A VARIATIONAL FORMULATION OF THE COMPRESSIBLE THROUGHFLOW PROBLEM

Gordon C. Oates, et al

Washington University

Prepared for:

Air Force Aero Propulsion Laboratory

August 1974

NOTICE PAGE

When Government drawings, specifications, or other data are used for any purpose other than in connection with a definitely related Government procurement operation, the United States Government thereby incurs no responsibility nor any obligation whatsoever; and the fact that the Government may have formulated, furnished, or in any way supplied the said drawings, specifications, or other data, is not to be regarded by implication or otherwise as in any manner licensing the holder or any other person or corporation, or conveying any rights or permission to manufacture, use, or sell any patented invention that may in any way be related thereto.

This report has been reviewed and cleared for open publication and/or public release by the appropriate Office of Information (OI) in accordance with AFR 190-17 and DODD 5230.9. There is no objection to unlimited distribution of this report to the public at large, or by DDC to the National Technical Information Service (NTIS).

This technical report has been reviewed and is approved for publication.

Francis R Ostdiek

FRANCIS R. OSTDIEK, GS-14
Project Engineer

FOR THE COMMANDER

Marvin F. Schmidt

MARVIN F. SCHMIDT, GS-14
Tech Area Manager, Compressors

AIR FORCE/56780/23 April 1975 — 50

UNCLASSIFIED

SECURITY CLASSIFICATION OF THIS PAGE (When Data Entered)

REPORT DOCUMENTATION PAGE		READ INSTRUCTIONS BEFORE COMPLETING FORM
1. REPORT NUMBER AFAPL-TR-74-78	2. GOVT ACCESSION NO.	3. RECIPIENT'S CATALOG NUMBER AD-A007 979
4. TITLE (and Subtitle) A VARIATIONAL FORMULATION OF THE COMPRESSIBLE THROUGHFLOW PROBLEM		5. TYPE OF REPORT & PERIOD COVERED Final March 1973 - April 1974
		6. PERFORMING ORG. REPORT NUMBER None
7. AUTHOR(s) Gordon C. Oates Graham F. Carey		8. CONTRACT OR GRANT NUMBER(s) F33615-73-C-2056
9. PERFORMING ORGANIZATION NAME AND ADDRESS University of Washington Aerospace Research Laboratory Seattle, WA 98195		10. PROGRAM ELEMENT, PROJECT, TASK AREA & WORK UNIT NUMBERS 30660406
11. CONTROLLING OFFICE NAME AND ADDRESS Air Force Aero Propulsion Laboratory Turbine Engine Division Wright-Patterson AFB, OH 45433		12. REPORT DATE August 1974 13. NUMBER OF PAGES 93
14. MONITORING AGENCY NAME & ADDRESS(if different from Controlling Office)		15. SECURITY CLASS. (of this report) Unclassified 15a. DECLASSIFICATION DOWNGRADING SCHEDULE

16. DISTRIBUTION STATEMENT (of this Report)

Approved for public release; distribution unlimited.

17. DISTRIBUTION STATEMENT (of the abstract entered in Block 20, if different from Report)

18. SUPPLEMENTARY NOTES

19. KEY WORDS (Continue on reverse side if necessary and identify by block number)

Internal Aerodynamics
Fluid Mechanics
Compressible Flow

20. ABSTRACT (Continue on reverse side if necessary and identify by block number)

A variational formulation of the compressible throughflow problem is developed. The method is suitable for the calculation of throughflow flow fields in which large rotational effects, large compressibility effects and large variations in hub and tip radii may exist. The formulation requires the absence of viscous forces between blade rows, though the effects of losses within the blade rows may be included through the variation of entropy across streamsurfaces. The meridional Mach number is restricted to be less than unity, though the (Cont'd)

DD FORM 1 JAN 73 1473 EDITION OF 1 NOV 65 IS OBSOLETE

UNCLASSIFIED

SECURITY CLASSIFICATION OF THIS PAGE (When Data Entered)

PRICES SUBJECT TO CHANGE

20. Abstract (Cont'd)

complete flow Mach number may be much in excess of unity. The variational formulation represents a complete statement of the problem in that the boundary conditions, far upstream and far downstream conditions, and matching conditions at all actuator discs are all natural conditions of the variational formulation. The numerical formulation of the problem is presented in detail and example calculations of flows with highly loaded actuator discs existing in annuli with large variations in hub and tip radii are given.

FOREWORD

This is the final Technical Report prepared by the Aerospace Research Laboratory of the University of Washington. The effort was sponsored by the Air Force Aero-Propulsion Laboratory, Air Force Systems Command, Wright-Patterson AFB, Ohio under Contract F33615-73-C-2056 for the period March 1973 to April 1974. The work herein was accomplished under Project 3066, Task 306604, Work Unit Number 30660406, A Variational Formulation of the Compressible Throughflow Problem, with Mr. Francis R. Ostdiek, AFAPL/TBC, as Project Engineer. Dr. Gordon C. Oates and Mr. Graham F. Carey of the University of Washington were technically responsible for the work.

TABLE OF CONTENTS

LIST OF FIGURES

LIST OF SYMBOLS

y,z	Dimensionless radial and axial coordinates ($\Psi = \Psi(y,z)$ system) Coordinates are non-dimensionalized with respect to the far upstream hub radius.
Y,x	Dimensionless radial and axial coordinates ($Y = Y(x,\Psi)$ system)
R	Dimensionless far upstream tip radius
G	Dimensionless tip radius ($G = G(x)$)
F	Dimensionless hub radius ($F = F(x)$)
Ψ	Dimensionless streamfunction, defined by Eqs (2) or Eqs (10)
U,V,W	Dimensionless velocity components in radial, azimuthal and axial directions. Velocities are non-dimensionalized with respect to the far upstream axial velocity.
$\bar{U}$	Dimensionless vector velocity, components (U,V,W)
ξ	Dimensionless angular momentum, $\xi = YV \equiv yV$
M	Mach number
ρ	Dimensionless density. Density is non-dimensionalized with respect to the far upstream static density.
T	Temperature
S	Entropy
C_v	Specific heat at constant volume
H	Dimensionless stagnation enthalpy. Enthalpies are non-dimensionalized with respect to the square of the far upstream axial velocity.
h	Dimensionless static enthalpy
P	Dimensionless pressure. Pressure is non-dimensionalized with respect to the product of the far upstream static density and square of the far upstream axial velocity.
K	Group of terms defined by Eq (15)
Γ	Variational functional, defined by Eq (14)
Ω	Dimensionless rotor angular velocity. Non-dimensionalized with respect to the far upstream axial velocity divided by the far upstream hub radius.

SUBSCRIPTS

d	Refers to (jump) conditions at a disc
o	Conditions far upstream
e	Conditions at exit
T	Stagnation conditions
$-\infty,\infty$	Conditions far upstream, far downstream

NOTE: Symbols used in finite element analysis and numerical analysis are introduced and defined within the text.

SECTION I

INTRODUCTION

The throughflow theory of flow in turbomachines describes the overall effect of an entire blade row or rows upon the fluid properties within the machine. The throughflow field is considered to be axially symmetric, and because of its position as the "parent" flow field to the cascade field and the secondary field, it is important that the throughflow field be accurately described.

An extensive description of throughflow theory for turbomachines is given in Refs. 1-3. In Ref. 3, a variational formulation of the incompressible throughflow problem suitable for the description of highly rotating flows existing in annuli with large variations in hub and tip radii is described. The present study, described herein, extends the study of Ref. 3 to include the effects of compressibility. The effects of entropy production within the blade rows is included in the formulation though the flow external to the blade rows must be considered perfect. In addition the meridional Mach number must be less than unity.

This latter restriction is not very limiting with regards to the extent of applicability of the results, because few (if any) turbines or compressors are contemplated that would utilize meridional Mach numbers in excess of unity. Of course, the full flow Mach number (including the swirl component of velocity) may be much in excess of unity. It should be noted, however, that it is the approach to unit meridional Mach number that is at the heart of the computational difficulties of any program that calculates near-sonic flow fields. Any iterative program utilizes, somewhere in the program, a "guess" for the streamline location that will later be adjusted to numerically satisfy the describing equations. A glance at subsonic flow tables (Ref. 4 for example) shows that a one percent error in streamtube area would lead to the prediction of sonic flow for a flow whose "true" Mach number should be 0.9. Without special corrective measures being taken, this error would lead to numerical divergence of the density calculation.

There are two reasons for the comparatively great difficulties encountered in the numerical calculation of highly rotating compressible flow fields. The presence of the large rotation leads to highly distorted axial velocity profiles, and the presence of the large swirl component of velocity leads to large total flow Mach numbers. The fluid density is, of course, determined by the total flow Mach number so the combination of axial velocity distortion and large density variations make it difficult to estimate an accurate "first guess" for streamline position. As a result erroneous "supersonic" portions of the flow field can easily appear in the initial portions of the calculations, even in a flow field that, when eventually determined, will have rather modest meridional Mach numbers throughout.

These preliminary remarks are intended to alert the reader to the importance of wisely selecting the iterative procedures of calculations such as those described herein, and to explain why such an emphasis has been placed upon the method and order of the several subsidiary calculations involved in the program.

SECTION II

VARIATIONAL FORMULATION OF THE COMPRESSIBLE THROUGHFLOW PROBLEM

1. FORMULATION OF THE EQUATIONS

The pertinent equations are developed in detail in Ref. 3, but for convenience non-dimensional forms of the resultant equations will be repeated here. When perfect flow is considered, conservation of angular momentum and Euler's momentum equation indicate that external to the blade rows the angular momentum and stagnation enthalpy, respectively, are conserved along streamsurfaces.

Information regarding variations across streamsurfaces is obtained by considering the normal component of the combined momentum and thermodynamic equations. The resultant equation gives a relationship for the tangential vorticity which may be written in the form:

$$\frac{\partial}{\partial z}\left(\frac{1}{\rho y}\frac{\partial \Psi}{\partial z}\right) + \frac{\partial}{\partial y}\left(\frac{1}{\rho y}\frac{\partial \Psi}{\partial y}\right) = \rho y\left[\frac{\partial H}{\partial \Psi} - T\frac{\partial S}{\partial \Psi} - \frac{1}{2y^2}\frac{\partial \xi^2}{\partial \Psi}\right] \tag{1}$$

This form is valid for flow external to the blade rows, provided only that the flow external to the blade rows may be considered nonviscous.

The dimensionless velocity components are related to the dimensionless streamfunction by:

$$\rho U = \frac{1}{y}\frac{\partial \Psi}{\partial z} \quad , \quad \rho W = -\frac{1}{y}\frac{\partial \Psi}{\partial y} \tag{2}$$

The boundary conditions on Ψ are

$$\Psi = -\frac{1}{2} \text{ on } y = F(z) \quad , \quad \Psi = -\frac{R^2}{2} \text{ on } y = G(z) \tag{3}$$

When actuator discs are considered to exist in the flow field, the matching conditions across the discs follow from the continuity equation and radial momentum (assuming no radial forces) to give respectively the jump conditions

$$[\Psi]_d = 0 \tag{4}$$

$$\left[\frac{1}{\rho y}\frac{\partial \Psi}{\partial z}\right]_d = 0 \tag{5}$$

In general there will be jumps in tangential momentum and stagnation enthalpy imparted by the blade rows, which must be related by the Euler momentum equation to give

$$[H]_d = \Omega[\xi]_d \tag{6}$$

Finally, the thermodynamic equation in conjunction with the equation for the (known) stagnation enthalpy gives the equation for the density.

$$H - \frac{1}{2}(U^2 + W^2 + \frac{\xi^2}{y^2}) = h = h_o \rho^{\gamma-1} e^{\frac{S-S_o}{c_v}} \tag{7}$$

Utilizing Eq (2), this may be rearranged to give:

$$(2H - \frac{\xi^2}{y^2})\rho^2 - 2h_o\rho^{\gamma+1} e^{\frac{S-S_o}{c_v}} - \{(\frac{1}{y}\frac{\partial\Psi}{\partial z})^2 + (\frac{1}{y}\frac{\partial\Psi}{\partial y})^2\} = 0 \tag{8}$$

Eqs (1) - (8) represent the mathematical statement of the problem. Fig. 1 indicates the various geometric relationships. It should be noted that any entropy variations occurring are considered to have been created within the blade rows, because Eq (1) has not included the effects of viscous terms. This being the case, external to the blade rows the entropy is a function of streamfunction only. This model gives a good approximation to the throughflow flow field,(1) and in this report only the special case of perfect flow ($S = S_o$ throughout) is actually calculated. The formulation, however, is not restricted to isentropic flow fields.

2. FORMULATION OF THE TRANSFORMED EQUATIONS

The numerical solutions to follow are conveniently obtained by formulating the equations to solve for the radial position as a function of axial position and streamfunction. We thus transform the independent variables from y and z to Ψ and x, where $x \equiv z$. We also write $y \equiv Y(x,\Psi)$ in order to facilitate simple conceptual separation of the two systems. Routine transformation of the appropriate equations leads to the following set of equations in the x,Ψ system.

Differential equation

$$-\frac{\partial}{\partial x}\left(\frac{1}{\rho}\frac{\frac{\partial Y}{\partial x}}{Y\frac{\partial Y}{\partial \Psi}}\right) + \frac{Y}{2}\frac{\partial}{\partial \Psi}\left\{\frac{1+\left(\frac{\partial Y}{\partial x}\right)^2}{\rho\left(Y\frac{\partial Y}{\partial \Psi}\right)^2}\right\} + \frac{Y}{2}\frac{1+\left(\frac{\partial Y}{\partial x}\right)^2}{\left(Y\frac{\partial Y}{\partial \Psi}\right)^2}\frac{\partial}{\partial \Psi}\frac{1}{\rho}$$

$$= \rho Y\left[\frac{\partial H}{\partial \Psi} - T\frac{\partial S}{\partial \Psi} - \frac{1}{2Y^2}\frac{\partial \xi^2}{\partial \Psi}\right] \tag{9}$$

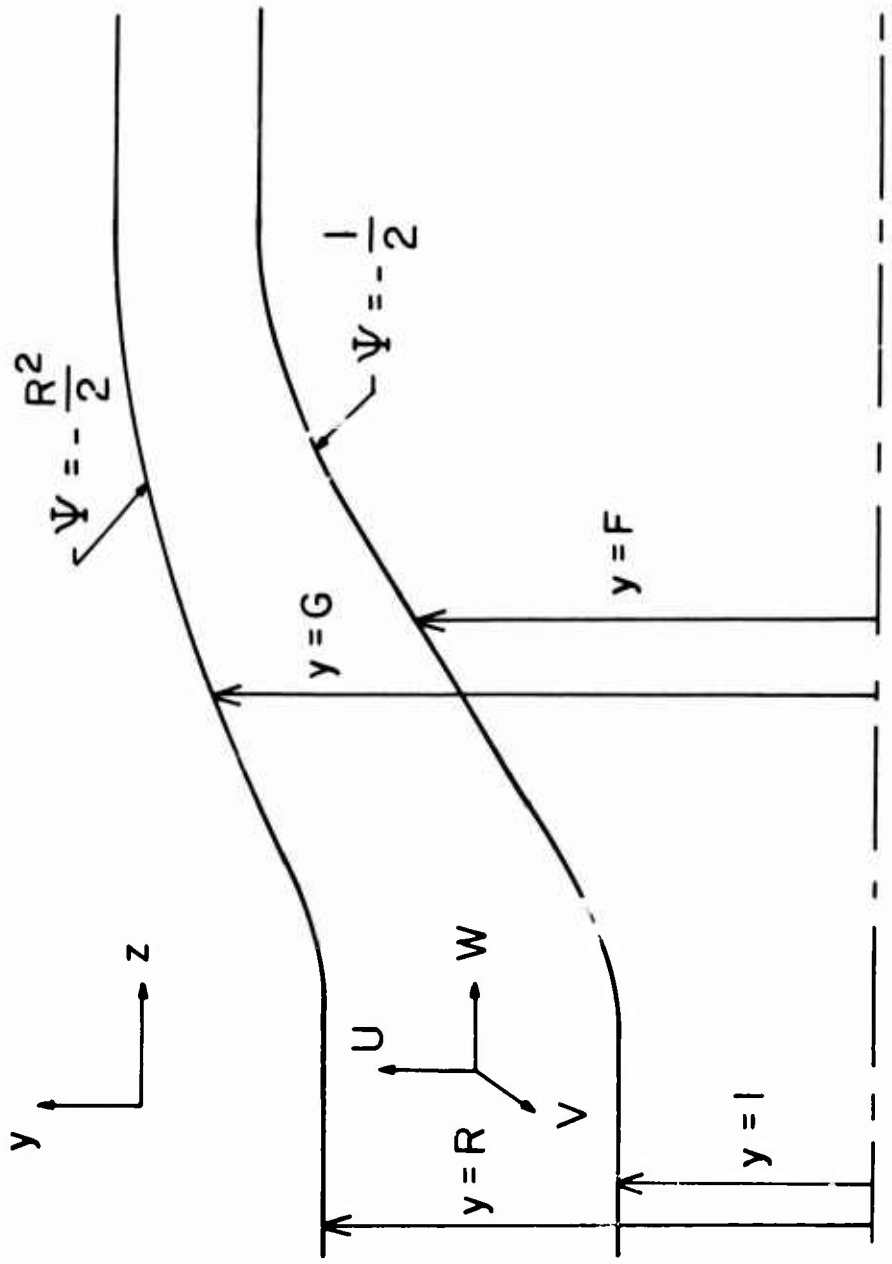

Figure 1. Nomenclature and Geometry

Velocity Relationships

$$\rho U = \frac{-\frac{\partial Y}{\partial x}}{Y\frac{\partial Y}{\partial \Psi}} \quad , \quad \rho W = \frac{-1}{Y\frac{\partial Y}{\partial \Psi}} \tag{10}$$

Boundary Conditions (enclosed flows only)

$$Y = F \text{ on } \Psi = -\frac{1}{2} \quad , Y = G \text{ on } \Psi = -\frac{R^2}{2} \tag{11}$$

Matching Conditions

$$[Y]_d = 0 \quad , \left[\frac{\frac{\partial Y}{\partial x}}{\rho Y\frac{\partial Y}{\partial \Psi}}\right]_d = 0 \tag{12}$$

Density Relationship

$$\left(2H - \frac{\xi^2}{Y^2}\right)\rho^2 - 2h_o\rho^{\gamma+1} e^{\frac{S-S_o}{c_v}} - \frac{1 + \left(\frac{\partial Y}{\partial x}\right)^2}{\left(Y\frac{\partial Y}{\partial \Psi}\right)^2} = 0 \tag{13}$$

The Euler equation remains as in Eq. (6).

3. VARIATIONAL STATEMENT OF THE PROBLEM

We now define a variational functional, Γ, by

$$\Gamma = \int_{-\infty}^{\infty}\int_{F}^{G} [P - P_e + \rho\{U^2 + W^2\}]ydydz \tag{14}$$

This, of course, is simply the integral of the meridional momentum over all space. For convenience in relating the compressible results to the incompressible results we define the parameter K by:

$$K = P - P_e + \frac{1}{2}\rho\bar{U}^2 \tag{15}$$

The thermodynamic equation may be written

$$T\nabla S = \nabla H - \nabla\frac{\bar{U}^2}{2} - \frac{1}{\rho}\nabla P \tag{16}$$

so that with Eq (15),

$$\nabla K = \rho\{\nabla H - T\nabla S\} + \frac{\overline{U}^2}{2}\nabla\rho \tag{17}$$

Utilizing the definitions of Eqs (14) and (15), we obtain the expression for Γ in the (x,Ψ) system as:

$$\Gamma = \int_{-\infty}^{\infty}\int_{-1/2}^{-R^2/2}\left[K + \frac{\rho}{2}\{U^2 + W^2 - V^2\}\right] Y \frac{\partial Y}{\partial \Psi}\, d\Psi dx \tag{18}$$

The variation of this quantity is now taken. Noting from Eq (17) that

$$\delta K = \rho\{\delta H - T\delta S\} + \frac{\overline{U}^2}{2}\delta\rho \tag{19}$$

the variation of Eq (18) utilizing Eqs (10) leads, after some manipulation, to

$$\delta\Gamma = \int_{-\infty}^{\infty}\int_{-1/2}^{-R^2/2}\left[\rho\{\delta H - T\delta S\} Y \frac{\partial Y}{\partial \Psi} + K\,\delta\left(Y \frac{\partial Y}{\partial \Psi}\right) + \frac{1}{2\rho}\delta\left(\frac{1 + \left(\frac{\partial Y}{\partial x}\right)^2}{Y \frac{\partial Y}{\partial \Psi}}\right) - \frac{\rho}{2}\delta\left\{\frac{\xi_2^2}{Y}\frac{\partial Y}{\partial \Psi}\right\}\right] d\Psi dx \tag{20}$$

In the flows considered in this report, perfect flow is assumed to exist outside the blade rows. This being the case, both the entropy and stagnation enthalpy are constant along streamsurfaces. When the variation is taken in the x,Ψ system, as it is here, the variation of functions of Ψ alone, is of course, zero. It follows that neither δH nor δS contribute in Eq (20). Utilizing this fact and rearranging the terms in Eq (20) we then obtain:

$$\delta\Gamma = \int_{-\infty}^{\infty}\int_{-1/2}^{-R^2/2}\left[\delta Y\left(-Y\frac{\partial K}{\partial \Psi} + \frac{1}{2Y}\frac{\partial \rho \xi_2^2}{\partial \Psi} - \frac{\partial}{\partial x}\frac{\frac{\partial Y}{\partial x}}{\rho Y \frac{\partial Y}{\partial \Psi}} + \frac{Y}{2}\frac{\partial}{\partial \Psi}\frac{1 + \left(\frac{\partial Y}{\partial x}\right)^2}{\rho\left(Y\frac{\partial Y}{\partial \Psi}\right)^2}\right)\right.$$

$$\left. + \frac{\partial}{\partial \Psi}\left(\left[KY - \frac{\rho}{2}\frac{\xi_2^2}{Y} - \frac{1}{2}\frac{1 + \left(\frac{\partial Y}{\partial x}\right)^2}{\left(Y\frac{\partial Y}{\partial \Psi}\right)^2}\frac{Y}{\rho}\right]\delta Y\right) + \frac{\partial}{\partial x}\left[\frac{\frac{\partial Y}{\partial x}\delta Y}{\rho Y \frac{\partial Y}{\partial \Psi}}\right]\right] d\Psi dx \tag{21}$$

Eq (17) with Eqs (10), gives us

$$\frac{\partial K}{\partial \Psi} = \rho\left\{\frac{\partial H}{\partial \Psi} - T\frac{\partial S}{\partial \Psi}\right\} - \frac{1}{2}\frac{1 + \left(\frac{\partial Y}{\partial x}\right)^2}{\left(Y\frac{\partial Y}{\partial \Psi}\right)^2}\frac{\partial}{\partial \Psi}\frac{1}{\rho} + \frac{\xi_2^2}{2Y^2}\frac{\partial \rho}{\partial \Psi} \tag{22}$$

Substituting this expression into Eq (21), and integrating the last two terms leads to

$$\delta\Gamma = \int_{-\infty}^{\infty}\int_{-1/2}^{-R^2/2} \delta Y \left[-\rho Y \left[\frac{\partial H}{\partial \Psi} - T\frac{\partial S}{\partial \Psi} - \frac{1}{2Y^2}\frac{\partial \xi^2}{\partial \Psi} \right] - \frac{\partial}{\partial x}\frac{\frac{\partial Y}{\partial x}}{\rho Y \frac{\partial Y}{\partial \Psi}} + \frac{Y}{2}\frac{\partial}{\partial \Psi}\frac{1+\left(\frac{\partial Y}{\partial x}\right)^2}{\rho\left(Y\frac{\partial Y}{\partial \Psi}\right)^2} \right.$$

$$\left. + \frac{1}{2}\frac{1+\left(\frac{\partial Y}{\partial x}\right)^2}{Y\left(\frac{\partial Y}{\partial \Psi}\right)^2}\frac{\partial}{\partial \Psi}\frac{1}{\rho} \right] d\Psi dx + \int_{-\infty}^{\infty} \left[\left[KY - \frac{\rho}{2}\frac{\xi^2}{Y} - \frac{1}{2}\frac{1+\left(\frac{\partial Y}{\partial x}\right)^2}{Y\left(\frac{\partial Y}{\partial \Psi}\right)^2}\frac{1}{\rho} \right] \delta Y \right]_{-1/2}^{-R^2/2} dx$$

$$- \int_{-1/2}^{-R^2/2} \left[\frac{\frac{\partial Y}{\partial x}\delta Y}{\rho Y \frac{\partial Y}{\partial \Psi}} \right]_{x=-\infty} d\Psi + \ldots + \int_{-1/2}^{-R^2/2} \left[\left[\frac{\frac{\partial Y}{\partial x}\delta Y}{\rho Y \frac{\partial Y}{\partial \Psi}} \right]_{x=x_{d-}} - \left[\frac{\frac{\partial Y}{\partial x}\delta Y}{\rho Y \frac{\partial Y}{\partial \Psi}} \right]_{x=x_{d+}} \right] d\Psi + \ldots$$

$$+ \int_{-1/2}^{-R^2/2} \left[\frac{\frac{\partial Y}{\partial x}\delta Y}{\rho Y \frac{\partial Y}{\partial \Psi}} \right]_{x=+\infty} d\Psi \qquad (23)$$

Interior to the domain, δY is arbitrary. It can be seen from Eq (9) that the first term gives the Euler-Lagrange equation governing $Y(x,\Psi)$. Utilizing Eqs (10) and (15), it is apparent that the second term vanishes if the boundary is specified ($\delta Y=0$ on $\Psi = -1/2, R^2/2$) or if the boundary is a free streamline ($P=P_e$). The remaining terms arise from the far upstream conditions, jump conditions at the actuator discs, and far downstream conditions. For enclosed flows, radial equilibrium at far upstream and far downstream ensures that $U = \dfrac{-\frac{\partial Y}{\partial x}}{\rho Y \frac{\partial Y}{\partial \Psi}}$ is zero. Eqs (12) indicate that the matching conditions at the actuator discs are also naturally satisfied by this variational statement.

It can now be seen that the variational principle represents a complete statement of the physical problem in which the effects of compressibility and entropy variations have both been included. The boundary conditions and all matching conditions are all natural conditions of the variational formulation. As a result, a finite element variational approach may be employed without prescription of these boundary and matching conditions, and they will automatically be satisfied within the numerical approximation.

4. FORMULATION OF THE VARIATIONAL EQUATION

It still remains to represent $\delta\Gamma$ in terms of prescribed variables (H,ξ) and functions of Y and δY. Eq (20) and the discussion immediately following Eq (20) lead to

$$\delta\Gamma = \int_{-\infty}^{\infty}\int_{-1/2}^{-R^2/2}\left[K\delta\left(Y\frac{\partial Y}{\partial\Psi}\right) + \frac{1}{2\rho}\delta\left(\frac{1+\left(\frac{\partial Y}{\partial x}\right)^2}{Y\frac{\partial Y}{\partial\Psi}}\right) - \frac{\rho}{2}\delta\left\{\frac{\xi^2}{Y}\frac{\partial Y}{\partial\Psi}\right\}\right]d\Psi dx \qquad (24)$$

We now restrict our attention to the calculation of isentropic flow fields. An expression for K is obtained by first noting that the dimensionless pressure may be written

$$P = \rho^{\gamma}P_o = \rho^{\gamma}\left(\frac{\gamma-1}{\gamma}h_o\right) \qquad (25)$$

Utilizing Eq (13) with $S = S_o$, it follows that

$$P = \frac{\gamma-1}{\gamma}\rho\left[H - \frac{1}{2}\left(\frac{1+\left(\frac{\partial Y}{\partial x}\right)^2}{\left(\rho Y\frac{\partial Y}{\partial\Psi}\right)^2} + \frac{\xi^2}{Y^2}\right)\right] \qquad (26)$$

Thus with Eqs (10), (15) and (26) it follows that

$$K = \frac{\gamma-1}{\gamma}\rho H + \frac{1}{2\gamma}\left[\frac{1}{\rho}\frac{1+\left(\frac{\partial Y}{\partial x}\right)^2}{\left(Y\frac{\partial Y}{\partial\Psi}\right)^2} + \rho\frac{\xi^2}{Y^2}\right] - P_e \qquad (27)$$

The desired form of the functional variation is then obtained to give:

$$\delta\Gamma = \int_{-\infty}^{\infty}\int_{-1/2}^{-R^2/2}\left[\left(\frac{\gamma-1}{\gamma}\rho H + \frac{1}{2\gamma}\left(\frac{1}{\rho}\frac{1+\left(\frac{\partial Y}{\partial x}\right)^2}{\left(Y\frac{\partial Y}{\partial\Psi}\right)^2} + \rho\frac{\xi^2}{Y^2}\right) - P_e\right)\delta\left(Y\frac{\partial Y}{\partial\Psi}\right)\right.$$

$$\left. + \frac{1}{2\rho}\delta\left(\frac{1+\left(\frac{\partial Y}{\partial x}\right)^2}{Y\frac{\partial Y}{\partial\Psi}}\right) - \frac{\rho}{2}\delta\left(\frac{\xi^2}{Y}\frac{\partial Y}{\partial\Psi}\right)\right]d\Psi dx \qquad (28)$$

The subsidiary equation for the density, for the case of isentropic conditions is:

$$\left(2H - \frac{\xi^2}{Y^2}\right) \rho^2 - 2h_o \rho^{\gamma+1} - \frac{1 + \left(\frac{\partial Y}{\partial x}\right)^2}{\left(Y \frac{\partial Y}{\partial \Psi}\right)^2} = 0 \tag{29}$$

Usually the far upstream approach Mach number will be prescribed, so we note

$$H_o - h_o = \frac{1}{2} = h_o \left(\frac{\gamma-1}{2} M_o^2\right)$$

hence $$h_o = \frac{1}{\gamma-1} \frac{1}{M_o^2} \tag{30}$$

and $$H_o = \frac{1}{\gamma-1} \frac{1 + \frac{\gamma-1}{2} M_o^2}{M_o^2} \tag{31}$$

The local stagnation enthalpy H follows from application of the Euler Momentum equation, Eq (6).

It is important to note that the density variations were included in the variation of functional Γ in Eq (18) to determine $\delta\Gamma$ in Eq (20). However, collecting terms involving $\delta\rho$ produces the governing differential equation multiplying $\delta\rho$ as the density variation contribution. Then, since the governing equation is satisfied as the Euler equation from consideration of variations δY, the expression involving $\delta\rho$ is zero. That is, we may write

$$\delta\Gamma = \frac{\partial \Gamma}{\partial Y} \delta Y + \frac{\partial \Gamma}{\partial \rho} \delta\rho \equiv \frac{\partial \Gamma}{\partial Y} \delta Y = 0$$

and the variational problem reduces to satisfying $\frac{\partial \Gamma}{\partial Y} \delta Y = 0$. Then the finite element approximation need introduce only an approximation to $Y(x,\Psi)$ in terms of solution point values Y_j^i and the variational problem requires $\frac{\partial \Gamma}{\partial Y_j^i} = 0$ subject to the prescribed boundary conditions.

The unknown density field still appears in the coefficients of the variations of position terms and satisfies the subsidiary equation, Eq (29). Thus given any streamfield, the associated density field is completely specified.

These two calculation steps, (a) the streamfield position, and (b) the corresponding density field, constitute the central feature of the coupled iterative scheme described in the following sections.

We remark that, as an alternative scheme, the density field could be included as an unknown in the variational problem itself, by expanding $Y(x,\Psi) = f_1(Y_j^i)$ and $\rho(x,\Psi) = f_2(\rho_j^i)$. The formulation and computation become complicated, since the subsidiary density equation must be imbedded as a constraint by Lagrange multiplier methods. The vector of finite element nodal unknowns is thereby increased to include $\{Y_j^i, \rho_j^i, \lambda_j^i\}$, where $\lambda(x,\Psi)$ is the Lagrange multiplier. In turn, this increases the vector of unknowns in the nonlinear algebraic system resulting, and the problem formulation is computationally inferior to that of the coupled position and density problems above.

5. INTERPRETATION OF TERM K

It is clear that the effect of finite Mach number is felt directly in the coefficients of the last two terms of Eq (28) through its effect on the dimensionless density ρ. It is of interest to consider also the effect of Mach number on the term K. Writing $\frac{\gamma-1}{\gamma} H = \frac{P_T}{\rho_T}$, we have from Eqs (10) and (27)

$$K = \rho \left(\frac{P_T}{\rho_T} + \frac{\bar{U}^2}{2\gamma} \right) - P_e = \rho \frac{P_T}{\rho_T} \{1 + \frac{a^2}{2a_T^2} M^2\} - P_e$$

$$= \rho \frac{P_T}{\rho_T} \frac{1 + \frac{\gamma}{2} M^2}{1 + \frac{\gamma-1}{2} M^2} - P_e$$

$$\text{or} \quad K = P_T \frac{1 + \frac{\gamma}{2} M^2}{\{1 + \frac{\gamma-1}{2} M^2\}} \frac{\gamma}{\gamma-1} - P_e$$

We note upon expansion that $K = P_T - P_e - \frac{\gamma}{8} M^4 P_T + \ldots$

Thus for small Mach numbers, the compressibility effect upon the parameter K is very small indeed.

SECTION III

FINITE ELEMENT METHOD

1. INTRODUCTION

The preceding analysis develops a variational formulation of the throughflow problem. The Euler equation is the governing partial differential equation for the throughflow, and natural boundary conditions prescribe conditions at the actuator discs and at downstream infinity. For the present, only enclosed flows are considered. In this analysis the fully-infinite flow domain is idealized as a finite but extensive region with boundary conditions at infinity applying on the remote boundaries $x = x_0$ and $x = x_N$. The finite domain approximation is not essential to the method. Since the asymptotic far field solution is known, this may be included in the finite element analysis as an "exterior" element approximant matching the solution at the remote boundaries x_0 and x_N.(5) However, it is simpler and adequate to use the finite domain approximation and the natural boundary condition insures parallel flow as the solution approaches the radial equilibrium condition at the ends.

It was remarked in the variational development that the inverse formulation in $Y(x,\Psi)$ achieved by transformation to (x,Ψ) coordinates is particularly advantageous. There, it was pointed out that enthalpy H and angular momentum ξ are constant along streamsurfaces in the flow between discs. In addition, the domain is mapped to a rectangular region bounded by $\Psi = \Psi_{hub} = -1/2$ and $\Psi = \Psi_{tip} = -\frac{R^2}{2}$ streamlines and with intermediate Ψ lines parallel to the bounding streamlines. A representation of rectangular elements is a natural choice in the (x,Ψ) plane. There is no domain error at the hub and tip and the use of parametric element forms, necessary in an accurate (x,y) plane approximation at the walls, is thereby avoided.

The finite element description of the problem is now developed for a general element form. Following this, detailed derivation is presented for a low order element approximant, the bilinear interpolant.

2. NATURE OF THE FINITE ELEMENT SYSTEM

The desired variational functional, Γ, was described in the previous section. We now utilize the notation $\frac{\partial f}{\partial \Psi} \equiv f_\Psi$, $\frac{\partial f}{\partial x} \equiv f_x$, f any function to rewrite the variation $\delta\Gamma$ as given in Eq (28) as:

$$\delta\Gamma = \int_{-\infty}^{\infty} \int_{-1/2}^{-R^2/2} \left[\left[\frac{\gamma-1}{\gamma} \rho H + \frac{1}{2\gamma} \left(\frac{1}{\rho} \frac{1 + Y_x^2}{(YY_\Psi)^2} + \rho \frac{\xi^2}{Y^2} \right) \right] \delta(YY_\Psi) + \frac{1}{2\rho} \delta \left(\frac{1 + Y_x^2}{YY_\Psi} \right) - \frac{\rho}{2} \delta \left(\frac{\xi^2}{Y} Y_\Psi \right) \right] d\Psi dx \qquad (32)$$

It is to be noted that the term P_e has been excluded for algebraic simplicity. In the situation considered here of enclosed flows only, P_e makes no contribution to the flow behavior.

Assume Lagrangian interpolation on any given mesh of elements and let the nodes be numbered consecutively. For example, on a rectangular mesh of size S = (MxN) the general node k defined by the ordinate index pair (i,j) is k = (i-1)N + j. The finite element approximation may be written in terms of the nodal values $\{Y^k\}$, k=1, ...,S, as

$$Y(x,\Psi) = Y^k \phi_k(x,\Psi) \tag{33}$$

where the repeated index implies summation.

The functions $\phi_k(x,\Psi)$ are termed nodal or global basis functions. They are non-zero only over those elements immediately adjacent to node k, assume unit value at node k and are zero at all other nodes.

Substituting for $Y(x,\Psi)$ into $\Gamma(Y)$, then $\Gamma(Y)$ becomes $\Gamma(\underset{\sim}{Y}, \{\phi_k\})$, with

$$\delta\Gamma = \frac{\partial\Gamma}{\partial Y^k} \delta Y^k = 0$$

which implies

$$\frac{\partial\Gamma}{\partial Y^k} = 0 \quad , k=1,\ldots,S \tag{34}$$

This represents the system of finite element equations for the discretized throughflow problem. From Eq (32), the detailed expression for Eq (34) is

$$0 = \frac{\partial\Gamma}{\partial Y^k} = \int_{-\infty}^{\infty} \int_{-1/2}^{-R^2/2} \left[\left[\frac{\gamma-1}{\gamma} \rho H + \frac{1}{2\gamma} \left(\frac{1 + Y_x^2}{\rho (YY_\psi)^2} + \rho \frac{\xi^2}{Y^2} \right) \right] \frac{\partial}{\partial Y^k} (YY_\psi) \right.$$

$$\left. + \frac{1}{2\rho} \frac{\partial}{\partial Y^k} \left(\frac{1 + Y_x^2}{YY_\psi} \right) - \frac{\rho}{2} \frac{\partial}{\partial Y^k} \left(\frac{\xi^2 Y_\psi}{Y} \right) \right] d\Psi dx \tag{35}$$

We examine the expression $\frac{\partial}{\partial Y^k}(YY_\psi)$ in detail:

$$\frac{\partial}{\partial Y^k}(YY_\psi) = \frac{\partial}{\partial Y^k}(Y^\alpha \phi_\alpha Y^\beta (\phi_\beta)_\psi)$$

$$= \frac{\partial}{\partial Y^k}(Y^\alpha Y^\beta \phi_\alpha (\phi_\beta)_\psi)$$

$$= \delta_{k\alpha} Y^\beta \phi_\alpha (\phi_\beta)_\psi + \delta_{k\beta} Y^\alpha \phi_\alpha (\phi_\beta)_\psi$$

$$= Y^\beta \phi_k (\phi_\beta)_\psi + Y^\alpha \phi_\alpha (\phi_k)_\psi$$

or $$\frac{\partial}{\partial Y^k}(YY_\psi) = Y^\alpha \{\phi_k (\phi_\alpha)_\psi + \phi_\alpha (\phi_k)_\psi\}$$

The other terms of interest, $\frac{\partial}{\partial Y^k}\left(\frac{1 + Y_x^2}{YY_\psi}\right)$ and $\frac{\partial}{\partial Y^k}\left(\frac{\xi^2 Y_\psi}{Y}\right)$ may be similarly expanded. Substitution into Eq (35) and integration over the "patch" of elements connected at node k determines the general finite element equation corresponding to node k.

The additional variables, enthalpy $H(\Psi)$ and angular momentum $\xi(\Psi)$, are known functions throughout the flow field; the density ρ is an implicit function of the streamline field and is assumed known corresponding to the prior position iteration. This completes the most general finite element description of the problem.

3. THE ELEMENT APPROXIMATIONS

In the above statement, a very general nodal or global basis $\{\phi_k(x,\Psi)\}$ was introduced. The problem reduces to quadrature on each nodal patch. In turn, this quadrature is most conveniently evaluated as an accumulated quadrature from each element of a given patch. To do so, the global basis $\{\phi_k(x,\Psi)\}$ is resolved to a local element basis on each element.

Consider a partition of the flow field by rectangular elements. The simplest approximation uses bilinear interpolation on each element and is developed here. The extension to higher order elements is immediate. A general element and nodal patch with global basis function is shown in Fig. 2.

For convenience of notation in deriving the finite element equations, replace node k by the ordinate node pair (m,n) as marked with $k = (m-1)N + n$. Let $x_{m+1} - x_m = a$ and $\Psi_{n+1} - \Psi_n = b$ and introduce the normalized element

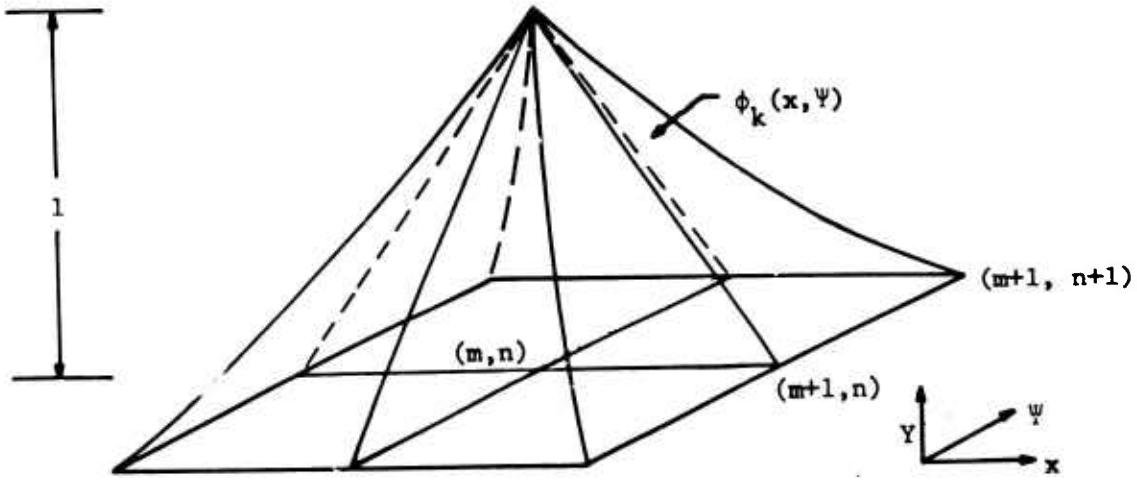

Figure 2. Patch of Four Elements Centered at k ≡ (m,n) and Nodal Basis Function $\phi_k(x,\Psi)$ Composed of Bilinear Element Approximants

coordinates $\bar{x} = (x - x_m)/a$ and $\bar{\Psi} = (\Psi - \Psi_n)/b$. In bilinear interpolation on an element e, $Y_e(x,\Psi) = a_0^m + a_1 x + a_2\Psi + a_3 x\Psi$ with the $\{a_i\}$ determined such that $Y_e(x,\Psi)$ interpolates the four corner values Y_n^m, Y_n^{m+1}, Y_{n+1}^m, and Y_{n+1}^{m+1}. In normalized coordinates, the bilinear interpolant is

$$Y_e(\bar{x},\bar{\Psi}) = (1 - \bar{x})(1 - \bar{\Psi})\, Y_n^m + \bar{x}(1 - \bar{\Psi})\, Y_n^{m+1} + \bar{x}\bar{\Psi}\, Y_{n+1}^{m+1} + (1 - \bar{x})\bar{\Psi}\, Y_{n+1}^m \quad (36)$$

The statement of Eq (34) may be rephrased in terms of element contributions. The functional Γ is represented as a sum of element quadratures by

$$\Gamma = \sum_e (\Gamma)_e = \sum_{m=1}^{M-1} \sum_{n=1}^{N-1} \Gamma_n^m$$

where $\Gamma_e \equiv \Gamma_n^m$ is the contribution to Γ of element e identified by the lower-left index pair (m,n).

Eq (34) becomes for any node (i,j),

$$\frac{\partial \Gamma}{\partial Y_j^i} = \sum_e \frac{\partial \Gamma_e}{\partial Y_j^i} = \sum_{m=1}^{M-1} \sum_{n=1}^{N-1} \frac{\partial \Gamma_n^m}{\partial Y_j^i} \quad (37)$$

Consider the contribution of a single element at (m,n) to the system. Then, writing,

$$K(x,\Psi) = \frac{\gamma-1}{\gamma}\rho H + \frac{1}{2\gamma}\left[\frac{1}{\rho}\left(\frac{1 + Y_x^2}{(YY_\Psi)^2}\right) + \rho\frac{\xi^2}{Y^2}\right]$$

the element contribution is

$$\frac{\partial \Gamma_n^m}{\partial Y_j^i} = \int_{x_m}^{x_{m+1}} \int_{\Psi_n}^{\Psi_{n+1}} \left[K(x,\Psi)\frac{\partial}{\partial Y_j^i}(YY_\Psi) + \frac{1}{2\rho}\frac{\partial}{\partial Y_j^i}\left(\frac{1 + Y_x^2}{YY_\Psi}\right) - \frac{\rho}{2}\frac{\partial}{\partial Y_j^i}\left(\frac{\xi^2}{Y}Y_\Psi\right)\right] d\Psi dx \quad (38)$$

In the interests of developing as simple a numerical problem as possible for this initial analysis, and motivated by the analogous assumption that H_e = constant for the incompressible calculations,[3] the quadrature problem is simplified by the assumption $K(x,\Psi) = K_e$ = constant in an element. This approximation is involved only in the quadrature. The enthalpy and

angular momentum are constant along Ψ lines in a given element. For the quadrature $H_e = (H_n + H_{n+1})/2$ and $\xi_e^2 = (\xi_n^2 + \xi_{n+1}^2)/2$ are assumed constant in an element. Similarly, the density ρ is constant at the mean value $\bar{\rho} = \rho_e = 1/4\{\rho_n^m + \rho_n^{m+1} + \rho_{n+1}^m + \rho_{n+1}^{m+1}\}$.

Under these assumptions the quadrature of Eq (38) becomes

$$\frac{\partial r_n^m}{\partial Y_j^i} = K_e \frac{\partial}{\partial Y_j^i} \int_{x_m}^{x_{m+1}} \int_{\Psi_n}^{\Psi_{n+1}} (YY_\Psi)\, d\Psi dx$$

$$+ \frac{1}{2}\,\frac{1}{\bar{\rho}} \frac{\partial}{\partial Y_j^i} \int_{x_m}^{x_{m+1}} \int_{\Psi_n}^{\Psi_{n+1}} \left(\frac{1 + Y_x^2}{YY_\Psi}\right) d\Psi dx - \frac{\xi_e^2}{2}\,\bar{\rho} \int_{x_m}^{x_{m+1}} \int_{\Psi_n}^{\Psi_{n+1}} \frac{Y_\Psi}{Y}\, d\Psi dx \tag{39}$$

The three integrals in Eq (39) are evaluated in turn. Consider the first integral,

$$I_1 = \int_{x_m}^{x_{m+1}} \int_{\Psi_n}^{\Psi_{n+1}} (YY_\Psi)\, d\Psi dx$$

$$= \int_{x_m}^{x_{m+1}} \int_{\Psi_n}^{\Psi_{n+1}} \left(\frac{1}{2} Y^2\right)_\Psi d\Psi dx$$

$$= \frac{1}{2} \int_{x_m}^{x_{m+1}} \{Y^2(x, \Psi_{n+1}) - Y^2(x, \Psi_n)\}\, dx$$

Applying the trapezoidal rule,

$$I_1 \approx \frac{1}{4}\left[(Y_{n+1}^m)^2 + (Y_{n+1}^{m+1})^2 - (Y_n^m)^2 - (Y_n^{m+1})^2\right](x_{m+1} - x_m) \tag{40}$$

In the second integral, since the element interpolant is bilinear, the approximant varies linearly along the element sides. Derivatives Y_x and Y_Ψ at the corner nodes can be replaced by the corresponding difference quotients in the 4-point quadrature formula

$$\int_{x_m}^{x_{m+1}} \int_{\Psi_n}^{\Psi_{n+1}} f(x,\Psi)\, d\Psi dx = \frac{1}{4}\left[f_n^m + f_n^{m+1} + f_{n+1}^m + f_{n+1}^{m+1}\right](\Psi_{n+1}-\Psi_n)(x_{m+1}-x_m)$$

to give

$$I_2 \approx \frac{1}{4}\left[\frac{1+\left(\frac{Y_{n+1}^{m+1}-Y_{n+1}^m}{x_{m+1}-x_m}\right)^2}{Y_{n+1}^{m+1}\left(Y_{n+1}^{m+1}-Y_n^{m+1}\right)} + \frac{1+\left(\frac{Y_{n+1}^{m+1}-Y_{n+1}^m}{x_{m+1}-x_m}\right)^2}{Y_{n+1}^{m}\left(Y_{n+1}^{m}-Y_n^{m}\right)} + \frac{1+\left(\frac{Y_{n}^{m+1}-Y_{n}^m}{x_{m+1}-x_m}\right)^2}{Y_{n}^{m+1}\left(Y_{n+1}^{m+1}-Y_n^{m+1}\right)}\right.$$

$$\left. + \frac{1+\left(\frac{Y_{n}^{m+1}-Y_{n}^m}{x_{m+1}-x_n}\right)^2}{Y_n^m(Y_{n+1}^m-Y_n^m)}\right](\Psi_{n+1}-\Psi_n)^2(x_{m+1}-x_m) \quad (41)$$

Similarly, the third quadrature gives

$$I_3 \approx \frac{1}{4}\left[\frac{(Y_{n+1}^{m+1})^2-(Y_n^{m+1})^2}{Y_{n+1}^{m+1}\,Y_n^{m+1}} + \frac{(Y_{n+1}^m)^2-(Y_n^m)^2}{Y_{n+1}^m\,Y_n^m}\right](x_{m+1}-x_m) \quad (42)$$

Writing $I_\alpha = I_\alpha(Y_n^m, Y_{n+1}^m, Y_n^{m+1}, Y_{n+1}^{m+1})$, $\alpha = 1,2,3$, then the following permutation relations are evident on inspection

$$I_\alpha(Y_n^m, Y_{n+1}^m, Y_n^{m+1}, Y_{n+1}^{m+1}) = -I_\alpha(Y_{n+1}^m, Y_n^m, Y_{n+1}^{m+1}, Y_n^{m+1})$$

$$= I_\alpha(Y_n^{m+1}, Y_{n+1}^{m+1}, Y_n^m, Y_{n+1}^m) = -I_\alpha(Y_{n+1}^{m+1}, Y_n^{m+1}, Y_{n+1}^m, Y_n^m) \quad (43)$$

Then differentiating I_α with respect to Y_j^i we have,

$$\frac{\partial I_\alpha}{\partial Y_j^i} = \delta_{im}\delta_{jn}\frac{\partial I_\alpha}{\partial Y_n^m} + \delta_{im}\delta_{j(n+1)}\frac{\partial I_\alpha}{\partial Y_{n+1}^m} + \delta_{i(m+1)}\delta_{jn}\frac{\partial I_\alpha}{\partial Y_n^{m+1}} + \delta_{i(m+1)}\delta_{j(n+1)}\frac{\partial I_\alpha}{\partial Y_{n+1}^{m+1}}$$

The term $\frac{\partial I_\alpha}{\partial Y^m_n}$ can be evaluated and $\frac{\partial I_\alpha}{\partial Y^m_{n+1}}$, $\frac{\partial I_\alpha}{\partial Y^{m+1}_n}$, $\frac{\partial I_\alpha}{\partial Y^{m+1}_{n+1}}$ all follow directly from the permutation relations in Eq (43).

The integrated expressions $\frac{\partial I_\alpha}{\partial Y^i_j}$, $\alpha = 1,2,3$ may be substituted into $\frac{\partial \Gamma^m_n}{\partial Y^i_j}$. We write

$$F^m_n\left(Y^m_n\ ,\ Y^m_{n+1}\ ,\ Y^{m+1}_n\ ,\ Y^{m+1}_{n+1}\right) = \left[K_e \frac{\partial I_1}{\partial Y^m_n} + \frac{1}{2\bar{\rho}} \frac{\partial I_2}{\partial Y^m_n} - \xi_e^2 \frac{\partial I_3}{\partial Y^m_n}\right] \delta_{im}\delta_{jn} \tag{44}$$

Then, using the permutation relations

$$\begin{aligned}\frac{\partial \Gamma^m_n}{\partial Y^i_j} = {} & F^m_n\left(Y^m_n\ ,\ Y^m_{n+1}\ ,\ Y^{m+1}_n\ ,\ Y^{m+1}_{n+1}\right) - F^m_n\left(Y^m_{n+1}\ ,\ Y^m_n\ ,\ Y^{m+1}_{n+1}\ ,\ Y^{m+1}_n\right) \\ & + F^m_n\left(Y^{m+1}_n\ ,\ Y^{m+1}_{n+1}\ ,\ Y^m_n\ ,\ Y^m_{n+1}\right) - F^m_n\left(Y^{m+1}_{n+1}\ ,\ Y^{m+1}_n\ ,\ Y^m_{n+1}\ ,\ Y^m_n\right)\end{aligned} \tag{45}$$

Eq (45) is the contribution of the general element e to the finite element equation at node (i,j). The product of delta functions in F^m_n ensures that the correct non-zero element contributions are accumulated. For example, if $(i,j) \equiv (m+1,n)$ then the contribution of the element is

$$\frac{\partial \Gamma^m_n}{\partial Y^{m+1}_n} = F^m_n\left(Y^{m+1}_n\ ,\ Y^{m+1}_{n+1}\ ,\ Y^m_n\ ,\ Y^m_{n+1}\right)$$

Individual element contributions are now collected to determine the finite element system.

$$\frac{\partial \Gamma}{\partial Y^i_j} = \sum_m \sum_n \frac{\partial \Gamma^m_n}{\partial Y^i_j}$$

An arbitrary internal node point (m,n) has four adjacent elements and collecting element contributions at this node,

$$0 = \frac{\partial \Gamma}{\partial Y_n^m} = -F_{n-1}^{m-1}\left(Y_n^m, Y_{n-1}^m, Y_n^{m-1}, Y_{n-1}^{m-1}\right) - F_{n-1}^{m}\left(Y_n^m, Y_{n-1}^m, Y_n^{m+1}, Y_{n-1}^{m+1}\right)$$
$$+ F_n^{m-1}\left(Y_n^m, Y_{n+1}^m, Y_n^{m-1}, Y_{n+1}^{m-1}\right) + F_n^{m}\left(Y_n^m, Y_{n+1}^m, Y_n^{m+1}, Y_{n+1}^{m+1}\right) \quad (46)$$

At a nodal point (m,n) on the boundary only 2 elements are adjacent except at the region corners where there is a single element. For example, at a point (m,n) on the lower boundary,

$$F_1^{m-1}\left(Y_2^{m-1}, Y_1^{m-1}, Y_2^m, Y_1^m\right) + F_1^m\left(Y_2^{m+1}, Y_1^{m+1}, Y_2^m, Y_1^m\right) = 0$$

A similar relation holds on the upper boundary and at the remote upstream and downstream boundaries.

The boundary conditions are now included in the formulation of the discrete problem. The enclosed flows, for instance, imply that Y_1^i and Y_j^N are prescribed for all i and j, and these values are set directly into the nonlinear system. The remote end conditions are retained as the natural boundary condition resulting from arbitrary end node variations, and satisfy

$$-F_{n-1}^{1}\left(Y_n^1, Y_{n-1}^1, Y_n^2, Y_{n-1}^2\right) + F_n^1\left(Y_n^1, Y_{n+1}^1, Y_n^2, Y_{n+1}^2\right) = 0$$

and $$-F_{n-1}^{M-1}\left(Y_n^M, Y_{n-1}^M, Y_n^{M-1}, Y_{n-1}^{M-1}\right) + F_n^{M-1}\left(Y_n^M, Y_{n+1}^M, Y_n^{M-1}, Y_{n+1}^{M-1}\right) = 0 \quad (47)$$

Eqs (46), (47) and the prescribed boundary conditions (known position) determine the nonlinear system of finite element equations for streamline position for a prescribed density field. The nonlinear system may be solved and the new streamfield used to improve the density field solution. The coupled solution of streamline position and density is then iterated to convergence.

SECTION IV

NUMERICAL ANALYSIS

1. FORMULATION OF COUPLED ITERATIONS

The streamline position $Y(x,\Psi)$ and the density $\rho(x,\Psi)$ are the primary unknowns in this formulation. One approach is to interpolate both unknown functions Y and ρ in the piecewise bilinear basis and solve for vectors $\underset{\sim}{Y}$ and $\underset{\sim}{\rho}$ from a variational problem that incorporates the density relation $f(\rho) = 0$ as a constraint condition by the use of Lagrange multipliers. This approach has not been developed since the earlier variational analysis indicated that the density variation expressions are zero.

The procedure advanced and applied here involves a coupled iteration for position $Y(x,\Psi)$, and density $\rho(x,\Psi)$. The function $Y(x,\Psi)$ is approximated on the finite element discretization, and substituted in the variational problem determining $\frac{\partial \Gamma}{\partial Y_j^i} = 0$. This leads to a nonlinear algebraic system of finite element equations for Y and dependent on the unknown density $\rho(x,\Psi)$. If the correct density were known, then solution of the algebraic system could be achieved by a gradient method such as Newton-Raphson iteration. Starting with an initial streamfield guess, the method iteratively improves the position vector, solving a linear Jacobian system at each iterative step. The approach can be extended to include the unknown density as follows. Select an appropriate streamline guess for the solution, based on the wall geometry. The scalar density equation $f(\rho) = 0$ is solved iteratively with this prescribed streamline position to determine the corresponding density field. With this density field (as if it were the exact result), the Newton-Raphson iteration for position is commenced. Interrupting the iteration at an appropriate point returns an improved streamline solution. The density field is recomputed for the new streamfield, and the Newton-Raphson iteration for position recommences with the new density field. The coupled process of scalar density iteration and vector position iteration is repeated to convergence within a prescribed error tolerance on the nonlinear system. The linking of iterations is depicted in the chart of Fig. 3.

2. DENSITY ITERATION

Given a streamline configuration $Y(x,\Psi)$, the density function satisfies the nonlinear scalar equation, Eq (29). This equation can be solved at each node point (i,j) where H, ξ and Y are known values.

Newton iteration for the root α of the scalar equation $f(\rho) = 0$ is

$$\rho_{k+1} = \rho_k - \frac{f(\rho_k)}{f'(\rho_k)} \quad , \text{ provided } f'(\alpha) \neq 0 \tag{48}$$

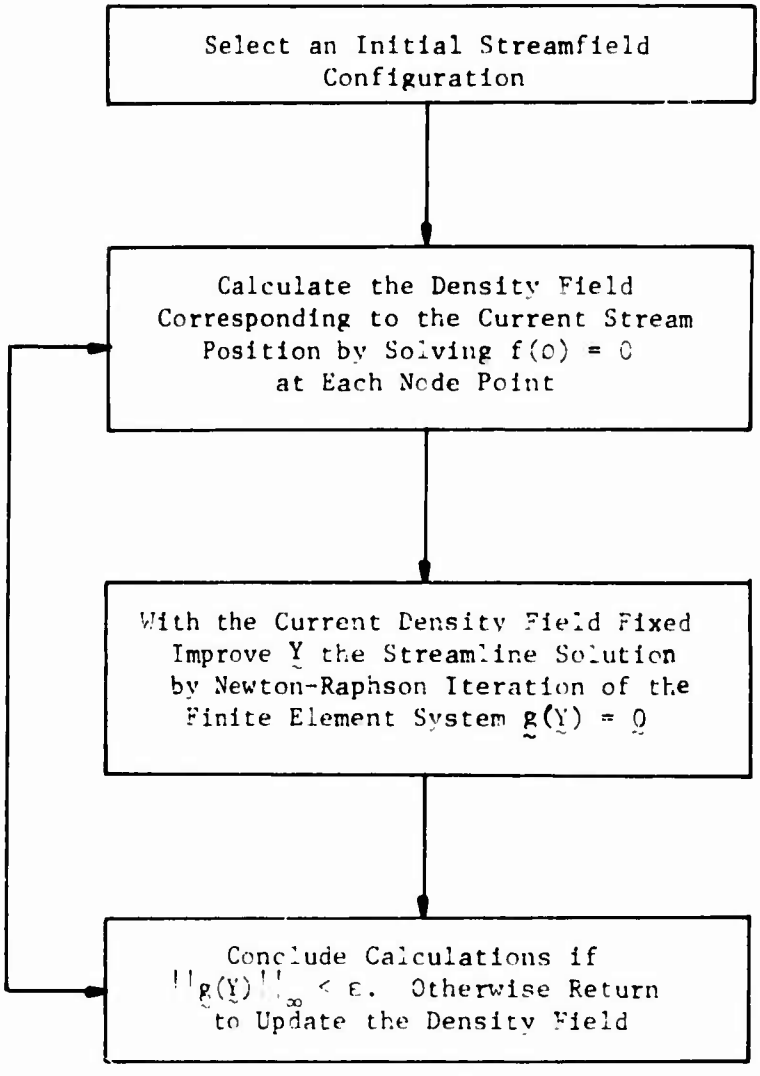

Figure 3. Coupling of Density and Streamline Calculations as an Iteration

Differentiating Eq (29)

$$f'(\rho) = 2(2H - \frac{\xi^2}{Y^2})\rho - (\gamma + 1)2h_o\rho^{\gamma}$$

Substituting in Eq (48) and simplifying,

$$\rho_{k+1} = \rho_k\left[1 - \frac{2H - \xi^2/Y^2 - 2h_o\,\rho_k^{\gamma+1} - \frac{1 + Y_x^2}{(YY_\psi)^2}}{2(2H - \xi^2/Y^2)\rho_k^{\,2} - 2(\gamma + 1)h_o\rho_k^{\gamma+1}}\right] \tag{49}$$

The iteration is considered to have converged when the difference in successive iterates is less than a specified error tolerance. The starting guess for the initial calculation is $\rho = 1$. Thereafter, the iterates begin from the previous flow field estimate. The scalar iteration is carried out for each node point in the mesh.

3. POSITION VECTOR ITERATION

Let $\underset{\sim}{J}$ be the Jacobian matrix $J_{ij} = \partial g_i/\partial Y_j$. The vector Newton iteration follows directly, as in the scalar case, by Taylor series expansion of $\underset{\sim}{g}(\underset{\sim}{Y} + \Delta\underset{\sim}{Y})$ about $\underset{\sim}{Y}$. Then the vector iteration is

$$\underset{\sim}{Y}^{k+1} = \underset{\sim}{Y}^{k} - \underset{\sim}{J}^{-1}\underset{\sim}{g}(\underset{\sim}{Y}^{k}) \tag{50}$$

In practice, the Jacobian derivatives $\partial g_i/\partial Y_j$ are determined as finite difference approximations,

$$\frac{\partial g_i}{\partial Y_j} \sim \frac{g_i(Y_1,\ldots,Y_{j-1},Y_j + \Delta Y_j, Y_{j+1},\ldots,Y_N) - g_i(Y_1,\ldots,Y_N)}{\Delta Y_j} \tag{51}$$

The iterate $\underset{\sim}{Y}^{k+1}$ is obtained as the solution of the linear system

$$\underset{\sim}{J}\Delta\underset{\sim}{Y}^{k+1} = \underset{\sim}{g}(\underset{\sim}{Y}^{k}) \tag{52}$$

with $\Delta\underset{\sim}{Y}^{k+1} = \underset{\sim}{Y}^{k+1} - \underset{\sim}{Y}^{k}$ and $g_p = \frac{\partial \Gamma}{\partial Y_p}$.

The coefficient matrix $\underset{\sim}{J}$ is positive definite, symmetric, and sparse. Positive definiteness results from the convexity of the functional Γ whose stationary value is sought. Writing $\underset{\sim}{g}^{k} = \underset{\sim}{E} = \{E_n^m\}$ for node (m,n) the symmetry follows from

$$\frac{\partial E^k_\ell}{\partial Y^i_j} = \frac{\partial}{\partial Y^i_j}\left(\frac{\partial \Gamma}{\partial Y^k_\ell}\right) = \sum_{m,n} \frac{\partial}{\partial Y^i_j}\left(\frac{\partial \Gamma^m_n}{\partial Y^k_\ell}\right) = \sum_{m,n} \frac{\partial}{\partial Y^k_\ell}\frac{\partial \Gamma^m_n}{\partial Y^i_j} = \frac{\partial E^i_j}{\partial Y^k_\ell}$$

The sparseness is evident as the algebraic equation corresponding to any given node has possible non-zero coefficients only for those nodes belonging to elements adjacent to the node concerned. Finally, it is important to note that a judicious numbering of the nodes will produce an algebraic problem that is neatly banded. Then highly efficient bandsolvers can be employed to solve Eq (52) for $\Delta \underset{\sim}{Y}^{k+1}$. In the particular instance of the throughflow problem, the characteristic span between hub and tip walls is small compared with the axial length between the remote upstream and downstream stations. Furthermore, the solution is well-behaved in the radial direction so that a coarse mesh gradation in this direction is appropriate; that is, few Ψ lines are necessary. On the other hand, there will be a much larger number of axial mesh lines corresponding to a graduated mesh, especially fine near the actuator discs and becoming coarse towards the remote boundaries. With this knowledge of the flow behavior and mesh nature, the optimal nodal-numbering scheme is evident: beginning at the remote upstream boundary, number radially across the streamlines. Then node k, corresponding to mesh pair (m,n) for a mesh of N Ψ-lines and M axial mesh lines (with M >> N), is (m-1) N + n. The half-bandwidth is N and the coefficient matrix is block-tridiagonal. Only the bandedness will be exploited in this algorithm as there is non-zero "fill" between the tridiagonal blocks during decomposition.

For direct solution of symmetric, positive-definite systems, the Cholesky method is preferable. The Cholesky decomposition is the triangular decomposition, $\underset{\sim}{J} = \underset{\sim}{L}\,\underset{\sim}{L}^T$, where $\underset{\sim}{L}$ is lower triangular. In the program code an equivalent form of Cholesky decomposition was used, expressing $\underset{\sim}{J}$ as $\underset{\sim}{U}^T\underset{\sim}{U}$ where $\underset{\sim}{U}$ is upper triangular. This allowed more convenient computation and display of the compactly stored jacobian and its decomposed form. Writing $\underset{\sim}{J} = \underset{\sim}{U}^T\underset{\sim}{U}$ so that $\underset{\sim}{U}^T\underset{\sim}{U}\,\Delta \underset{\sim}{Y}^{k+1} = g(\underset{\sim}{Y}^k)$, implies:

$$\underset{\sim}{U}^T\underset{\sim}{\beta} = \underset{\sim}{g}(\underset{\sim}{Y}^k) \quad , \quad \text{forward reduction}$$

and $$\underset{\sim}{U}\Delta \underset{\sim}{Y}^{k+1} = \underset{\sim}{\beta} \quad , \quad \text{back substitution,}$$

to determine the solution $\Delta \underset{\sim}{Y}^{k+1}$.

Only the non-zero upper half-band of $\underset{\sim}{J}$ need be stored and $\underset{\sim}{U}$ is overstored on $\underset{\sim}{J}$ as decomposition proceeds.

4. STABILITY AND CONVERGENCE

Fixed point theory for scalar and vector iterations is quite extensively developed and the Newton-Raphson iteration has been investigated. Standard contraction arguments([6]) indicate that the iteration converges if the initial

guess is within the contraction interval. The streamline position iteration is generally well-behaved, as the wall geometry suggests a reasonable starting guess which is coded directly in the program and need not be developed as data. The density iteration requires more care. Given an initial streamline configuration, the starting guess is incompressibility, $\rho = 1$, and Newton iteration of the nonlinear scalar equation at each grid point is generally convergent. However, in regions where there is a dramatic change in density, such as on the hub axis immediately beyond a stator imparting large swirl, the density iteration may not converge. An inadequate streamline configuration estimate, together with a poor initial density iterate, may predict meridional Mach number values greater than unity when the real physical flow has a subsonic meridional Mach number.

To stabilize the density iteration, the successive Newton iterates are scrutinized: if the iteration at a particular grid point begins to diverge, the physical constraint to subsonic meridional Mach numbers is enforced by setting axial velocity $W = 1$ and radial velocity $U = 0$. This determines a reasonable interim approximation at the troublesome point. Subsequent position iterations improve the streamline guess, and the later density iteration generally converges, with the exceptions of borderline cases where the physical flow is very demanding and sonic meridional Mach numbers are being closely approached. This approximate measure then serves to stabilize the numerical iterations and extends the numerical stability to include essentially the full range of flows of interest.

The graphs in Figs. 4 and 5 plot the error at a point on the hub wall beyond a stator, for several computations at various incident, free-stream Mach numbers. The graphs show very clearly the influence of the stabilizing density approximation.

Another technique for stabilizing the density calculation is to moderate the flow transition through the blade row. This can be done readily by using several actuator discs closely nested with a very fine separating grid, rather than use a single disc. Such an example is later examined in SECTION VI.

The exploration of the density calculation brings forth the question of stability of the global coupled iteration process, rather than that of the position or density iterations alone. In particular, should the position iteration at a fixed density be iterated to convergence (a quasi-incompressible analysis) and the density then updated, or should the position iteration be terminated earlier. Early computations explored the former scheme and it was found that in many cases the coupled process diverged. The use of under-relaxation attempting complete position iteration was similarly unsuccessful in these cases. Limiting the number of position iterations and successively reducing the limit eventually led to a coupled sequence that was stable and converged. The best results were obtained using a single position iteration to improve the streamline pattern. This analysis indicated the necessary close coupling of the numerical schemes.

Computationally, the global rate of convergence of the coupled calculations is only linear, whereas the Newton processes are asymptotically quadratic. For each case the rate of convergence of both position and density is somewhat slower for the first few iterations. The density point computations

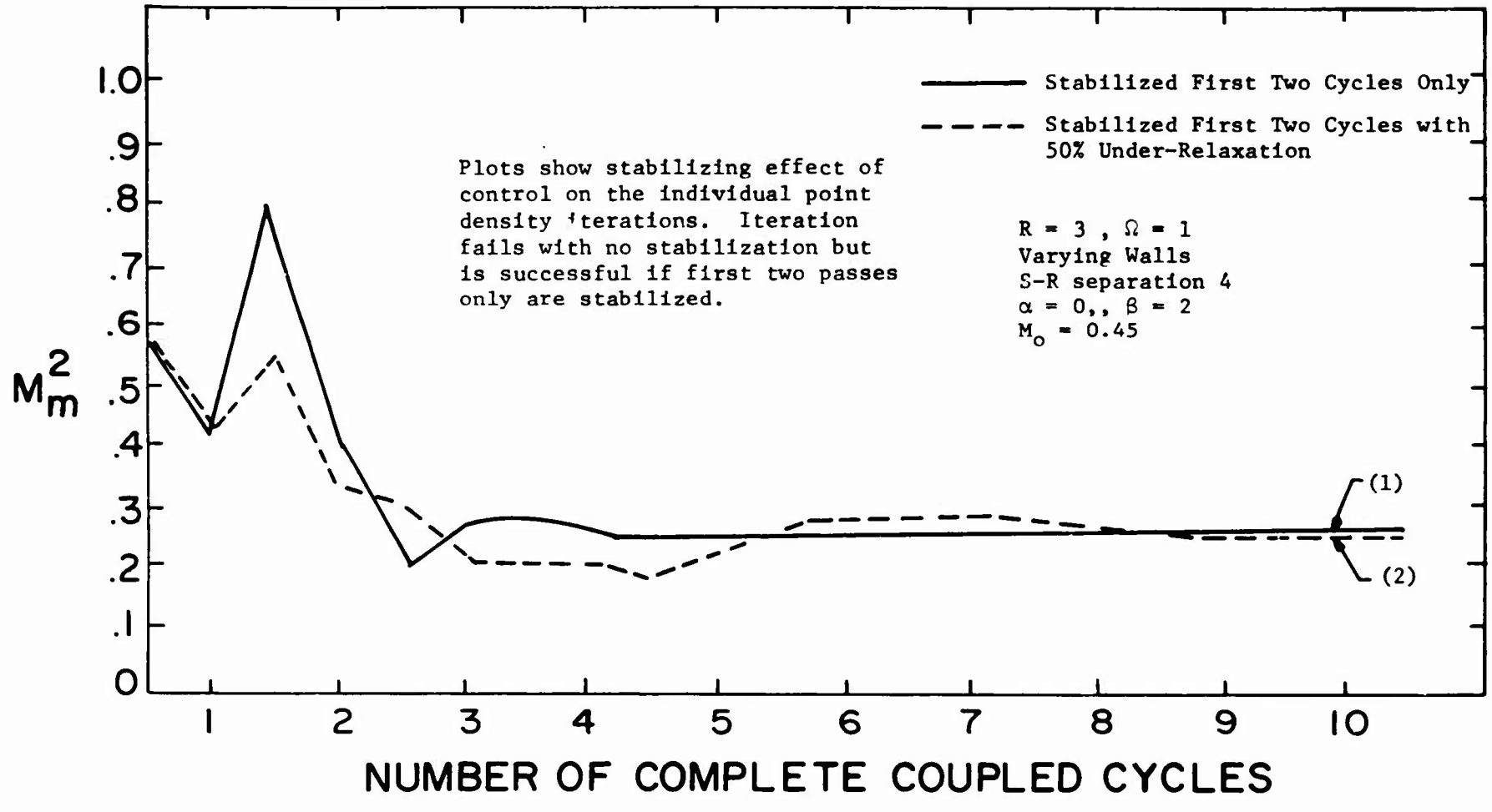

Figure 4. Plots of Peak Meridional Mach Number on the Hub Streamline Immediately Following the Stator

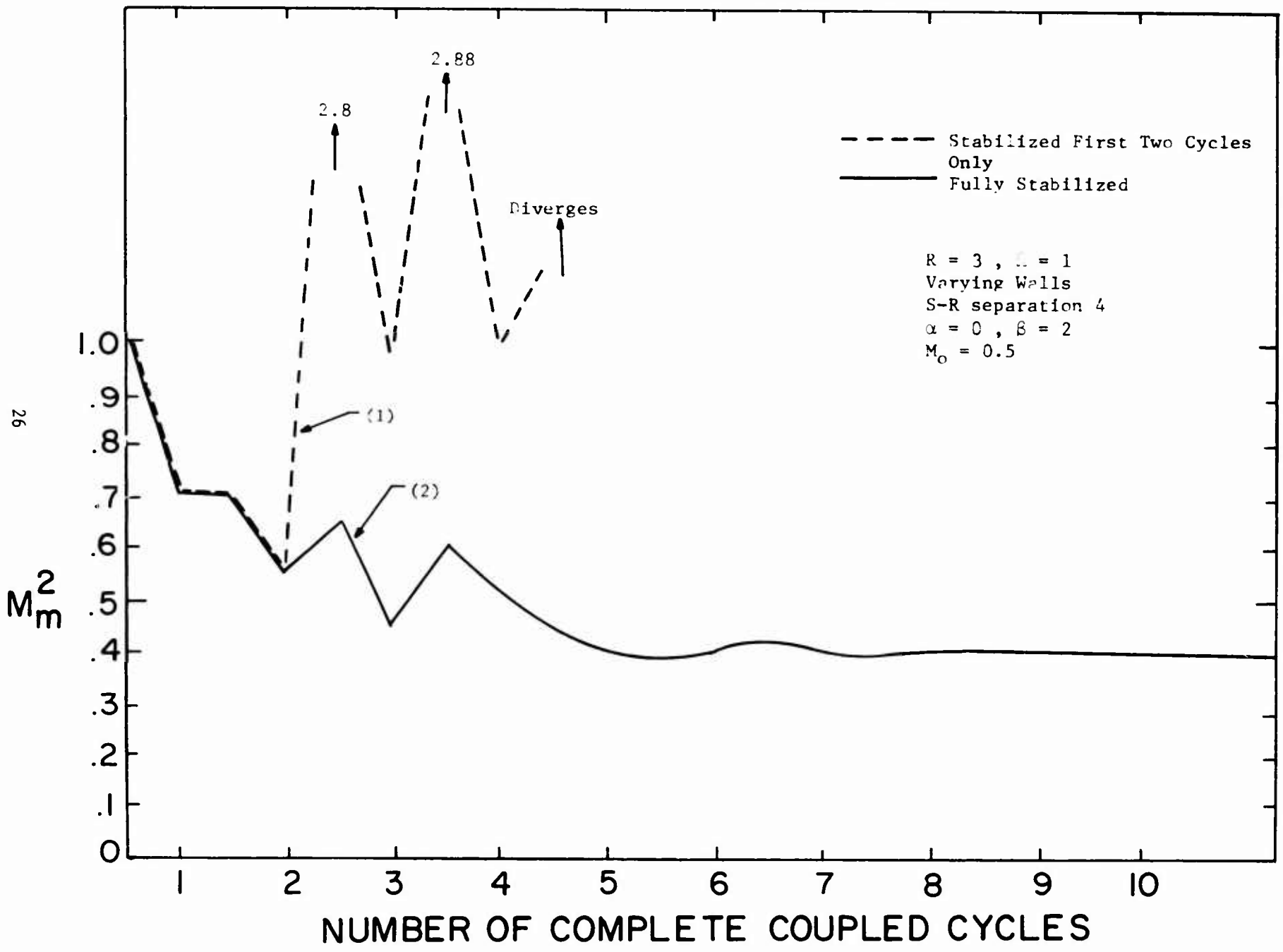

Figure 5. Plots of Peak Meridional Mach Number on the Hub Streamline Immediately Following the Stator

required several iterations in the starting calculations. However, for most incident Mach numbers and away from heavily loaded discs, subsequent point density calculations required only one or two iterations to give six significant figure accuracy.

Finally, the scheme is naturally sensitive to the incident Mach number. As Mach number increases the calculation becomes more demanding, stabilization is necessary, and the rate of convergence decreases. This is due in part to the physical nature of the higher Mach number flows, attainment of a sonic meridional Mach number being associated with "choking." In addition, sequences of flows computed at successively higher incident Mach numbers, on the same configuration and at the same loading, all used the same starting streamline pattern. This pattern is best for nearly incompressible flows and deteriorates with increased incident Mach number. Thus it takes increasingly more iterations to improve the starting guess. Relaxation and extrapolation techniques are possible ways to accelerate convergence but have not yet been explored, the present scheme affording adequate results in fewer than ten coupled iterations for most applications.

SECTION V

THE THROUGHFLOW PROGRAM

1. BASIC PROGRAM STRUCTURE

The throughflow problem is specified by input data to the program, the finite element idealization is established, and, beginning with a preset streamfield, the coupled iterations in density and position are carried out. Each position iteration is associated with solution of a banded linear system of equations. The general computational procedure and subroutine inter-relations are depicted in the macrochart of Fig. 6.

The function of each module and its relation to other stages in the layout are described briefly below.

a. Input

The input instructions reside within the controlling program, TCOMFLO. Input data defining the problem is read from cards for each flow problem analyzed.

b. TCOMFLO

This is the main calling program. It determines the finite element idealization in the (x,Ψ) coordinate system, and controls the data input and solution output steps.

c. GUESS

The initial guess for $Y(x,\Psi)$ at the mesh points is prescribed.

d. RSOLVE

This contains the density iteration and position vector iteration, returning the final values to the main controlling module, TCOMFLO.

e. BANSOL

This subprogram is called from RSOLVE and bandsolves the linear jacobian system for $\Delta\underset{\sim}{Y}$.

f. MERMACH

The meridional Mach number is computed at each node point between streamfield position iterations to monitor convergence of the coupled iterations.

g. Output

The final streamline coordinates and associated nodal velocity components are printed by axial mesh section.

Important details of the program are now developed.

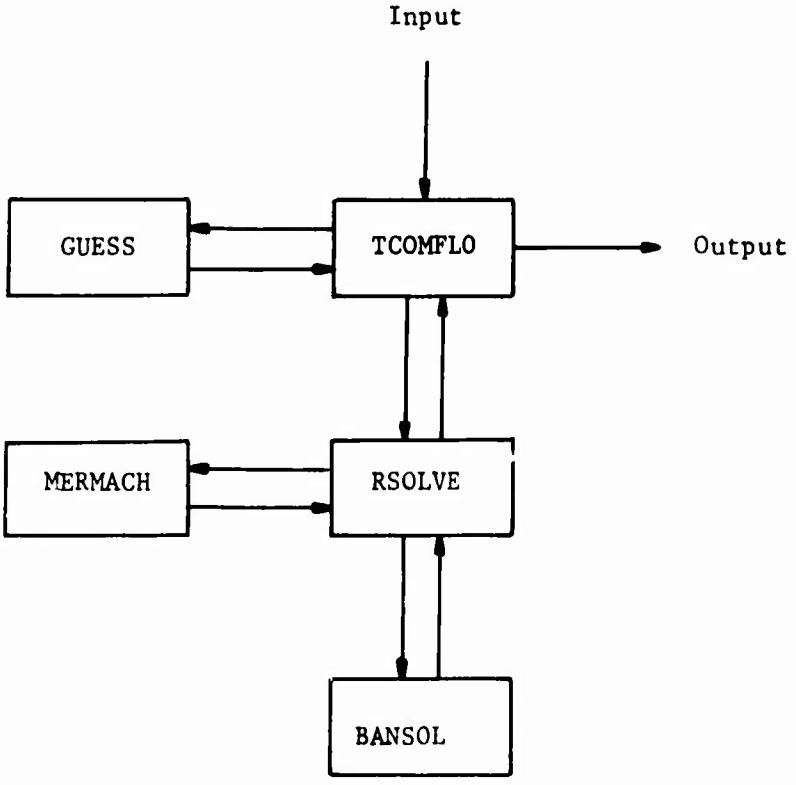

Figure 6. Modular Subroutine Layout of Programs for Throughflow Calculations

2. PROGRAM METHOD

Finite element mesh generation. The sections of uniform flow between discs are delimited by variables set in the program code. For a single stage, the separation between stator and rotor is input, and a uniform fine mesh established between the disc pair. Away from the discs, the grid spacing increases with $\Delta x_{j\pm1} = \kappa\, x_j$ where $\Delta x_{j+1} = x_{j+1} - x_j$ downstream and $\Delta x_{j-1} = x_j - x_{j-1}$ upstream and κ is set in the program as 1.25. Most of the results described later employed this restricted mesh algorithm. For general purposes, problems with several stages will require more flexible data-generation schemes or simply input the values $\{x_j\}$ as in Ref. 3.

Initial Streamfield Pattern. The starting pattern is determined from the hub and tip wall shapes and the uniform flow at the remote upstream boundary. At the spstream boundary the flow is uniform with axial velocity $W_{-\infty} = 1$ and $f = 1$. Then the axial velocity satisfies $\rho W = -\frac{1}{Y}\frac{\partial \Psi}{\partial Y}$ and leads in the (x,Ψ) system, to $\frac{1}{2}(Y^2)_\Psi = 1$. Integrating with respect to Ψ gives $\frac{1}{2}Y^2 = -\Psi$ so that

$$Y(x_o, \Psi) = \sqrt{-2\Psi} \tag{53}$$

and determines the Ψ-line distribution at the remote upstream boundary. The Ψ-line spacing for the initial guess is chosen so that the separation of adjacent streamlines is constant along any radial mesh line from hub to tip. In the (x,Ψ) plane, then $\Psi_{i+1} - \Psi_i = -\frac{1}{2}\left[\left(Y^j_{i+1}\right)^2 - \left(Y^j_i\right)^2\right]$. Clearly the spacing ΔY will vary from one mesh line j to the next as the hub wall $f(x)$ or tip wall $g(x)$ change. Then for a mesh line at x_j,

$$Y(x_j,\Psi_i) = Y^j_i = f(x_j) + (\sqrt{-2\Psi_i} - f(x_o))\,\frac{(g(x_j) - f(x_j))}{(g(x_o) - f(x_o))} \tag{54}$$

The Density Iteration. The density at any node point (x_j,Ψ_i) is determined by Newton iteration applied to the equation $f(\rho) = 0$ as described in the preceding section. For highly rotating flows at high incident Mach number, the density iteration may require stabilization. This is particularly true in the early stages of coupled iteration as the streamline pattern will be poor in some regions. The density calculation is indicated in the chart of Fig. 7.

Streamline Position Adjustment. The variational finite element formulation for strealine position $Y(x,\Psi)$ leads to the nonlinear system of equations

$$\frac{\partial \Gamma}{\partial Y^i_j} = \sum_{m,n} \frac{\partial \Gamma^m_n}{\partial Y^i_j} = 0$$

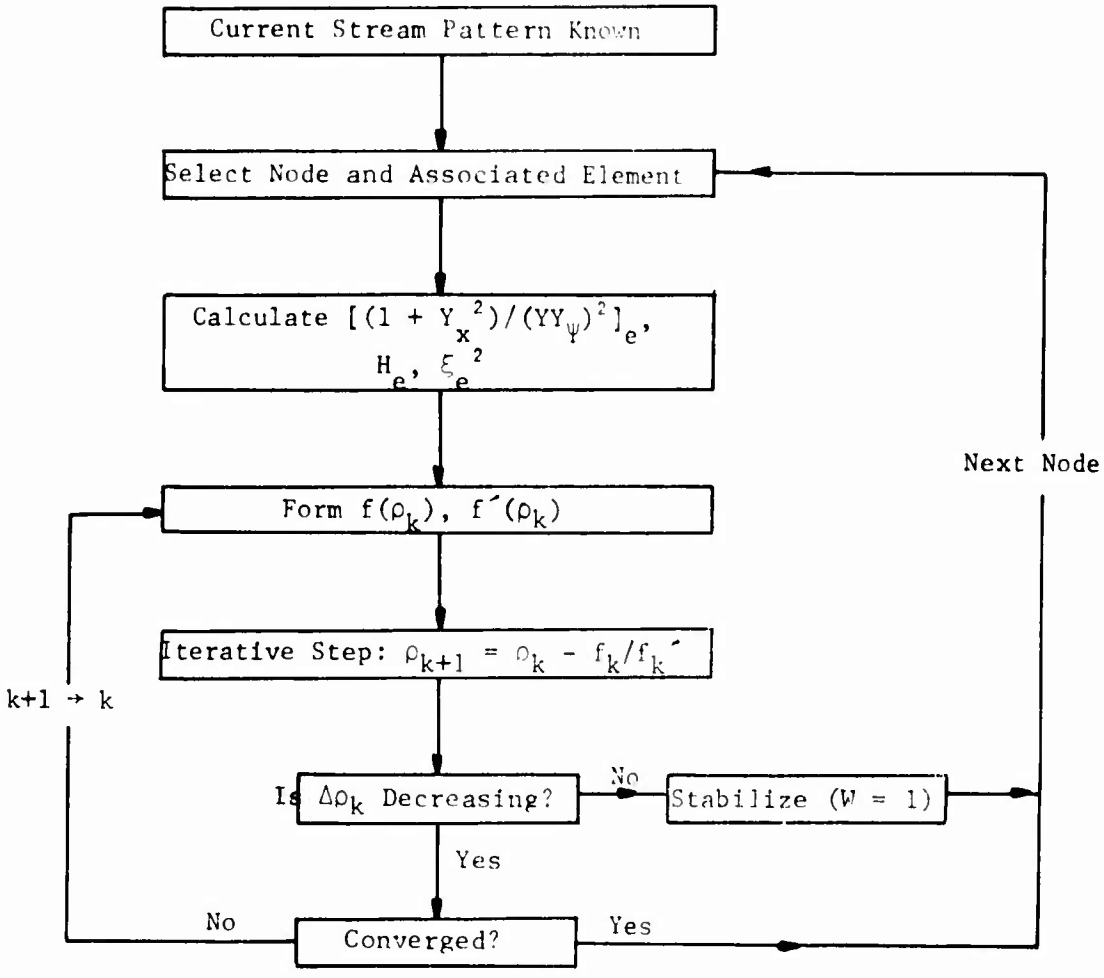

Figure 7. Newton Iteration for Density with Stabilization at Critical Points

Writing this as $\underset{\sim}{g}(\underset{\sim}{Y}) = \underset{\sim}{0}$, the solution $\underset{\sim}{Y}$ is sought by Newton-Raphson iteration. Let $\underset{\sim}{Y}^k$ correspond to the k'th intermediate solution pattern. Then $\underset{\sim}{g}(\underset{\sim}{Y}^k) = \underset{\sim}{e}^k \neq \underset{\sim}{0}$, and is the error vector. The solution adjustment is achieved as a single step of the jacobian system iteration

$$\underset{\sim}{J}\Delta\underset{\sim}{Y}^{k+1} = -\underset{\sim}{e}^k$$

In SECTION IV, the element contributions to $\partial\Gamma/\partial Y^i_j$ were developed and permutation relations noted. These permutation relations allow an elegant coding for accumulation of $\underset{\sim}{g}^k = \underset{\sim}{e}^k$ at each node point, and similarly for the jacobian evaluation. A single statement function definition, $F(Y^m_n, Y^m_{n+1}, Y^{m+1}_n, Y^{m+1}_{n+1})$ determines the element contribution to a given node, and permutation of the corner coordinates (Y^α_β) ascertain the other nodal contributions from the element (Fig. 8).

The compuational procedure is outlined in Fig. 9. Using the density field calculated from the current streamline position, the new adjusted streamline pattern is computed. Proceeding sequentially by elements, the element contribution of $\partial\Gamma^m_n/\partial Y^i_j$ to each of the four corner nodes is determined by use of the statement function. The nodal contributions are accumulated to give the error vector

$$\left\{\frac{\partial\Gamma}{\partial Y^i_j}\right\} = \underset{\sim}{g}(\underset{\sim}{Y}^k) = \underset{\sim}{e}^k$$

and the infinity norm of $\underset{\sim}{e}^k$ is tested to determine if the solution has converged. The jacobian $J_{pq} = \partial g_p/\partial Y_q$ is formed numerically by differencing,

$$\frac{\partial g_p}{\partial Y_q} = \frac{g(Y_1,\ldots Y_{p-1}, Y_p + \Delta Y_p, Y_{p+1},\ldots, Y_N) - g(Y_1,\ldots Y_N)}{\Delta Y_p}$$

Again, this difference quotient is formed sequentially by elements, evaluating $g(Y_1,\ldots,Y_p + \Delta Y_p,\ldots,Y_N)$ and $g(Y_1,\ldots,Y_N)$ by accumulating element contributions to the nodes as in the preceding calculation of $\underset{\sim}{e}^k$. The value $\Delta Y_p = 10^{-6}$ is set in the program code. Only the banded upper-half of the jacobian is stored during formation. The linear jacobian system is solved by banded Cholesky decomposition, followed by forward and backward substitution sweeps on the right-hand side vector $\underset{\sim}{e}^k$. During decomposition, only the upper triangular decomposed matrix is needed, and is stored over the coefficient matrix $\underset{\sim}{J}$ as decomposition proceeds. Solution for $\Delta\underset{\sim}{Y}^{k+1}$ determines the adjusted streamline

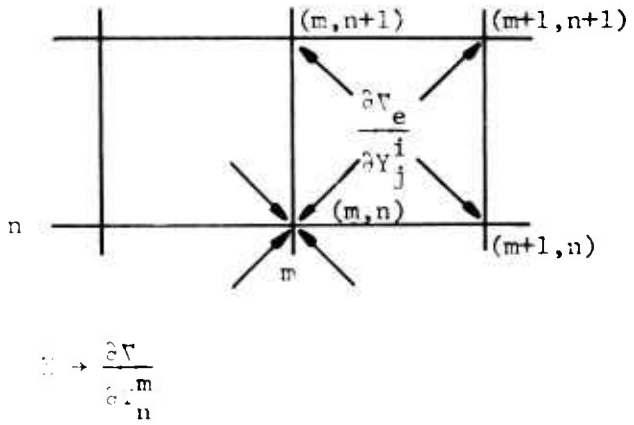

Figure 8. Distribution of Element Contributions and Corresponding Accumulation at Each Node

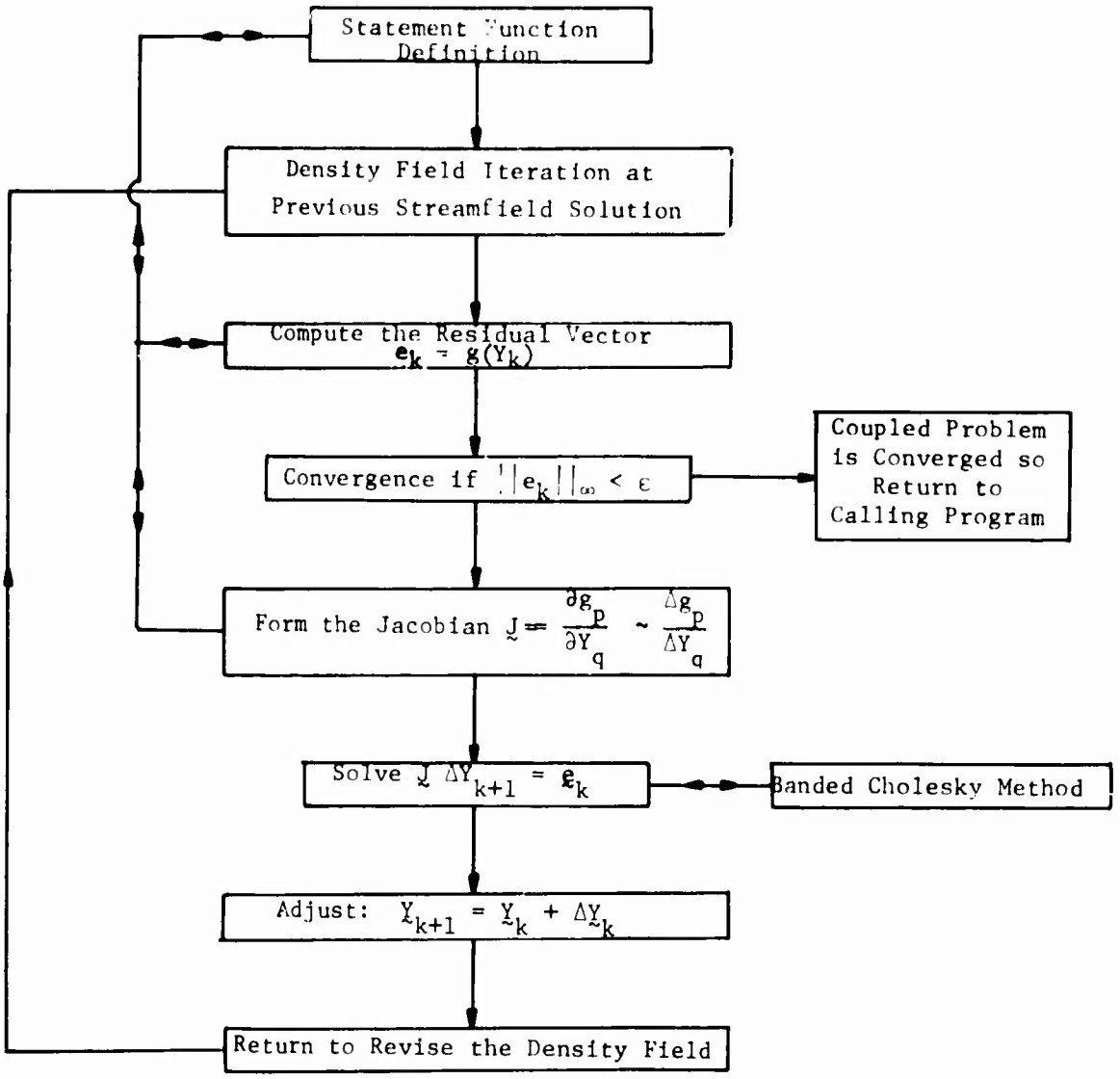

Figure 9. Layout of Procedure in RSOLVE to Adjust the Streamline Pattern

pattern. After the new position solution, we return to the density calculation and the next coupled iteration commences.

3. PROGRAM USAGE

Idealization Description. The turbine configuration is described in two dimensions, and consists of a sequence of sections of continuous flow separated by line interfaces representing actuator discs. The lower and upper boundaries correspond to hub and tip surfaces respectively, and the remote left and right boundaries simulate uniform flow regions far upstream and far downstream. The flow is characterized by a discrete streamline pattern, and the problem formulated in the (x,Ψ) plane to solve for streamline location. In (x,Ψ) coordinates the domain is rectangular and a finite element idealization of rectangular is introduced, with grid lines $\Psi = \Psi_i$ determined in the program, and $x = x_j$ input as data. Angular momentum and enthalpy far upstream and at the discs are prescribed for each section of continuous flow. A typical configuration with three discs and varying hub and tip walls is shown in Fig. 10. The finite element idealization in the (x,Ψ) plane is indicated in Fig. 11.

A typical rectangular element, shaded in section 2 of Fig. 11, is defined by enclosing horizontal Ψ-lines and vertical x-lines. The section limits $Nz_{\ell,k}$ with $\ell = 1,\ldots$ sections and $k = 1,2$ delimit each domain of continuous flow and are the x-line index pairs marked.

Computer application requires specification of: the idealization as grid point ordinates in the (x,Ψ) plane and identification of flow sections; angular momentum and enthalpy at each interface between adjacent sections. The rectangular domain in the (x,Ψ) plane simplifies the finite element representation and for flexibility the prescription of the x-partition is required as card input. The Ψ-partition is set in the program and corresponds to ΔY = constant at the upstream boundary. The fully-infinite problem is modelled as a finite but extensive region, and natural boundary conditions at the remote ends of the flow approximate the free-stream conditions.

List of Program Variables.[†]

ALFA(K):	Coefficient of momentum fit across disc, $yV = -\underline{\underline{\alpha}}\Psi + \underline{\beta}$
BETA(K):	Coefficient of momentum fit across disc, $yV = -\underline{\underline{\alpha}}\Psi + \underline{\beta}$
C(N,M):	Upper half-band of symmetric jacobian matrix
E(N):	Error residual vector of nonlinear system
F(J):	Vector defining lower wall (hub) ordinate boundary, f(x)
G(J):	Vector defining upper wall (tip) ordinate boundary, g(x)
H(I,K):	Total enthalpy on streamline I in section K
IDEN:	Maximum number of cycles of coupled calculation
ITMX:	Maximum number of position iterations per cycle, usually 1
MNMAX:	Maximum number of density iterations per cycle
NR:	Row dimension of jacobian, $\underline{\underline{C}}$

[†]Indices: K = section, I = streamline, J = x-line, N = node (I,J)

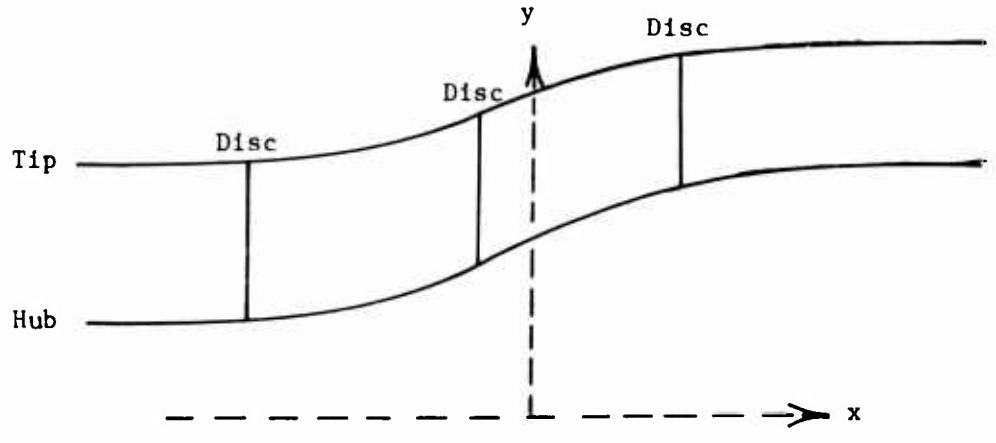

Figure 10. Multiple Disc Throughflow Configuration

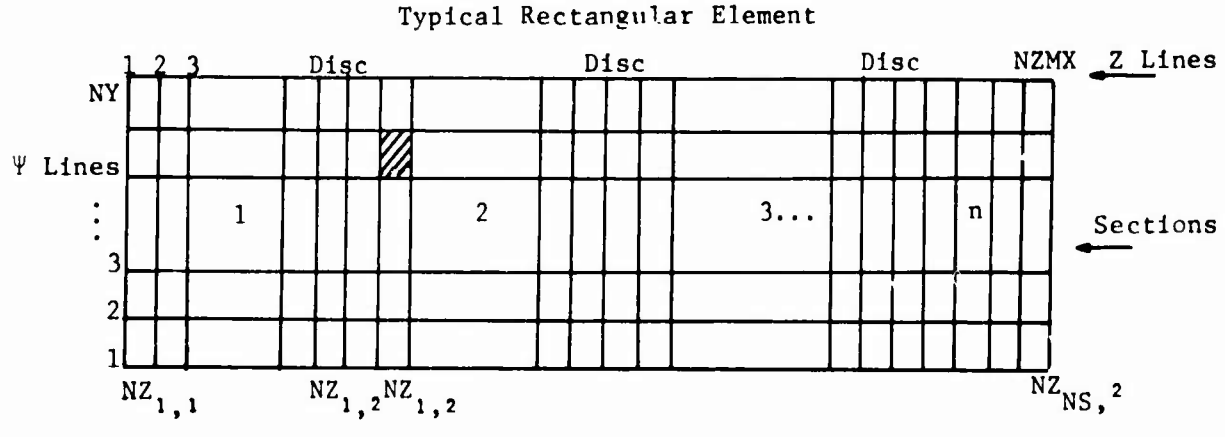

Figure 11. Idealization of Turbine Flow Problem to a Finite Element Representation in the (x,Ψ) Plane

NS:	Number of flow sections
NY:	Number of horizontal Ψ-lines
NZ(K,L):	Section delimiters in pairs, L = 1,2
NZMX:	Number of vertical x-lines
OMEGA(K):	Angular velocity introduced to each section (Ω_k)
RON(I,J):	Density at node (I,J)
T(I,K):	Section angular momentum on each Ψ-line, $T = (yV)^2 = \xi^2$
X(I,J):	Solution array of Ψ-line ordinates, (Y^i_j)
Y(I):	Stream function values, Ψ_i
Z(J):	x-grid abscissas, x_j

Input Preparation. The input scheme is described sequentially by card type. Numbers in parentheses following each listed number indicate the number of cards of this type required. Variables are listed within each card type in order, and correspond to the column fields as sequenced.

(a) Card Type 1 (1)

Cols:	1-5, 6-10, 11-15, 16-20
Format:	4I5
Variables:	NY, NZMX, NS, NF
Description:	NY - Number of Ψ-lines NZMX - Number of x-lines NS - Number of sections NF - Flag: 0 = enclosed, 1 = free exit
Comments:	Use NF = 0 for this program version.

(b) Card Type 2 (NZMX)

Cols:	1-5, 6-15, 16-25, 26-35
Format:	I5, 3F10.5
Variables:	J, Z(J), F(J), G(J)
Description:	J - Vertical grid-line z-index Z(J) - Z-abscissa F(J) - Hub-surface boundary G(J) - Tip-surface boundary
Comments:	Repeat each card to end of z-lines; J = 1, NZMX

(c) Card Type 3 ([NS/3] + 1)

Cols:	1-10, 11-20, 21-30, 31-40, 41-50, 51-60
Format:	3(2F10.5)
Variables:	NZ(L,K)
Description:	NZ(L,K) - Flow section delimiters in pairs, L = 1,2
Comments:	Set up in sequence with 3 sections per card till end of sections, e.g., the first card will have in order: NZ(1,1), NZ(2,1); NZ(1,2), NZ(2,2); NZ(1,3), NZ(2,3).

(d) Card Type 4 (1)

Cols:	1-2
Format:	I2
Variables:	IFLAG
Description:	IFlag (= 1 implies read card types 6b and 7) (≠ 1 implies read card type 6a only)
Comments:	IFlag determines mode of prescribed enthalpy and momentum within sections.

(e) Card Type 5 (1)

Cols:	1-10
Format:	F10.5
Variables:	AMD
Description:	AMD - Incident Mach number for upstream.

(f) Card Type 6a (NS)

Cols:	1-10, 11-20, 21-30
Format:	3F10.5
Variables:	ALFA(K), BETA(K), OMEGA(K)
Description:	Momentum (rv) = -ALFA(K)*Ψ + BETA(K) ALFA(K) -- Swirl component BETA(K) - Translation component OMEGA(K) - Angular velocity
Comments:	Linear fit to momentum introduced by disc at section entrance. Repeat each card to end of sections K = 1, NS. Repeat sequential sets for parametric studies (see Recommendations).

(g) Card Type 6b ([NS/8] + 1)

Cols:	1-10, 11-20, 21-30, 31-40, 41-50, 51-60, 61-70, 71-80
Format:	8F10.5
Variables:	OMEGA(K)
Description:	OMEGA(K) - Angular velocity introduced to each flow section
Comments:	Repeat to end of sections.

(h) Card Type 7 ([NS*NY/8])

Cols:	1-10, 11-20, 21-30, 31-40, 41-50, 51-60, 61-70, 71-80
Format:	8F10.5
Variables:	T(I,K)
Description:	T(I,K) - Angular momentum (rv) at Ψ-line I for section K
Comments:	Repeat each card to end of sections, K = 1, NS in sequential order by streamlines I = 1, NY. Repeat sets 6b and 7 for parametric studies (see Recommendations).

Recommendations. Multiple data sets can be processed and are to be separated by END-OF-RECORD cards (7-8-9 multipunch in column 1). Parametric studies for varied section angular velocities and momenta can be run within each full data set by duplicating card types 6 and 7. Also, the incompressible flow calculation is available as a default, by setting MNMAX = 0 as the iteration limit for density calculations.

Restrictions. Arrays currently are dimensioned in the main program TCOMFLO to accommodate at most: 15 streamlines, 42 z-lines, 3 sections. Note that NR is set to 630, the current row dimension of C(M,N). The corresponding dimension statements can be altered readily. Subprograms are variably dimensioned and require no adjustment. Array usage is:

NZ(2, ≥ NS), F(≥ NZMX), G(≥ NZMX), H(NY, ≥ NS), T(NY, ≥ NS),
X(NY, ≥ NZMX), Y(≥ NY), Z(≥ NZMX), C(NR, ≥ NY + 2), E(≥ NODE),
ALFA(≥ NS), BETA(≥ NS), OMEGA(≥ NS), RON(NY, ≥ NZMX)

To change the array dimensions the relevant source cards are: cards 2, 3, 4 and 12 in program TCOMFLO. The iterations are controled by the following variables set in RSOLVE:

IDEN = 10	;	the maximum number of coupled cycles allowed
MNMAX = 5	;	the maximum number of Newton iterations for density at each grid point
ITMX = 1	;	the maximum number of position iterations of the finite element system
ETOL = 10^{-5}	;	error-bound tolerance for iterate convergence
DX = 10^{-6}	;	difference increment for jacobian derivative

Convergence is accepted if the infinity norm of $\underset{\sim}{E}$ is less than ETOL. If more than IDEN cycles are necessary the program terminates with a message, and prints: the current contents of the streamline position solution, the last position adjustment, and the velocity components at each node.

Diagnostics. The following diagnostic comments may appear during program execution:

"IMPROPER ARRAY SIZE FOR EXECUTION" -- accompanied by the input NR, NS, NY, NZMX, NODE values. This is triggered by either incorrect data (prescribing NR) or the need to redimension arrays in the program to accommodate a "larger" problem. The program terminates after printing the diagnostic.

"SOLUTION DID NOT CONVERGE" -- the maximum number of full cycles was completed and $||\underset{\sim}{E}||_\infty$ had not yet decreased to the prescribed tolerance ETOL. The control returns to the calling program, whereupon the velocity field is calculated and printed.

"ENCOUNTERED MERIDIONAL MACH NUMBER IN EXCESS OF UNITY" -- printed from subroutine MERMACH, this indicates that the current position and density is predicting a supersonic meridional Mach number. For physically realistic problems this is corrected in later cycles by density and position adjustment. Computation continues to complete the analysis. Physically ill-posed problems will lead to an arithmetic error in the band-solver, caused by divergence of the solution.

"DENSITY ADJUSTED TO STABILIZE COUPLED PROBLEM" -- this occurs when the position guess is so poor that locally the Newton iteration for density fails. A physical argument resets the density to an approximate estimate and calculation proceeds.

Subprograms and Calling Sequences.

GUESS: Call GUESS (X,F,G,NZMX,NY,Y,XT,XH,YT,YH) [also call COORD (X,F,G,NZMX,NY,Y,XT,XH,YT,YH) as a second entry point]. GUESS determines the Ψ-line distribution and the starting streamfield pattern.

RSOLVE: Call RSOLVE (NF,NR,NS,NY,NZ,C,E,F,G,H,T,PE,X,Y,Z, RON). RSOLVE solves for density and position adjustments as an iterative cycle.

MERMACH: Call MERMACH (NS,NR,NZ,H,T,NY,X,Y,RON,Z,NDEN). MERMACH calculates the meridional Mach number at each node in the idealization.

BANSOL: Call BANSOL (NBAN,NODE,NR,C,E). BANSOL solves the symmetric positive-definite jacobian system for each position adjustment, using a banded Cholesky decomposition and substitution sweeps.

Machine Requirements. The program has been developed on the CDC 6400 computer at the University of Washington. It is coded completely in FORTRAN with no machine-dependent instructions, and so can be adapted to alternate hardware. With current array dimensions the program requires 42,000 octal central memory storage locations and takes approximately 90 seconds CDC 6400 central processor time for solution at the maximum array size allowed. A detailed breakdown of timing for sample calculations follows.

Timing. Timing profiles for a sample problem with coarse and fine mesh idealizations are shown in Figs 12 and 13. The calculation is broken down to its main components -- the density iteration (D), jacobian calculation (J), bandsolver (B), position adjustment (P), and total coupled iteration (T). The graphs indicate that the density iteration is quite inexpensive and confirm the earlier reasoning in formulating the coupled process.

Output. An echo-check of the input data is displayed; the density, position, and error arrays are printed during each cycle together with the peak meridional Mach number on each Ψ-line and in each section. Finally, the position, stream function, axial velocity and tangential velocity are printed by Ψ-line beginning at the hub and for each x-line segment.

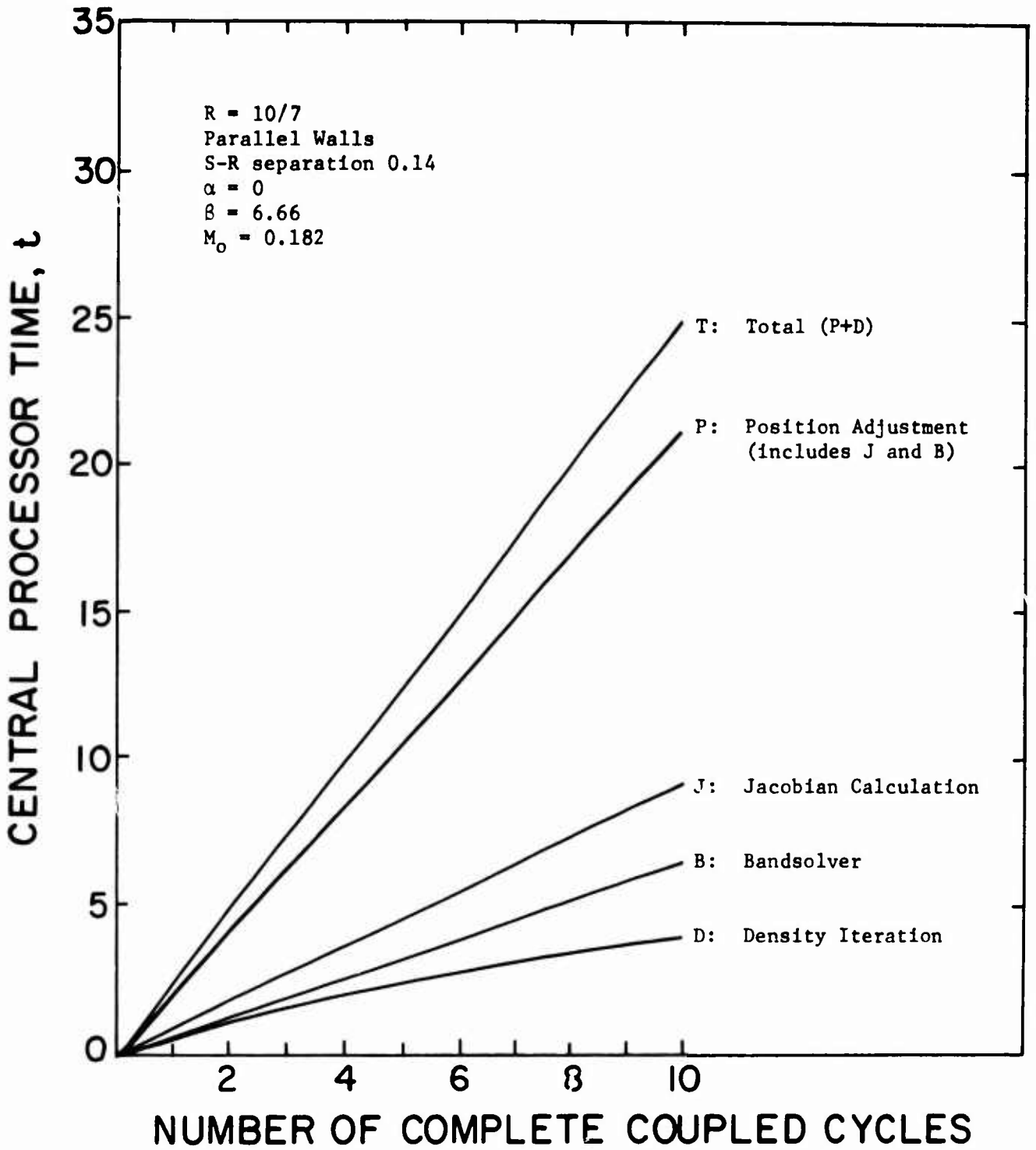

Figure 12. Timing in Central Processor Seconds for Coarse Mesh (8 x 24) Calculation

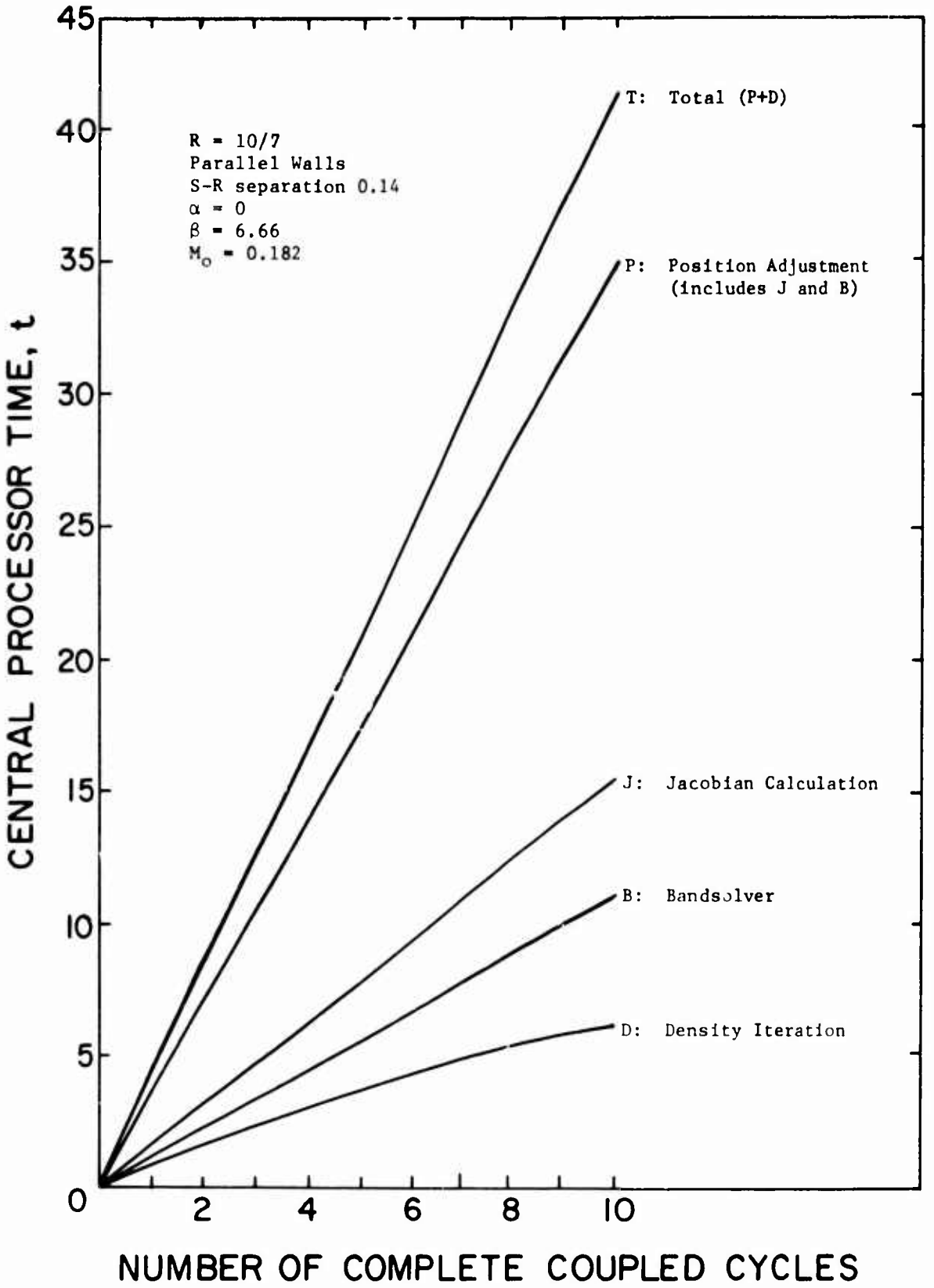

Figure 13. Timing in Central Processor Seconds for Fine Mesh (8 x 42) Calculation

Deck Structure for Compile and Execute from Source Code.

```
JOB CARD
RUN(S)                          (Compile)           Job Control
LGO                             (Load and execute)  Record
END-OF-RECORD CARD

PROGRAM CODE                                        Source Deck
END-OF-RECORD CARD
   1st Data Set
END OF RECORD CARD

FINAL DATA SET
END-OF-RECORD CARD
END-OF-FILE CARD
```

Sample Problem. A simple throughflow example with single stage and varying tip surface is identified in three sections in Fig 14. The corresponding finite element idealization in the (x,Ψ) plane is given in Fig 15.

Input.

```
  8      24    3     0
  1    -9.42        1.0          3.0
  2    -7.04        1.0          3.0
  3    -5.13        1.0          3.0
  4    -3.60        1.0          3.0
  5    -2.38        1.0          3.0
  6    -1.41        1.0          3.0
  7    -0.63        1.0          3.0017
  8    -0.0         1.0          3.0085
  9     0.5         1.0          3.0172
 10     1.0         1.0          3.0283
 11     1.5         1.0          3.0410
 12     2.0         1.0          3.0546
 13     2.5         1.0          3.0681
 14     3.0         1.0          3.0808
 15     3.5         1.0          3.0919
 16     4.0         1.0          3.1006
 17     4.63        1.0          3.1074
 18     5.41        1.0          3.1086
 19     6.38        1.0          3.1086
 20     7.60        1.0          3.1086
 21     9.13        1.0          3.1086
 22    11.04        1.0          3.1086
 23    13.42        1.0          3.1086
 24    16.40        1.0          3.1086
         1          8            9              16          17          23
22
  .2
 .          0.          0.
.0          2.          0.
.0          0.          0.
```

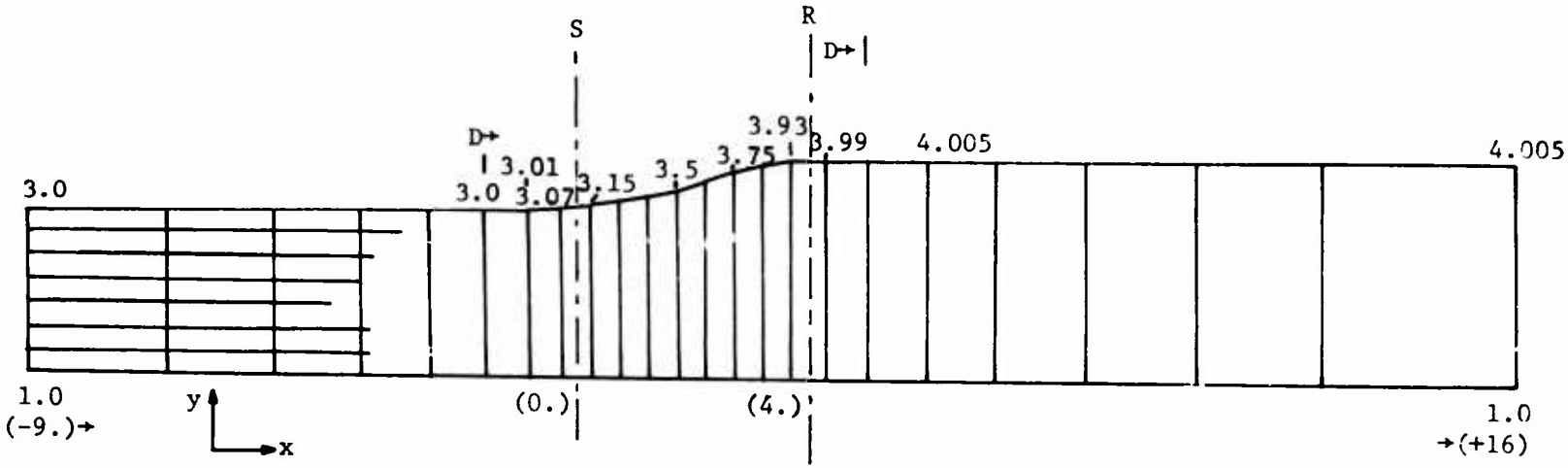

Figure 14. Flow Field in (x,y) Plane with Single Stage S-R within Diffusing Region D-D

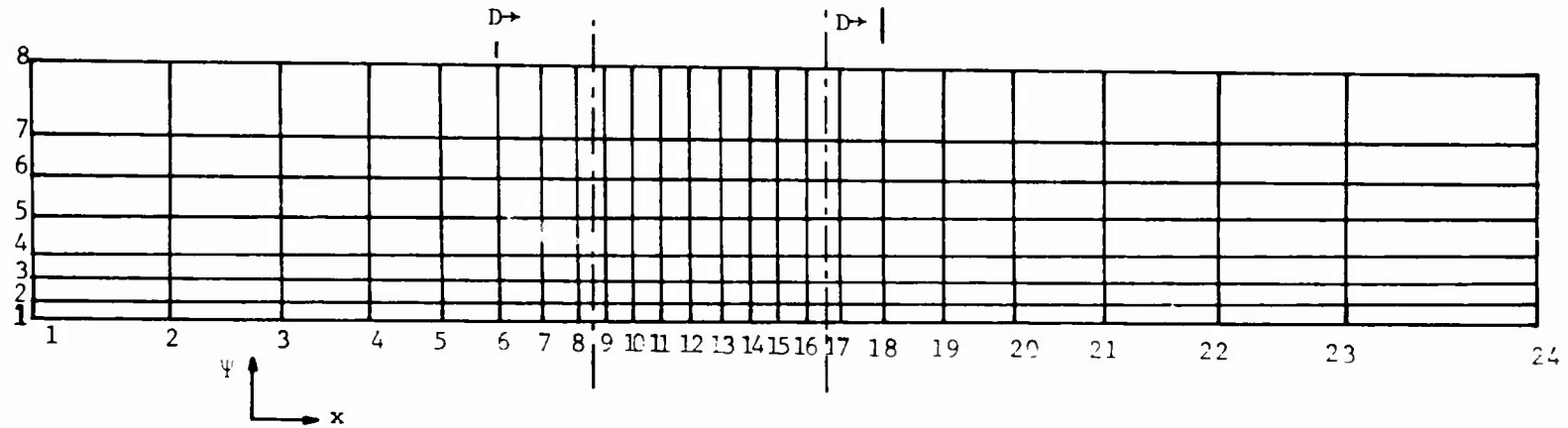

Figure 15. Idealization as Rectangular Finite Elements in the (x,Ψ) Plane

```
RUN  VERSION FEB 74     16:47 06/24/74

                SUBROUTINE RSOLVE(NF,NR,NS,NY,NZ,C,E,F,G,H,T,PE,X,Y,Z,RON)
          C
          C     SOLVES A NONLINEAR SET OF FINITE ELEMENT EQUATIONS GIVING
          C     A THROUGHFLOW MODEL OF AN ANNULAR TURBOMACHINE INCLUDING
          C     VARIABLE WALL GEOMETRY AND THE POSSIBILITY OF A NEARBY EXIT
          C     WITH FREE-STREAMLINES. THE TREATMENT IS BASED ON RADIUS(X)
          C     AS A FUNCTION OF PSI(Y) AND AXIAL-POSITION(Z). THE MACHINE
          C     IS DIVIDED INTO NS SEGMENTS OF CONTINUOUS FLOW WITH NS-1
          C     ACTUATOR DISCS BETWEEN INTERNAL DIVISIONS. NY PSI-LINES
          C     ARE IN EACH SEGMENT, AND NZ(JE,JS) DEFINES THE END Z-DIVI-
          C     SION NUMBERS. WHERE SPECIFIED, THE INNER WALL SHAPE IS
          C     GIVEN BY F(J) AND THE OUTER WALL BY G(J).
          C     NF=0    EXIT FAR DOWNSTREAM (NO FREE-STREAMLINES)
          C     NF=1    LAST SEGMENT IS FREE (F AND G TO BE DETERMINED)
          C     H(I,JS) AND T(I,JS) DEFINE THE STAGNATION ENTHALPY AND
          C     TANGENTIAL VELOCITY FUNCTIONS IN THE INTERVAL Y(I),Y(I+1)
          C     FOR EACH SEGMENT (JS=1,...,NS). PE DEFINES THE EXTERNAL
          C     CONDITIONS ON THE FREE-STREAMLINES. IT NEED NOT BE SPECI-
          C     FIED IF NF=0 ... PE=0 IS THEN AUTOMATICALLY SET.
          C     NR IS THE ROW DIMENSION OF THE MATRIX C(K,L) AS SET IN
          C     THE MAIN PROGRAM. C IS USED FOR COMPACT STORAGE OF THE
          C     BANDED, SYMMETRIC JACOBIAN MATRIX USED IN SOLVING THE NON-
          C     LINEAR SYSTEM BY NEWTON-RAPHSON ITERATION. THE ERROR RESI-
          C     DUALS ARE STORED IN E(K) BY PSI-LINE.
          C     VERSION .... FINITE DIFFERENCE JACOBIAN EVALUATION
          C
    23            DIMENSION NZ(2,1),F(1),G(1),H(NY,1),T(NY,1)
    23            DIMENSION X(1),Y(1),Z(1),C(NR,1),E(1)
    23            DIMENSION RON(NY,1)
    23            DIMENSION V(4)
    23            LOGICAL NTST
    23            REAL MMN
          C
          C     ELEMENT-CHARACTERISTIC FUNCTION (MEAN-VALUE APPROXIMATION)
    23            D(R1,R2,R3,R4) = DZ*( 2*(FF-FN)*R4-0.5*TT*(1/R3+R3/(R4*R4))
               *  +DY*DY*( (R4-R2)*(1/(R4*(R4-R3))+1/(R2*(R2-R1)))/(DZ*DZ)
               *           -0.5*( (1+((R4-R2)/DZ)**2)*(2*R4-R3)/(R4*R4)
               *+(1+((R3-R1)/DZ)**2)/R3)/(R4-R3)**2)/RN2)*RN
          C
    112           NY1=NY-1     $ NZMX=NZ(2,NS)+1
    116           NBAN=NY+2    $ NODE=NY*NZMX
    121           ITMX=1  $  ETOL=1.E-6  $  DX=1.E-5  $  IDEN=10
    126           GAM=1.4
    130           RF=1.0
    131           NPRT=5
    132           MNMAX=5
    133           ITMX=1
    134           NPSS=2
    135           IDEN=10
    136           IP=ITMX-1
    140           IF(NF.EQ.0) PE=0.
    142           IF(NR.GE.NODE) GO TO 1
    144           WRITE(6,201) NR,NS,NY,NZMX,NODE
    162           CALL EXIT
    163         1 CONTINUE



RSOLVE
```

```
RUN  VERSION FEB 74      16:47 06/24/74

        C
        C  STARTING GUESS IS INCROPRESSIBLE FLOW
   163          DO 50 I=1,NY
   170          DO 50 J=1,NZMX
   171       50 RON(I,J)=1.0
   204          DO 26 NDEN=1,IDEN
   205            CALL MERMACH(NS,NR,NZ,H,T,NY,X,Y,RON,Z,NDEN)
   221          DO 25 JS=1,NS
   226          J1=NZ(1,JS)   $J2=NZ(2,JS)
   232          DO 24 I=1,NY
   234          ITEST=0
   235          IF(I.NE.NY)GO TO 1000
   236          I=I-1
   240          ITEST=1
   241     1000 HH=H(I,JS)
   246          TT=T(I,JS)
   252           DY=Y(I+1)-Y(I)
   255          H0=H(I,1)-0.5
   262          DO 23 J=J1,J2
   264          DZ=Z(J+1)-Z(J)
   270          IF(I.EQ.NY)I=I-1
   273          JNYI=J*NY+I
   275          K1=JNYI-NY   $  K2=K1+1   $ K3=JNYI   $K4=K3+1
   302          X1=X(K1)    $  X2=X(K2)    $  X3=X(K3)   $    X4=X(K4)
   314          T1=(1+((X4-X2)/DZ)**2)/(X4*(X4-X3))**2
   324          T2=(1+((X4-X2)/DZ)**2)/(X2*(X2-X1))**2
   333          T3=(1+((X3-X1)/DZ)**2)/(X3*(X4-X3))**2
   343          T4=(1+((X3-X1)/DZ)**2)/(X1*(X2-X1))**2
   353          TS=(T1+T2+T3+T4)*DY**2/4.0
   361          IF(ITEST.NE.1)GO TO 1001
   363          I=NY
   364          X1=X2
   365     1001  CONTINUE
   365          KR=0
   366          QT=1.0
   370          DO 21 MNIT=1,MNMAX
   371          QTP=ABS(QT)
   373          EPSM=RON(I,J)
   400          A1=(2.*HH-TT/X1**2)*RON(I,J)**2
   412           A2=2.*H0*RON(I,J)**(GAM+1.)
   424          A3=A2*(GAM+1.)
   427          QT=(A1-A2-TS)/(2.*A1-A3)
   434          QT=QT*RF
   436          IF(QTP.LT.ABS(QT))GO TO 211
   441          RON(I,J)=RON(I,J)*(1.-QT)
   447          IF(ABS(EPSM-RON(I,J)).LE.ETOL)GO TO 22
   457       21 CONTINUE
   461          GO TO 212
   462      211 TVAR=(1.0+TT/(X1**2))/2.0
   467          RON(I,J)=SQRT(((HH-TVAR)/H0)**5)
   505          RPM=RON(I,J)
   510          WRITE(6,204)I,J,RPM
   522      204 FORMAT(5X,*DENSITY ADJUSTED TO STABILIZE COUPLED PROBLEM*,5X,
               1*I=*,I2,*J=*,I2,*DENSITY SET*,E12.4)
   522      212 CONTINUE
   522       22 CONTINUE



RSOLVE
```

```
RUN  VERSION FEB 74     16:47 06/24/74

   522       23 CONTINUE
   530          IF(JS.EQ.NS)RON(I,NZMX)=RON(I,J2)
   541       24 CONTINUE
   544       25 CONTINUE
   546            CALL MERNACH(NS,NR,NZ,H,T,NY,X,Y,RON,Z,NDEN)
         C        ************************************
         C        BEGIN THE NEWTON-RAPHSON ITERATION   *
         C        ************************************
         C
   562            DO 20 IT=1,ITMX
         C
         C        EVALUATE THE RESIDUAL VECTOR ...
   567            DO 2 K=1,NODE
   570         2 E(K)=0.
         C             SUM THE ELEMENT CONTRIBUTIONS TO RESIDUALS
   575            DO 5 JS=1,NS
   576            J1=NZ(1,JS) $ J2=NZ(2,JS)
   602            DO 4 I=1,NY1
   604            DY=Y(I+1)-Y(I)
   610            HH=H(I,JS)
   614            TT=T(I,JS)
   620            DO 3 J=J1,J2
   622            DZ=Z(J+1)-Z(J)                $ JNYI=J*NY+I
   630            K1=JNYI-NY   $ K2=K1+1        $ K3=JNYI       $ K4=K3+1
   635            X1=X(K1)     $ X2=X(K2)       $ X3=X(K3)      $ X4=X(K4)
   647            T1=(1+((X4-X2)/DZ)**2)/(X4*(X4-X3))**2
   657            T2=(1+((X4-X2)/DZ)**2)/(X2*(X2-X1))**2
   666            T3=(1+((X3-X1)/DZ)**2)/(X3*(X4-X3))**2
   676            T4=(1+((X3-X1)/DZ)**2)/(X1*(X2-X1))**2
   706            TS=(T1+T2+T3+T4)*DY**2/4.0
   714            RN=(RON(I,J)+RON(I,J+1)+RON(I+1,J)+RON(I+1,J+1))/4.0
   736            IF(J.EQ.J2)RN=(RON(I,J)+RON(I+1,J))/2.0
   747            RN2=RN**2
   751            TS=TS/RN2
   752            SS=(1.0/X1**2+1.0/X2**2+1.0/X3**2+1.0/X4**2)/4.0
   764            FF=(GAM-1.0)*HH/GAM+(TS+TT*SS)/(2.0*GAM)
   776            PN=PE/RN
  1000            E(K1)=E(K1)-D(X4,X3,X2,X1)
  1012            E(K2)=E(K2)+D(X3,X4,X1,X2)
  1024            E(K3)=E(K3)-D(X2,X1,X4,X3)
  1036            E(K4)=E(K4)+D(X1,X2,X3,X4)
  1050         3 CONTINUE
  1052         4 CONTINUE
  1055         5 CONTINUE
         C             MODIFY RESIDUALS AT SPECIFIED WALL NODES
  1057            IF(NF.EQ.0) J2=NZMX
  1061            IF(NF.EQ.1) J2=NZ(1,NS)
  1065            DO 6 J=1,J2
  1067            JU=J*NY      $ JL=JU-NY+1
  1072            E(JU)=X(JU)-G(J)
  1100            E(JL)=X(JL)-F(J)
  1106         6 CONTINUE
         C
         C        RESIDUAL NORM AND CHECK FOR CONVERGENCE ...
  1110            EMAX=0.
  1111            DO 7 K=1,NODE



RSOLVE
```

```
RUN  VERSION FEB 74     16:47 06/24/74

  1112        7 EMAX=AMAX1(EMAX,ABS(E(K)))
  1123          IF(MOD(NDEN,NPRT).NE.0)GO TO 777
  1126          WRITE(6,299)
  1132      299 FORMAT(1H1)
  1132          WRITE(6,300)NDEN
  1140      300 FORMAT(3(/),5X,*ITERATION*,I3,5X,*SOLUTION AND ERROR RESIDUAL*)
  1140          WRITE(6,301)(X(K),K=1,NODE)
  1162          WRITE(6,301)(E(K),K=1,NODE)
  1204      301 FORMAT(/,(5X,8E11.3))
  1204      777 CONTINUE
  1204          IF(EMAX.LE.ETOL)GO TO 31
        C
        C     EVALUATE THE JACOBIAN ELEMENTS NUMERICALLY ...
  1212          DO 9 K=1,NODE
  1214          DO 8 L=1,NBAN
  1215        8 C(K,L)=0.
  1224        9 CONTINUE
        C           SUM THE ELEMENT CONTRIBUTIONS TO JACOBIAN
  1227          DO 12 JS=1,NS
  1230          J1=NZ(1,JS) $ J2=NZ(2,JS)
  1234          DO 11 I=1,NY1
  1236          DY=Y(I+1)-Y(I)
  1242          HH=H(I,JS)
  1246          TT=T(I,JS)
  1252          DO 10 J=J1,J2
  1254          DZ=Z(J+1)-Z(J)                  $ JNYI=J*NY+I
  1262          K1=JNYI-NY   $ K2=K1+1          $ K3=JNYI       $ K4=K3+1
  1267          X1=X(K1)     $ X2=X(K2)         $ X3=X(K3)      $ X4=X(K4)
  1301          T1=(1+((X4-X2)/DZ)**2)/(X4*(X4-X3))**2
  1311          T2=(1+((X4-X2)/DZ)**2)/(X2*(X2-X1))**2
  1320          T3=(1+((X3-X1)/DZ)**2)/(X3*(X4-X3))**2
  1330          T4=(1+((X3-X1)/DZ)**2)/(X1*(X2-X1))**2
  1340          TS=(T1+T2+T3+T4)*DY**2/4.0
  1346          RN=(RON(I,J)+RON(I,J+1)+RON(I+1,J)+RON(I+1,J+1))/4.0
  1370          IF(J.EQ.J2)RN=(RON(I,J)+RON(I+1,J))/2.0
  1401          RN2=RN**2
  1403          TS=TS/RN2
  1404          SS=(1.0/X1**2+1.0/X2**2+1.0/X3**2+1.0/X4**2)/4.0
  1416          PE=(GAM-1.0)*HH/GAM+(TS+TT+SS)/(2.0*GAM)
  1430          PN=PE/RN
  1432          D10=D(X4,X3,X2,X1)              $ D20=D(X3,X4,X1,X2)
  1450          D30=D(X2,X1,X4,X3)              $ D40=D(X1,X2,X3,X4)
  1466          C(K1,1)=C(K1,1)-(D(X4,X3,X2,X1+DX)-D10)/DX
  1504          C(K1,2)=C(K1,2)-(D(X4,X3,X2+DX,X1)-D10)/DX
  1522          C(K1,NY+1)=C(K1,NY+1)-(D(X4,X3+DX,X2,X1)-D10)/DX
  1542          C(K1,NY+2)=C(K1,NY+2)-(D(X4+DX,X3,X2,X1)-D10)/DX
  1561          C(K2,1)=C(K2,1)+(D(X3,X4,X1,X2+DX)-D20)/DX
  1576          C(K2,NY)=C(K2,NY)+(D(X3+DX,X4,X1,X2)-D20)/DX
  1614          C(K2,NY+1)=C(K2,NY+1)+(D(X3,X4+DX,X1,X2)-D20)/DX
  1633          C(K3,1)=C(K3,1)-(D(X2,X1,X4,X3+DX)-D30)/DX
  1650          C(K3,2)=C(K3,2)-(D(X2,X1,X4+DX,X3)-D30)/DX
  1666          C(K4,1)=C(K4,1)+(D(X1,X2,X3,X4+DX)-D40)/DX
  1704       10 CONTINUE
  1707       11 CONTINUE
  1711       12 CONTINUE
        C           MODIFY JACOBIAN AT SPECIFIED WALL NODES


RSOLVE
```

```
RUN  VERSION FEB 74     16:47 06/24/74

 1714          IF(NF.EQ.0) J2=NZMX
 1716          IF(NF.EQ.1) J2=NZ(J,NS)
 1722          DO 14 J=1,J2
 1724          JU=J*NY      $ JL=JU-NY+1
 1727          C(JU,1)=C(JL,1)=1.
 1737          DO 13 L=2,NBAN
 1740          C(JU,L)=C(JL,L)=0.
 1750       13 CONTINUE
 1753          C(JU-1,2)=0.
 1757          IF((NF.EQ.1).AND.(J.EQ.J2)) GO TO 14
 1766          C(JL+1,NY)=0.
 1771          C(JU-1,NY+2)=0.
 1775       14 CONTINUE
       C
       C      SOLVE THE SYMMETRIC, POSITIVE-DEFINITE JACOBIAN SYSTEM
       C      USING A BANDED-CHOLESKY DECOMPOSITION ...
 2000          CALL BANSOL(NBAN,NODE,NR,C,E)
       C
       C
       C      NEW ESTIMATE OF THE SOLUTION VECTOR ...
 2004          DXMX=0.
 2005          DO 15 K=1,NODE
 2012          X(K)=X(K)-E(K)
 2016          DXMX=AMAX1(DXMX,ABS(E(K)))
 2025       15 CONTINUE
       C
 2027       20 CONTINUE
       C
 2032       26 CONTINUE
 2034          WRITE(6,202)
 2040       31 CONTINUE
 2041          NDEN=IDEN
 2042          CALL MERMACH(NS,NR,NZ,H,T,NY,X,Y,RON,Z,NDEN)
 2061      201 FORMAT(* IMPROPER ARRAY SIZE FOR EXECUTION *,
              *       * NR,NS,NY,NZMX,NODE *,5I5)
 2061      202 FORMAT(//,15X,*SOLUTION DID NOT CONVERGE*)
       C
 2061          RETURN
 2062          END
```

RSOLVE

```
RUN  VERSION FEB 74     16:47 06/24/74

                SUBROUTINE GUESS(X,F,G,NZMX,NY,Y,XT,XH,YT,YH)
    15          DIMENSION X(NY,1),Y(1),F(1),G(1)
    15          NY1=NY-1
          C END R VALUES
          C PRESCRIBE SURFACE PSI VALUES
    17          YH=-(XH**2)/2.
    22          YT=-(XT**2)/2.
          C CALCULATE INTERMEDIATE PSI VALUES
    24          Y(1)=YH
    26          DO 10 I=1,NY1
    27          R=XH+(XT-XH)*FLOAT(I)/FLOAT(NY1)
    40       10 Y(I+1)=-0.5*R*R
    45          RETURN
    45          ENTRY COORD
    72          XD=(XT/XH)**2-1.
    76          DO 15 J=1,NZMX
   100          A1=F(J)**2
   102          A2=G(J)**2
   104          B1=A2-A1
   106          DO 15 I=1,NY
   107          X(I,J)=F(J)+(SQRT(-2.*Y(I))-XH)*(G(J)-F(J))/(XT-XH)
   137       15 CONTINUE
   143          RETURN
   143          END
```

GUESS

```
RUN  VERSION FEB 74     16847 06/24/74

                PROGRAM TCOMFLO(INPUT,OUTPUT,TAPE5=INPUT,TAPE6=OUTPUT)
     3          DIMENSION NZ(2,3),F(24),G(24),H(8,3),T(8,3)
               1,X(8,24),Y(8),Z(24),C(192,10),E(192)
               1,RON(8,24)
     3          DIMENSION ALFA(3),BETA(3),OMEGA(3)
     3       666 READ(5,101)NY,NZMX,NS,NF
    17          IF(EOF,5)1,2
    22        1 CALL EXIT
    23        2 WRITE(6,1001)NY,NZMX,NS,NF
    37          PI=3.1415927
    41          NY1=NY-1
    43          NODE=NY*NZMX
    44          NR=192
    45       101 FORMAT(4I5)
    45      1001 FORMAT(1H1,3(/),15X,*NUMBER OF STREAMLINES =*,I2,
               1                /,15X,*NUMBER OF GRID SEGMTS =*,I2,
               1                /,15X,*NUMBER OF FLOW SECTNS =*,I2,
               1                /,15X,*0=ENCLOSED, 1=FREE EXIT*,I2)
    45          READ(5,102)(J,Z(J),F(J),G(J),J=1,NZMX)
    65       102 FORMAT(I5,3F10.5)
    65          WRITE(6,1002)(J,Z(J),F(J),G(J),J=1,NZMX)
   105       1002 FORMAT(2(/),5X,*SEGMENT*,5X,*ORDINATE*,5X,*HUB SURFACE*,5X,*TIP SU
               1RFACE*,      /,(5X,I4,6X,F10.5,5X,F10.5,5X,F10.5))
   105           READ(5,107) (NZ(1,J),NZ(2,J),J=1,NS)
   125       107   FORMAT(3(2I10))
   125           WRITE(6,1007)((NZ(I,J),I=1,2),J=1,NS)
   144       1007   FORMAT(3(/),5X,*SECTION DELIMITERS*,/,(3X,2I10))
             C PRESCRIBE SURFACE PSI VALUES
   144           XH=F(1)
   146            XT=G(1)
   147           YH=-0.5*XH**2
   152           YT=-0.5*XT**2
             C CALCULATE INTERMEDIATE PSI VALUES
             C SET HUB AND TIP COORDINATES
             C  SET PSI LINE VALUES
   153           CALL GUESS(X,F,G,NZMX,NY,Y,XT,XH,YT,YH)
             C ENTHALPY AND ANG MOM TERMS
   165           READ(5,103)IFLAG
   173        103 FORMAT(I2)
   173           READ(5,1041)HCONS
   201       1041 FORMAT(F10.5)
   201           WRITE(6,1042)HCONS
   207       1042 FORMAT(//,5X,*INCIDENT MACH NO. *,F5.2)
   207           HCONS=(5.0/(2.0*HCONS**2))*(1.0+0.2*HCONS**2)
   216        777 IF(IFLAG.EQ.1)GO TO 888
   220           READ(5,104)(ALFA(J),BETA(J),OMEGA(J),J=1,NS)
   237        104 FORMAT(3F10.5)
   237           IF(EOF,5)3,4
   242          3 GO TO 666
   243          4 WRITE(6,1003)(J,ALFA(J),BETA(J),OMEGA(J),J=1,NS)
   263       1003 FORMAT(3(/),5X,*SECTION*,5X,*ALFA-COEF*,5X,*BETA-COEF*,5X,
               1*OMEGA    *,/,(5X,I5,3(5X,F10.5)))
             C STARTING GUESS IN X
   263           CALL COORD(X,F,G,NZMX,NY,Y,XT,XH,YT,YH)
   275           DO 35 I=1,NY1


TCOMFLO
```

```
RUN  VERSION FEB 74     16:47 06/24/74

   277          H(I,1)=HCONS
   301           T(I,1) = 0.0
   302          DO 35 J=2,NS
   304          T(I,J)=(0.5*ALFA(J)*(Y(I+1)+Y(I))-BETA(J))**2
   314          DRV = SQRT(T(I,J))-SQRT(T(I,J-1))
   326    35    H(I,J) = H(I,J-1) + OMEGA(J)*DRV
   341          GO TO 41
   341     888 READ(5,105)(OMEGA(J),J=1,NS)
   354          IF(EOF,5)6,7
   357     105 FORMAT(8F10.5)
   357       6 GO TO 666
   360       7 READ(5,106)((T(I,J),I=1,NY),J=1,NS)
   377     106 FORMAT(8F10.5)
   377          WRITE(6,1006)(J,OMEGA(J),(T(I,J),I=1,NY),J=1,NS)
   422    1006 FORMAT(3(/),5X,*SECTION*,5X,*ANG.VEL.*,5X,*MOMENTUM*,/,
               1(5X,I4,3X,F10.5,3X,F10.5))
   422          DO 36 I=1,NY1
   424          H(I,1)=HCONS
   426           DO 36 J = 2,NS
   427          DRV = SQRT(T(I,J))-SQRT(T(I,J-1))
   441    36    H(I,J) = H(I,J-1) + OMEGA(J)*DRV
   453       41 CALL SECOND(T1)
   455          CALL RSOLVE(NF,NP,NS,NY,NZ,C,E,F,G,H,T,PE,X,Y,Z,FON)
   475          CALL SECOND(T2)
   477          WRITE(6,203)
   503    203   FORMAT(1H1,5(/),23X,*SOLUTION POINTWISE BY VERTICAL SECTIONS*)
   503          DO 40 J=1,NZMX
   505          WRITE(6,201)J,Z(J)
   514          WRITE(6,205)
   520    205   FORMAT(/,14X,*LINE*,3X,*STREAMFUNCTION*,5X,*RADIUS*,5X,*AXIAL VELO
               1C.*,3X,*TANG. VELOC.*)
   520          DO 40 I=1,NY
   522          IF(IFLAG.EQ.1)GO TO 37
   524          DO 33 M=1,NS
   525          IF(J.NE.NZ(1,M))GO TO 33
   530          K=M
   531       33 CONTINUE
   534          V=-(ALFA(K)*Y(I)+BETA(K))/(X(I,J)/XH)
   544          GO TO 371
   545       37 V=-SQRT(T(I,K))
   552      371 IF(I.NE.NY)GO TO 38
   554          P=Y(NY)-Y(NY-1)
   556          Q=Y(NY)-Y(NY-2)
   560          DE=P*Q*(P-Q)
   563          A1=P**2
   564          A2=Q**2
   565          A3=A1-A2
   567          F1=X(NY-2,J)**2
   572          F2=X(NY-1,J)**2
   574          F3=X(NY,J)**2
   576          W=-2.*DE/(-A1*F1+A2*F2+A3*F3)
   605          W=W/RON(I,J)
   611          GO TO 39
   611       38 CONTINUE
   611          W=-2.*(Y(I+1)-Y(I))/(X(I+1,J)**2-X(I,J)**2)
   623          W=W/RON(I,J)



TCOMFLO
```

```
RUN  VERSION FEB 74      16:47 06/24/74

   626       39 WRITE(6,202)I,Y(I),X(I,J),W,V
   646       40 CONTINUE
   653      201 FORMAT(//,2X,*SEGMENT*,I3,5X,*ORDINATE Z(J)*,E12.4)
   653    202   FORMAT(13X,I5,5X,E12.4,4X,E12.4,2X,E12.4,3X,E12.4)
   653          TIM=T2-T1
   655          WRITE(6,204)TIM
   663      204 FORMAT(3(/),5X,*SOLN. TIME*,F7.3,*  C.P. SECONDS*)
   663          GO TO 777
   664          END
```

TCOMFLO

```
RUN  VERSION FEB 74      16:47 06/24/74

                SUBROUTINE MERMACH(NS,NR,NZ,H,T,NY,X,Y,RON,Z,NDEN)
     16         DIMENSION NZ(2,1),H(NY,1),T(NY,1),X(1),Y(1),Z(1),RON(NY,1)
     16         DIMENSION VP(8,42)
     16         REAL MMN,MEM
           C  MERIDIONAL MACH NUMBER CALCULATION BEGINS
     16         NY1=NY-1
     20         DO 40 JS=1,NS
     21         J1=NZ(1,JS) $J2=NZ(2,JS)
     25         DO 40 I=1,NY1
     27         HH=H(I,JS)
     33         TT=T(I,JS)
     36         K=0   $  L=0
     40         VMMN=0.0
     41         DO 39 J=J1,J2
     43         JNYI=J*NY+I
     45         K1=JNYI-NY $K2=K1+1 $ K3=JNYI  $K4=K3+1
     53         X1=X(K1)  $X2=X(K2)  $X3=X(K3)  $X4=X(K4)
     65         V=SQRT(TT)/X1
     71         W=-2.*(Y(I+1)-Y(I))/(X2**2-X1**2)
    105         W=W/RON(I,J)
    112         U=-W*(X3-X1)/(Z(J+1)-Z(J))
    121         U=U**2
    122         W=W**2
    122         V=V**2
    123         TOT=U+V+W
    126         MMN=2.5*(U+W)/(HH-0.5*TOT)
    134         VP(I,J)=MMN
    136         MMN=ABS(MMN)
    140         IF(VMMN.GE.MMN)GO TO 38
    142         K=I   $  L=J
    145         VMMN=MMN
    145      38 CONTINUE
    145         IF(MMN.LE.1.)GO TO 39
    150         MEM=SQRT(MMN)
    152         WRITE(6,102)I,J,MEM
    163     102 FORMAT(5X,*ENCOUNTERED MERIDIONAL MACH NUMBER IN EXCESS OF UNITY*,
                15X,*I=*,I2,*J=*,I2,*MER. MACH NO. =*,F5.2)
    163      39 CONTINUE
    171      40 CONTINUE
           C  MERIDIONAL MACH NUMBER CALCULATION ENDS
    176         RETURN
    176         END
```

```
RUN  VERSION FEB 74     16:47 06/24/74

                SUBROUTINE BANSOL(M,N,NR,A,B)
      C
      C     SOLVES A BANDED, SYMMETRIC, POSITIVE-DEFINITE SYSTEM OF
      C     N LINEAR EQUATIONS USING PACKED STORAGE AND A CHOLESKY
      C     DECOMPOSITION FOLLOWED BY FORWARD AND BACK SUBSTITUTION.
      C     NR IS THE ROW DIMENSION OF A(I,J) WHEN IT WAS STORED.
      C     M IS THE HALF-BAND SIZE (SUPERDIAGONAL) PLUS ONE.
      C     ON ENTRY THE SINGLE RIGHT-HAND VECTOR IS STORED IN B(I),
      C     AND B(I) CONTAINS THE SOLUTION VECTOR ON EXIT.
   10         DIMENSION A(NR,1),B(1)
      C
      C     CHOLESKY DECOMPOSITION WITH PACKED STORAGE ...
   10         DO 5 I=1,N
   11         SUM=A(I,1)
   15         KMX=MIN0(I,M)
   20         IF(KMX.LT.2) GO TO 2
   22         DO 1 K=2,KMX
   24         TMP=A(I-K+1,K)
   30       1 SUM=SUM-TMP*TMP
   35       2 A(I,1)=RA=SQRT(SUM)
   46         RA=1./RA
   50         JMX=MIN0(M,N-I+1)
   54         IF(JMX.LT.2) GO TO 5
   56         DO 4 J=2,JMX
   60         SUM=A(I,J)
   64         KMX=MIN0(I,M-J+1)
   70         IF(KMX.LT.2) GO TO 4
   72         DO 3 K=2,KMX
   74       3 SUM=SUM-A(I-K+1,K)*A(I-K+1,J+K-1)
  111       4 A(I,J)=RA*SUM
  121       5 CONTINUE
      C
      C     FORWARD AND BACK SUBSTITUTION WITH PACKED STORAGE ...
  124         DO 7 I=1,N
  125         SUM=B(I)
  127         KMX=MIN0(I,M)
  132         IF(KMX.LT.2) GO TO 7
  134         DO 6 K=2,KMX
  136       6 SUM=SUM-A(I-K+1,K)*B(I-K+1)
  147       7 B(I)=SUM/A(I,1)
  156         DO 9 II=1,N
  160         I=N-II+1
  162         SUM=B(I)
  164         KMX=MIN0(II,M)
  167         IF(KMX.LT.2) GO TO 9
  171         DO 8 K=2,KMX
  173       8 SUM=SUM-A(I,K)*B(I+K-1)
  206       9 B(I)=SUM/A(I,1)
      C
  216         RETURN
  216         END

BANSOL
```

NUMBER OF STREAMLINES = 8
NUMBER OF GRID SEGMTS =24
NUMBER OF FLOW SECTNS = 3
0=ENCLOSED, 1=FREE EXIT 0

SEGMENT	ORDINATE	HUB SURFACE	TIP SURFACE
1	-9.42000	1.00000	3.00000
2	-7.04000	1.00000	3.00000
3	-5.13000	1.00000	3.00000
4	-3.60000	1.00000	3.00000
5	-2.38000	1.00000	3.00000
6	-1.41000	1.00000	3.00000
7	-.63000	1.00000	3.00170
8	-0.00000	1.00000	3.00850
9	.50000	1.00000	3.01720
10	1.00000	1.00000	3.02830
11	1.50000	1.00000	3.04100
12	2.00000	1.00000	3.05460
13	2.50000	1.00000	3.06810
14	3.00000	1.00000	3.08080
15	3.50000	1.00000	3.09190
16	4.00000	1.00000	3.10060
17	4.63000	1.00000	3.10740
18	5.41000	1.00000	3.10860
19	6.38000	1.00000	3.10860
20	7.60000	1.00000	3.10860
21	9.13000	1.00000	3.10860
22	11.04000	1.00000	3.10860
23	13.42000	1.00000	3.10860
24	16.46000	1.00000	3.10860

SECTION DELIMITERS

1	8
9	16
17	23

INCIDENT MACH NO. .20

SECTION	ALFA-COEF	BETA-COEF	OMEGA
1	0.00000	0.00000	0.00000
2	0.00000	2.00000	0.00000
3	0.00000	0.00000	0.00000

SOLUTION POINTWISE BY VERTICAL SECTIONS

SEGMENT 1 ORDINATE Z(J) -9.4200E+00

LINE	STREAMFUNCTION	RADIUS	AXIAL VELOC.	TANG. VELOC.
1	-5.0000E-01	1.0000E+00	9.9735E-01	-0.
2	-8.2653E-01	1.2866E+00	9.9689E-01	-0.
3	-1.2347E+00	1.5726E+00	9.9982E-01	-0.
4	-1.7245E+00	1.8583E+00	1.0005E+00	-0.
5	-2.2959E+00	2.1438E+00	1.0008E+00	-0.
6	-2.9490E+00	2.4293E+00	1.0013E+00	-0.
7	-3.6837E+00	2.7146E+00	1.0013E+00	-0.
8	-4.5000E+00	3.0000E+00	1.0013E+00	-0.

SEGMENT 2 ORDINATE Z(J) -7.0400E+00

LINE	STREAMFUNCTION	RADIUS	AXIAL VELOC.	TANG. VELOC.
1	-5.0000E-01	1.0000E+00	9.9734E-01	-0.
2	-8.2653E-01	1.2866E+00	9.9888E-01	-0.
3	-1.2347E+00	1.5726E+00	9.9981E-01	-0.
4	-1.7245E+00	1.8583E+00	1.0005E+00	-0.
5	-2.2959E+00	2.1438E+00	1.0009E+00	-0.
6	-2.9490E+00	2.4293E+00	1.0013E+00	-0.
7	-3.6837E+00	2.7146E+00	1.0013E+00	-0.
8	-4.5000E+00	3.0000E+00	1.0013E+00	-0.

SEGMENT 3 ORDINATE Z(J) -5.1300E+00

LINE	STREAMFUNCTION	RADIUS	AXIAL VELOC.	TANG. VELOC.
1	-5.0000E-01	1.0000E+00	9.9735E-01	-0.
2	-8.2653E-01	1.2866E+00	9.9887E-01	-0.
3	-1.2347E+00	1.5726E+00	9.9982E-01	-0.
4	-1.7245E+00	1.8583E+00	1.0005E+00	-0.
5	-2.2959E+00	2.1438E+00	1.0008E+00	-0.
6	-2.9490E+00	2.4293E+00	1.0013E+00	-0.
7	-3.6837E+00	2.7146E+00	1.0013E+00	-0.
8	-4.5000E+00	3.0000E+00	1.0013E+00	-0.

SEGMENT 4 ORDINATE Z(J) -3.6000E+00

LINE	STREAMFUNCTION	RADIUS	AXIAL VELOC.	TANG. VELOC.
1	-5.0000E-01	1.0000E+00	9.9744E-01	-0.
2	-8.2653E-01	1.2866E+00	9.9697E-01	-0.
3	-1.2347E+00	1.5726E+00	9.9992E-01	-0.
4	-1.7245E+00	1.8582E+00	1.0006E+00	-0.
5	-2.2959E+00	2.1439E+00	1.0009E+00	-0.
6	-2.9490E+00	2.4292E+00	1.0013E+00	-0.
7	-3.6837E+00	2.7146E+00	1.0012E+00	-0.
8	-4.5000E+00	3.0000E+00	1.0011E+00	-0.

SEGMENT 5 ORDINATE Z(J) -2.3800E+00

LINE	STREAMFUNCTION	RADIUS	AXIAL VELOC.	TANG. VELOC.

3	-1.2347E+00	1.6291E+00	9.6307E-01	-1.2277E+00
4	-1.7245E+00	1.9238E+00	9.6307E-01	-1.0396E+00
5	-2.2959E+00	2.2164E+00	9.6137E-01	-9.0234E-01
6	-2.9495E+00	2.5082E+00	9.5983E-01	-7.9737E-01
7	-3.6837E+00	2.7999E+00	9.5704E-01	-7.1432E-01
8	-4.5000E+00	3.0919E+00	9.5509E-01	-6.4685E-01

SEGMENT 16 ORDINATE Z(J) 4.0000E+00

LINE	STREAMFUNCTION	RADIUS	AXIAL VELOC.	TANG. VELOC.
1	-5.0000E-01	1.0000E+00	9.2990E-01	-2.0000E+00
2	-8.2653E-01	1.3270E+00	9.5696E-01	-1.5872E+00
3	-1.2347E+00	1.6283E+00	9.5788E-01	-1.2279E+00
4	-1.7245E+00	1.9253E+00	9.5615E-01	-1.0390E+00
5	-2.2959E+00	2.2193E+00	9.5340E-01	-9.0120E-01
6	-2.9495E+00	2.5135E+00	9.5129E-01	-7.9996E-01
7	-3.6837E+00	2.8065E+00	9.4744E-01	-7.1263E-01
8	-4.5000E+00	3.1006E+00	9.4497E-01	-6.4504E-01

SEGMENT 17 ORDINATE Z(J) 4.6300E+00

LINE	STREAMFUNCTION	RADIUS	AXIAL VELOC.	TANG. VELOC.
1	-5.0000E-01	1.0000E+00	8.7992E-01	-0.
2	-8.2653E-01	1.3190E+00	9.1192E-01	-0.
3	-1.2347E+00	1.6225E+00	9.2219E-01	-0.
4	-1.7245E+00	1.9215E+00	9.2709E-01	-0.
5	-2.2959E+00	2.2184E+00	9.2659E-01	-0.
6	-2.9495E+00	2.5147E+00	9.2966E-01	-0.
7	-3.6837E+00	2.8107E+00	9.2742E-01	-0.
8	-4.5000E+00	3.1074E+00	9.2629E-01	-0.

SEGMENT 18 ORDINATE Z(J) 5.4100E+00

LINE	STREAMFUNCTION	RADIUS	AXIAL VELOC.	TANG. VELOC.
1	-5.0000E-01	1.0000E+00	9.0714E-01	-0.
2	-8.2653E-01	1.3108E+00	9.1497E-01	-0.
3	-1.2347E+00	1.6149E+00	9.1936E-01	-0.
4	-1.7245E+00	1.9159E+00	9.2222E-01	-0.
5	-2.2959E+00	2.2151E+00	9.2363E-01	-0.
6	-2.9495E+00	2.5133E+00	9.2465E-01	-0.
7	-3.6837E+00	2.8109E+00	9.2399E-01	-0.
8	-4.5000E+00	3.1086E+00	9.2366E-01	-0.

SEGMENT 19 ORDINATE Z(J) 6.3800E+00

LINE	STREAMFUNCTION	RADIUS	AXIAL VELOC.	TANG. VELOC.
1	-5.0000E-01	1.0000E+00	9.1547E-01	-0.
2	-8.2653E-01	1.3063E+00	9.1792E-01	-0.
3	-1.2347E+00	1.6121E+00	9.1972E-01	-0.
4	-1.7245E+00	1.9134E+00	9.2114E-01	-0.
5	-2.2959E+00	2.2132E+00	9.2194E-01	-0.
6	-2.9495E+00	2.5122E+00	9.2274E-01	-0.
7	-3.6837E+00	2.8105E+00	9.2269E-01	-0.
8	-4.5000E+00	3.1086E+00	9.2268E-01	-0.

SEGMENT 20 ORDINATE Z(J) 7.6000E+00

LINE	STREAMFUNCTION	RADIUS	AXIAL VELOC.	TANG. VELOC.
1	-5.0000E-01	1.0000E+00	9.1774E-01	-0.
2	-8.2653E-01	1.3077E+00	9.1914E-01	-0.
3	-1.2347E+00	1.6112E+00	9.2016E-01	-0.

SECTION VI

EXAMPLE RESULTS

1. CALCULATION OF DESIRED AREA CHANGE

In the first series of examples considered below, a stator rotor pair are considered to exist in an annulus in which the area is expanded to make the outlet "average" Mach number approximately equal to the inlet average Mach number. Assuming for the moment that a single Mach number exists far downstream (as would be the case for free vortex machinery) it follows from consideration of continuity for isentropic flow that

$$\frac{A_2}{A_o} = \frac{M_o}{M_2}\left[\frac{1 + \frac{\gamma-1}{2} M_2^2}{1 + \frac{\gamma-1}{2} M_o^2}\right]^{\frac{\gamma+1}{2(\gamma-1)}} \left(\frac{H_o}{H_2}\right)^{\frac{\gamma+1}{2(\gamma-1)}} \tag{55}$$

or, in the case where $M_2 = M_o$,

$$\frac{A_2}{A_o} = \left(\frac{H_o}{H_2}\right)^{\frac{\gamma+1}{2(\gamma-1)}} \tag{56}$$

Here we calculate the desired area ratio using this formula, but considering the enthalpy to be a mass averaged enthalpy such that

$$H_{av} = \frac{-2}{R^2 - 1} \int_{-1/2}^{-R^2/2} H \, d\Psi \tag{57}$$

For convenience of interpretation the examples considered herein were all taken to be of the linear form considered in Ref. 3. That is to say the angular momentum in all sections is of the form $YV = -\alpha\Psi + \beta$. Thus it follows in this case of a stator followed by a rotor that removes the swirl, that:

$$\frac{H_{av}}{H_o} = 1 - \frac{\Omega}{H_o}\left\{\beta + \frac{\alpha}{4}(R^2 + 1)\right\} \tag{58}$$

The area ratio is then calculated from Eq (56). It is assumed in these examples that the hub radius remains at unity and the tip radius in the

expanding section of length L is given by

$$G = R + \frac{\Delta R}{2}\left(1 - \cos\frac{\pi x}{L}\right) = R + \frac{1}{2}\left[\left\{R^2 - (R^2 - 1)\left(1 - \frac{A_2}{A_o}\right)\right\}^{1/2} - R\right]\left(1 - \cos\frac{\pi x}{L}\right) \quad (59)$$

In the examples considered in this report, L was taken equal to 5.4063.

2. FREE VORTEX FLOWS

Figs.16 through 21 show the results of the calculations for flow through a stator rotor combination in which a free vortex swirl is introduced by the stator and removed by the rotor. In all cases the outlet area is adjusted to compensate for the reduced stagnation enthalpy as described in the previous section. The figures are arranged in order to illustrate the effect of increasing inlet Mach number, other pertinent parameters being supplied on the figures.

It is readily apparent that the perturbations in axial velocity brought about by the effect of compressibility increase substantially over the range of Mach numbers investigated. (For example, just following the rotor $W_h = 0.95$ for $M_o = 0.2$, whereas $W_h = 0.68$ for $M_o = 0.5$). The overall effect of the reduction in axial velocity at exit due to the reduced stagnation enthalpy is also evident in the same figures. ($W_\infty = .98$ for $M_o = 0.2$, $W_\infty = .91$ for $M_o = 0.5$). It is obvious that in these cases, where the vorticity is zero, that the outlet velocity must be uniform, and it is a simple check on the accuracy of the program to observe the predicted uniformity of the outlet velocity profile.

It is interesting to note that in the calculation of these free vortex examples, no spurious values of meridional Mach Numbers in excess of unity appeared throughout the iterations in the calculational procedures. This was true even though in the case where $M_o = 0.5$, meridional Mach number on the hub just following the stator was M = 0.74. (The total Mach number at this location was 1.36). In the examples to follow, the very important effect of the vorticity in distorting the axial velocity profiles becomes evident. The effect of the distortion is to actually introduce high Mach numbers, as well as to make the eventual streamline pattern more distant from the original guess.

3. FLOWS WITH VORTICITY

In order to illustrate the effects of vorticity two sets of calculations ($\alpha = 0.4$, $\beta = 1$ and $\alpha = 0.5$, $\beta = 0.75$) were investigated at inlet Mach numbers of 0.2 and 0.3. The results of the flow field calculations are presented in Figs. 22 to 27. The distortion of axial velocity profile due to the presence of the non-free vortex swirl velocities is very evident in the figures. Note, for example the distorted outlet profiles far downstream. Thus, for flows with seemingly low approach Mach numbers, the distortion of the profile can lead to large meridional Mach numbers occurring in the field. The very strong effect

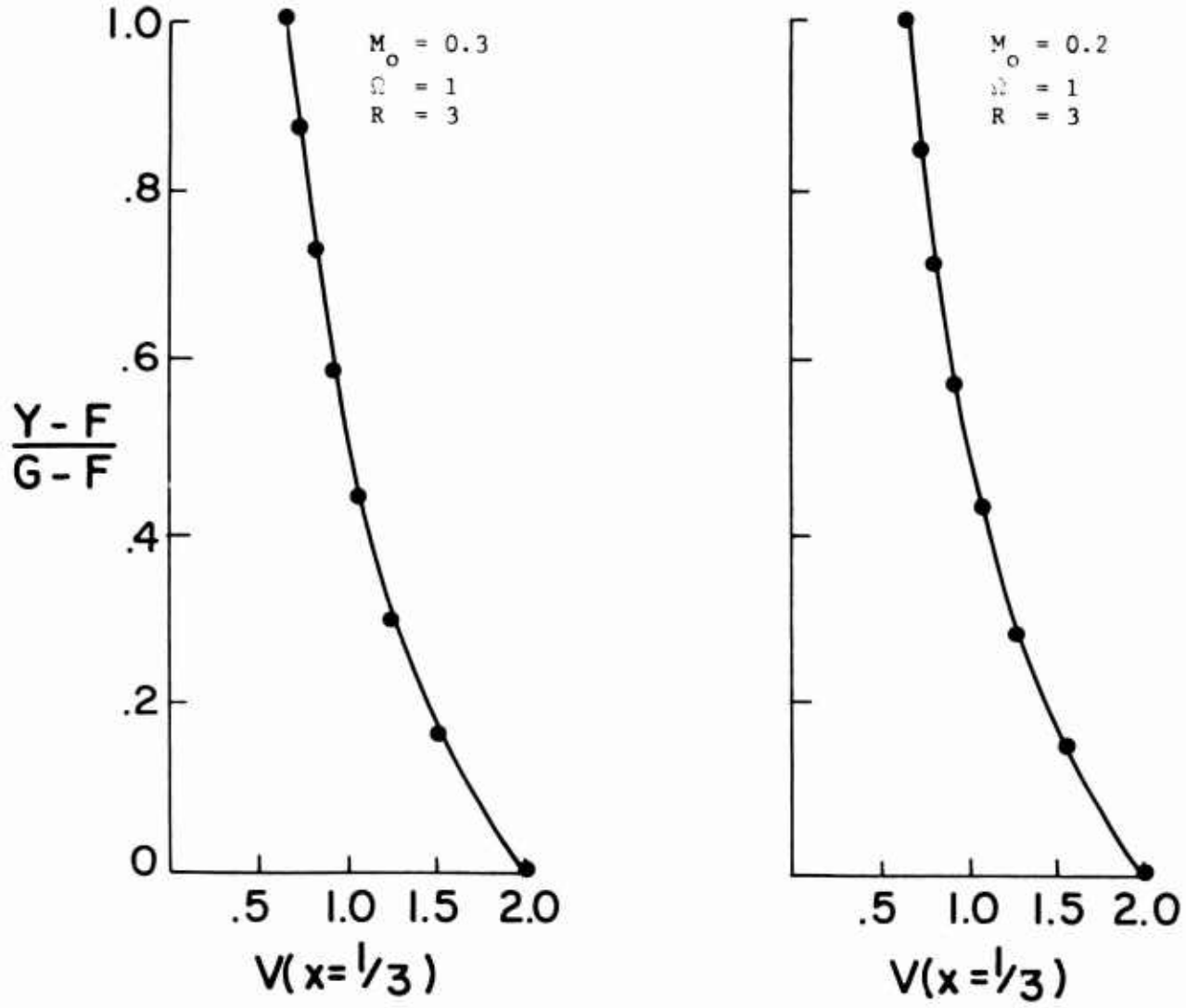

Figure 16. Tangential Velocity Profiles Immediately Following Stator; M_o = 0.2,0.3; α = 0, β = 2

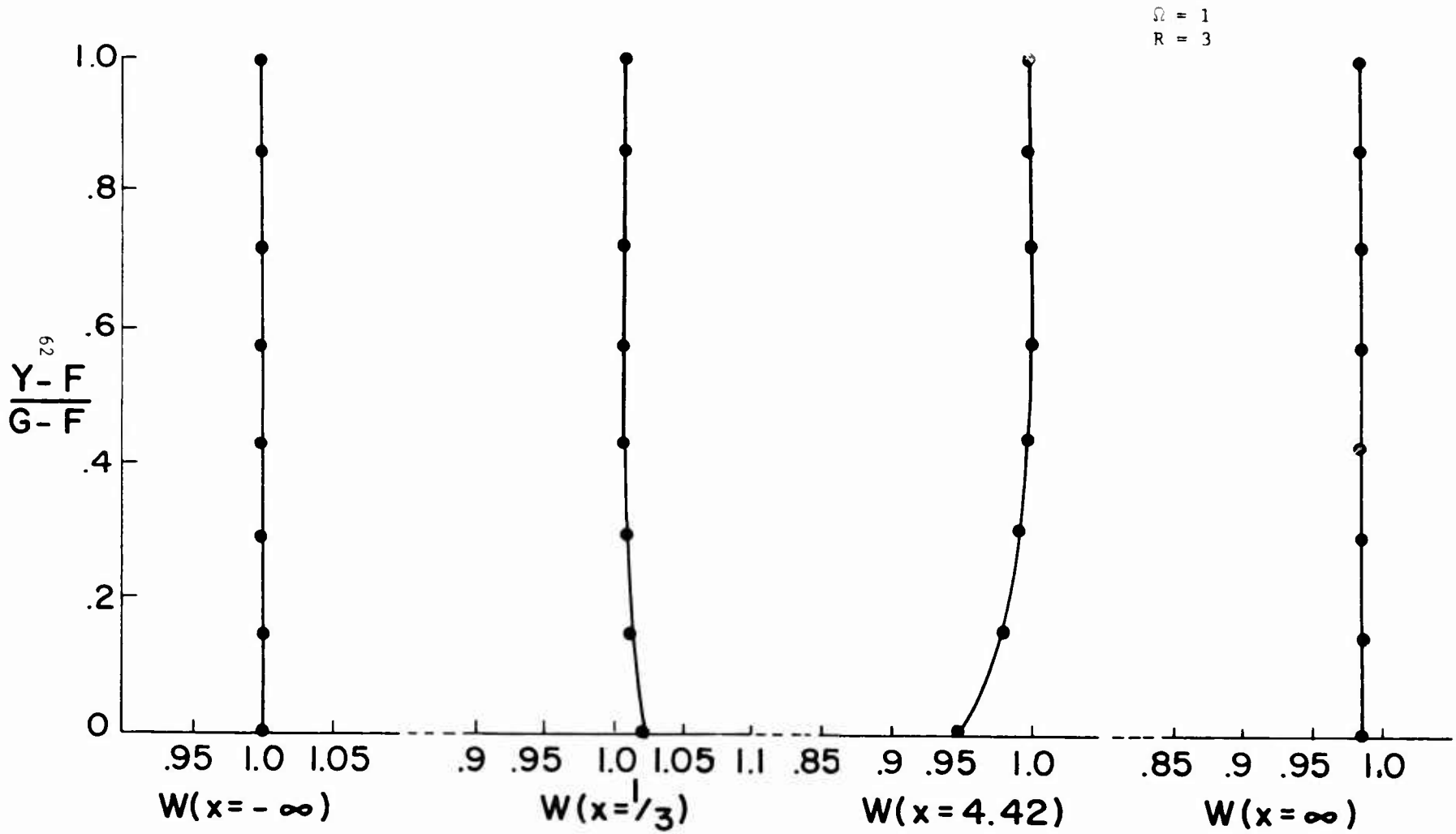

Figure 17. Axial Velocity Profiles at Four Axial Stations; $M_o = 0.2$; $\alpha = 0$, $\beta = 2$

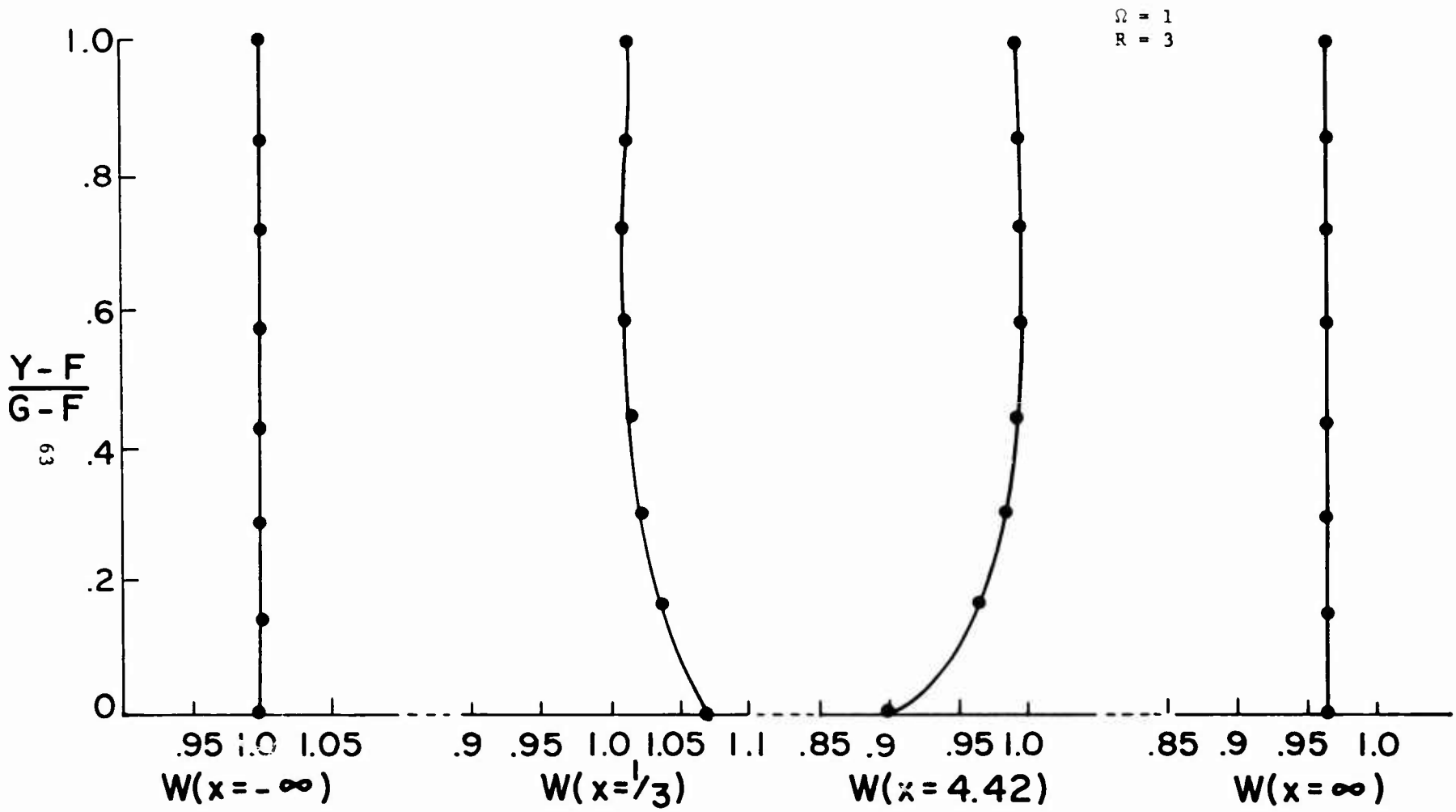

Figure 18. Axial Velocity Profiles at Four Axial Stations; $M_o = 0.3$; $\alpha = 0$, $\beta = 2$

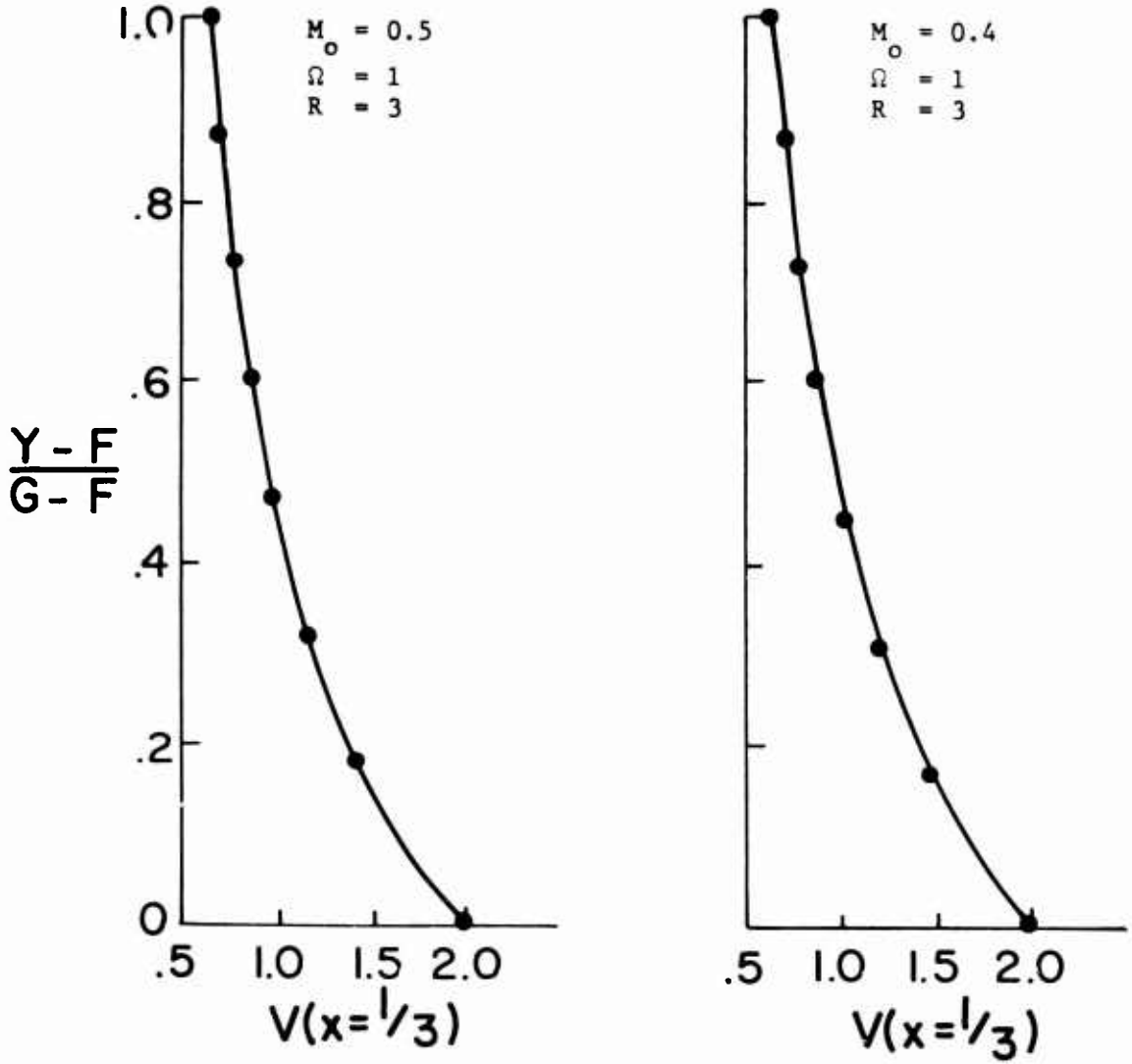

Figure 19. Tangential Velocity Profiles Immediately Following Stator; M_o = 0.4,0.5; α = 0, β = 2

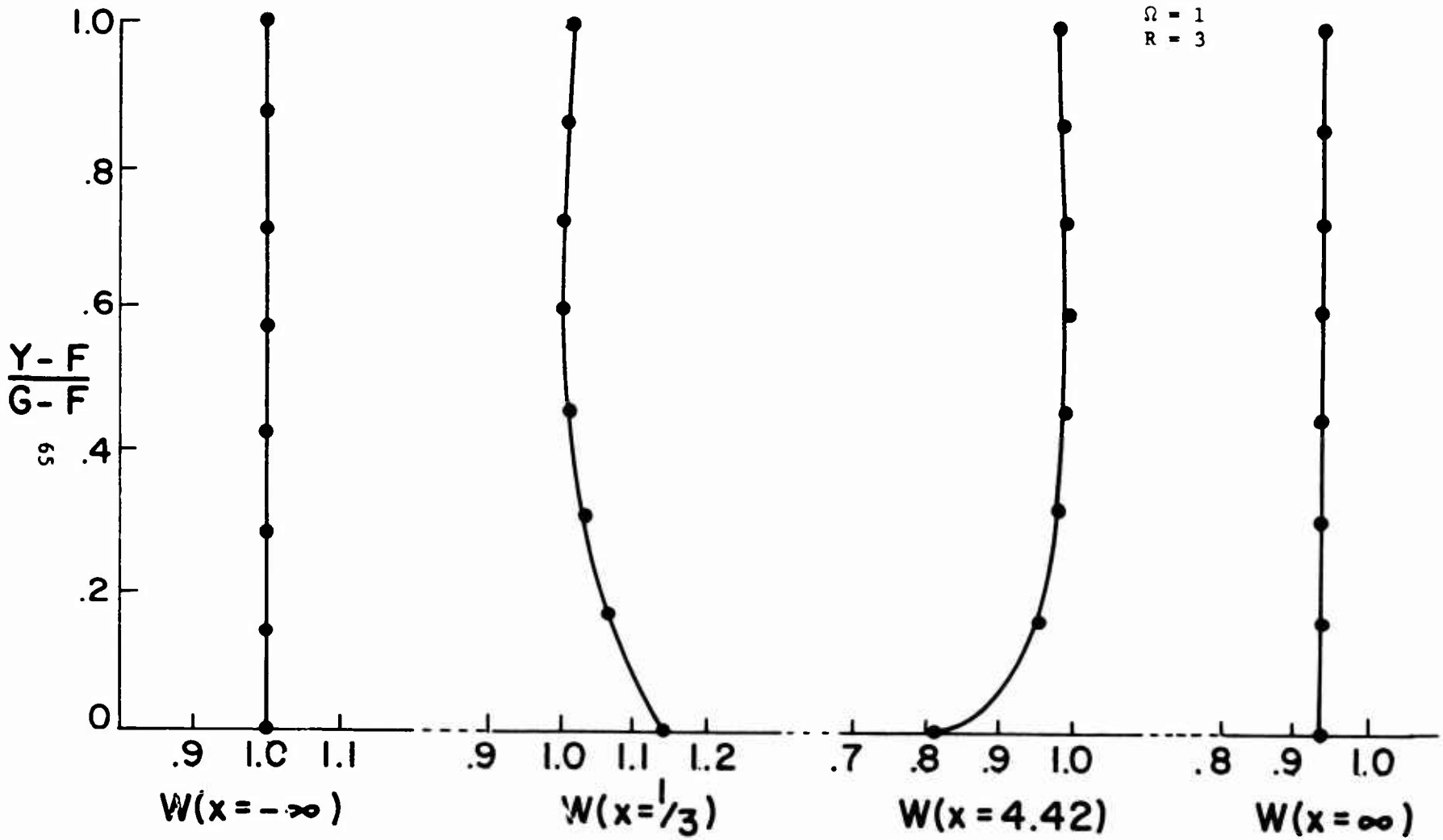

Figure 20. Axial Velocity Profiles at Four Axial Stations; $M_o = 0.4$; $\alpha = 0$, $\beta = 2$

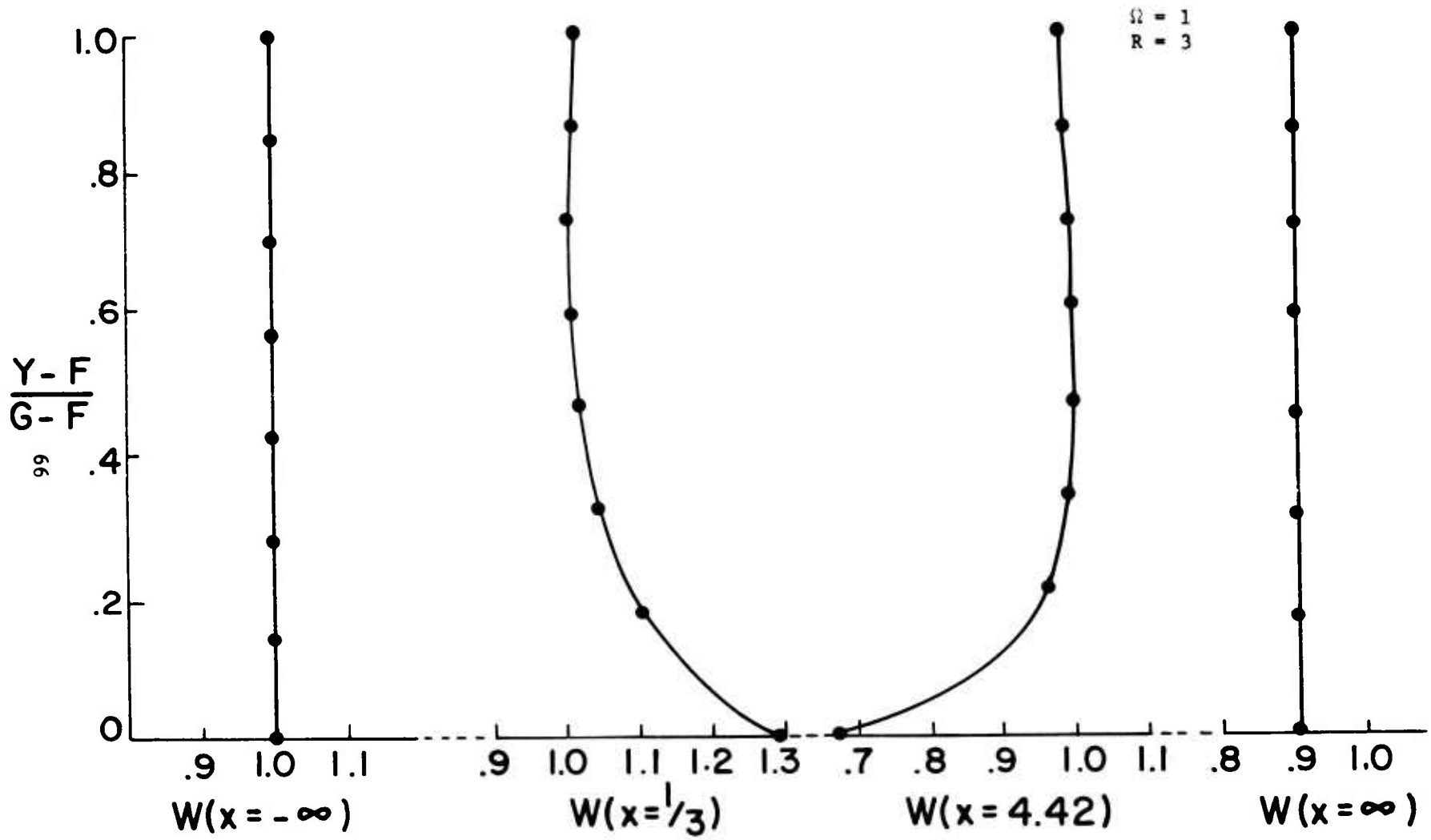

Figure 21. Axial Velocity Profiles at Four Axial Stations; $M_o = 0.5$; $\alpha = 0$, $\beta = 2$

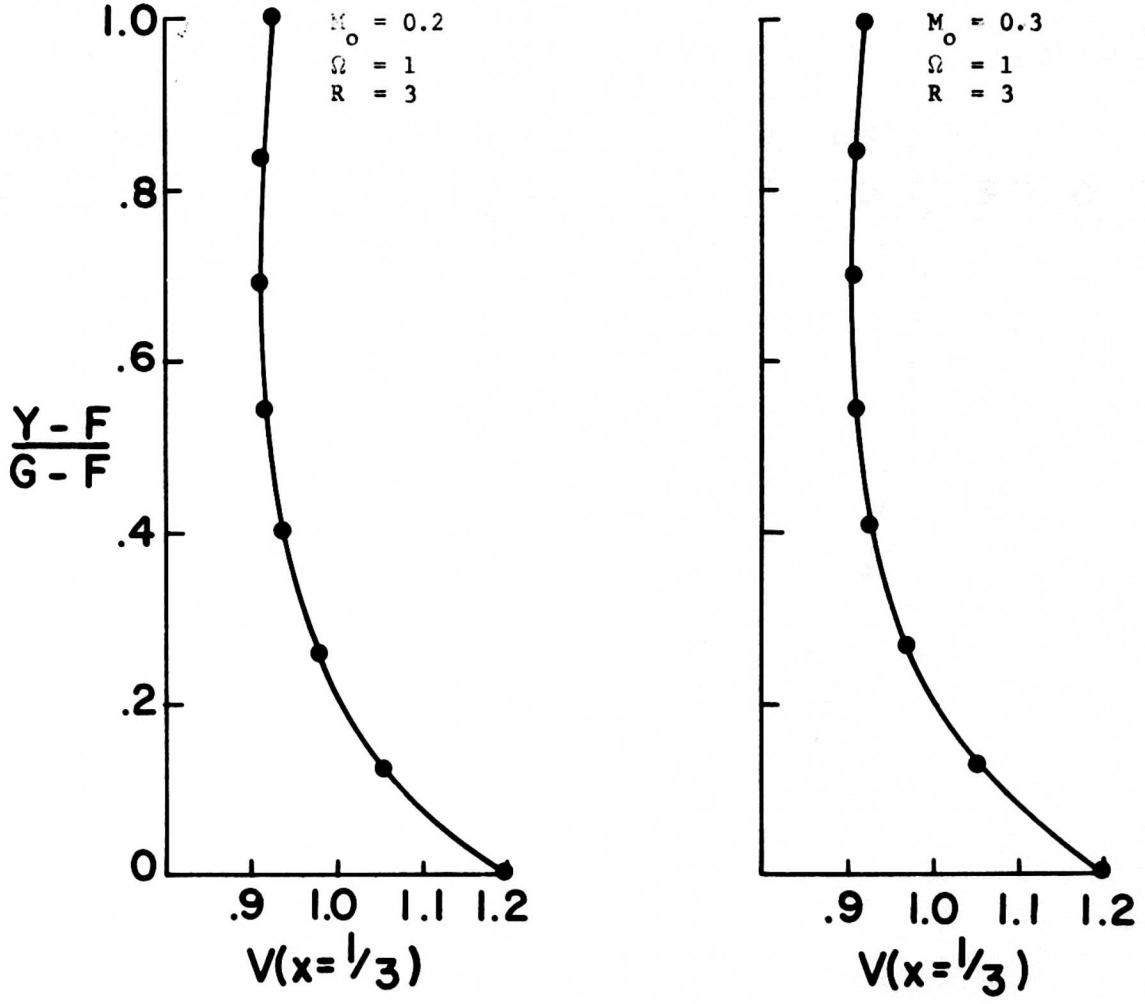

Figure 22. Tangential Velocity Profiles Immediately Following Stator; M_o = 0.2,0.3; α = 0.4, β = 1

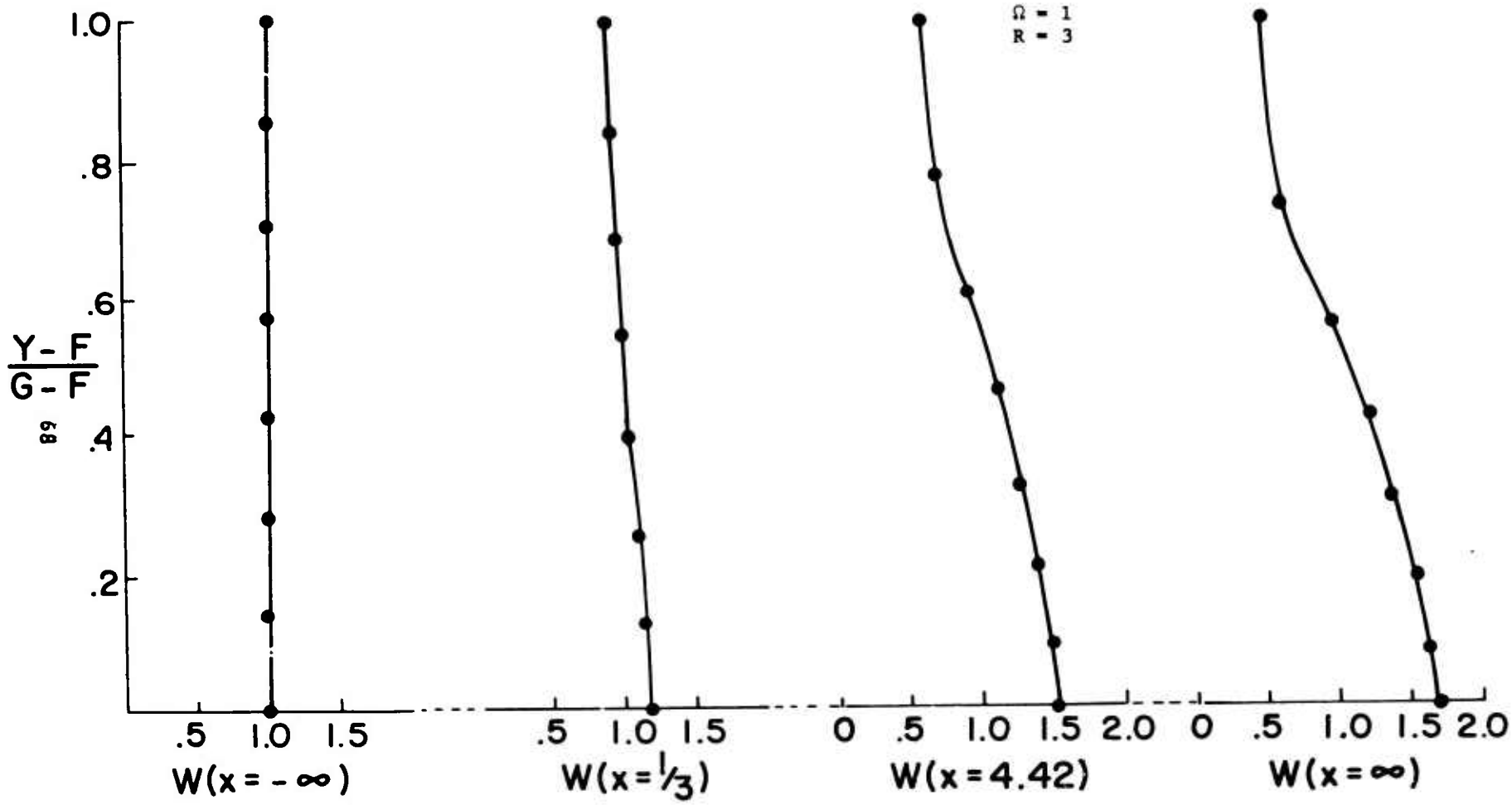

Figure 23. Axial Velocity Profiles at Four Axial Stations; $M_o = 0.2$; $\alpha = 0.4$, $\beta = 1$

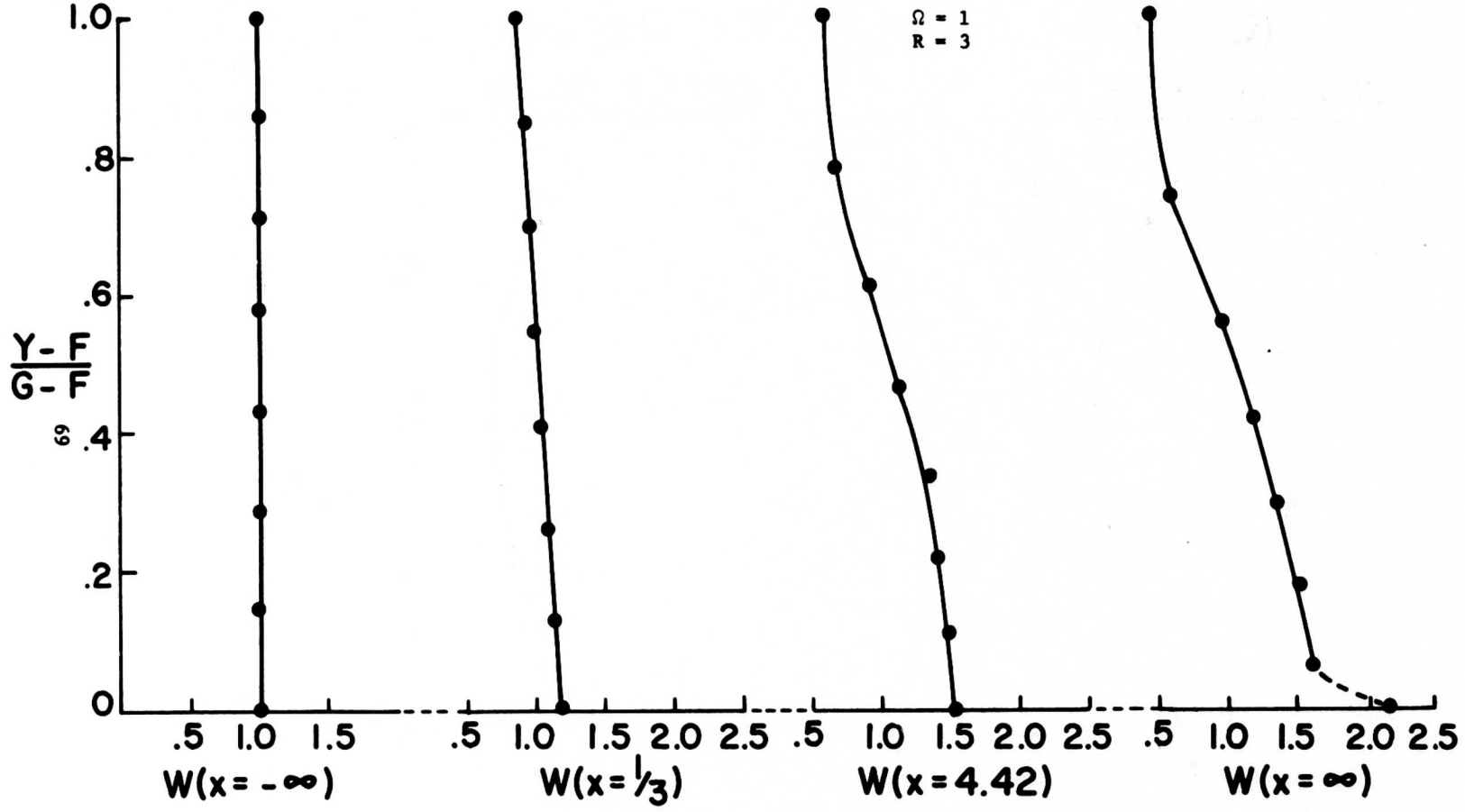

Figure 24. Axial Velocity Profiles at Four Axial Stations; $M_o = 0.3$; $\alpha = 0.4$, $\beta = 1$

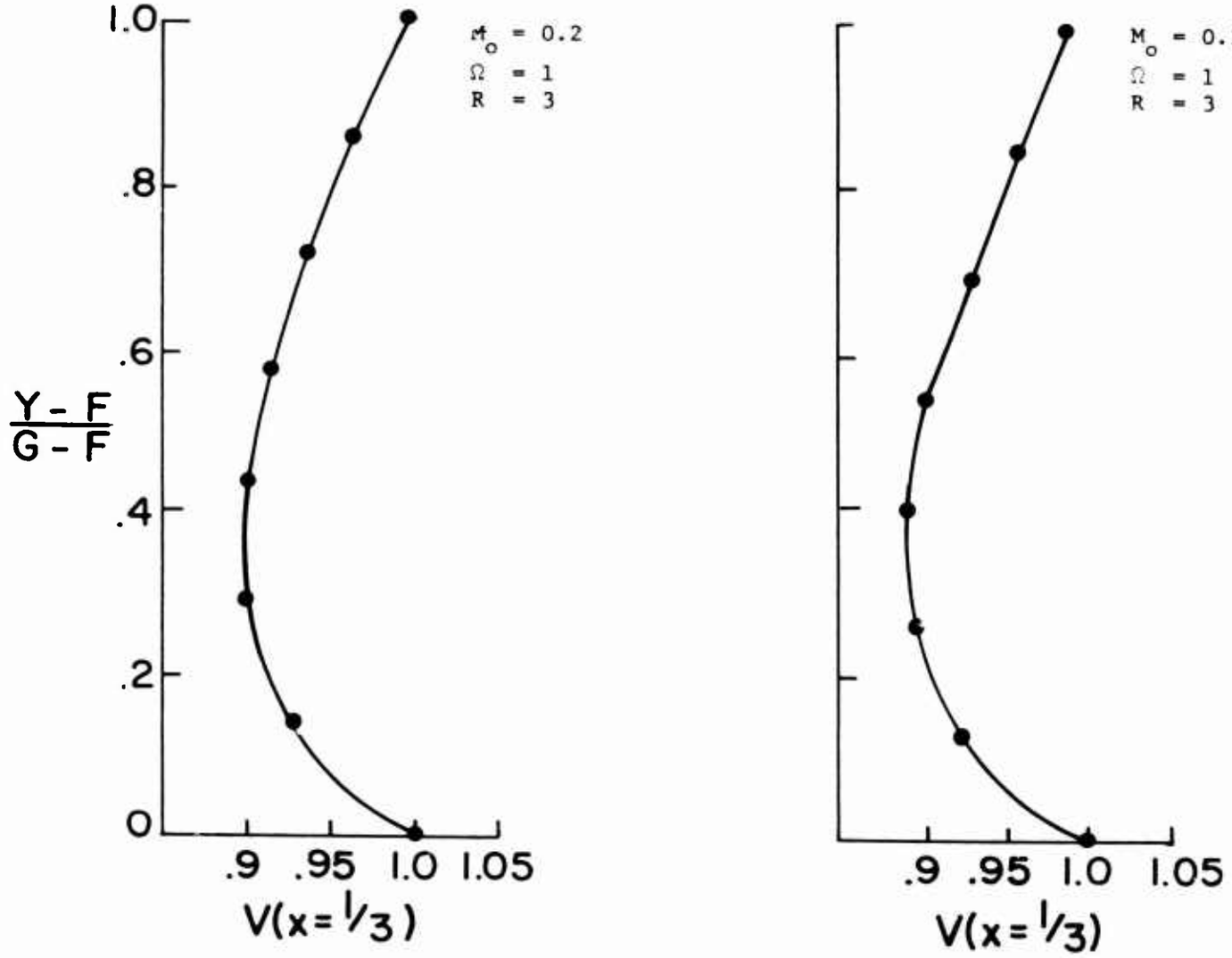

Figure 25. Tangential Velocity Profiles Immediately Following Stator; M_o = 0.2,0.3; α = 0.5, β = 0.75

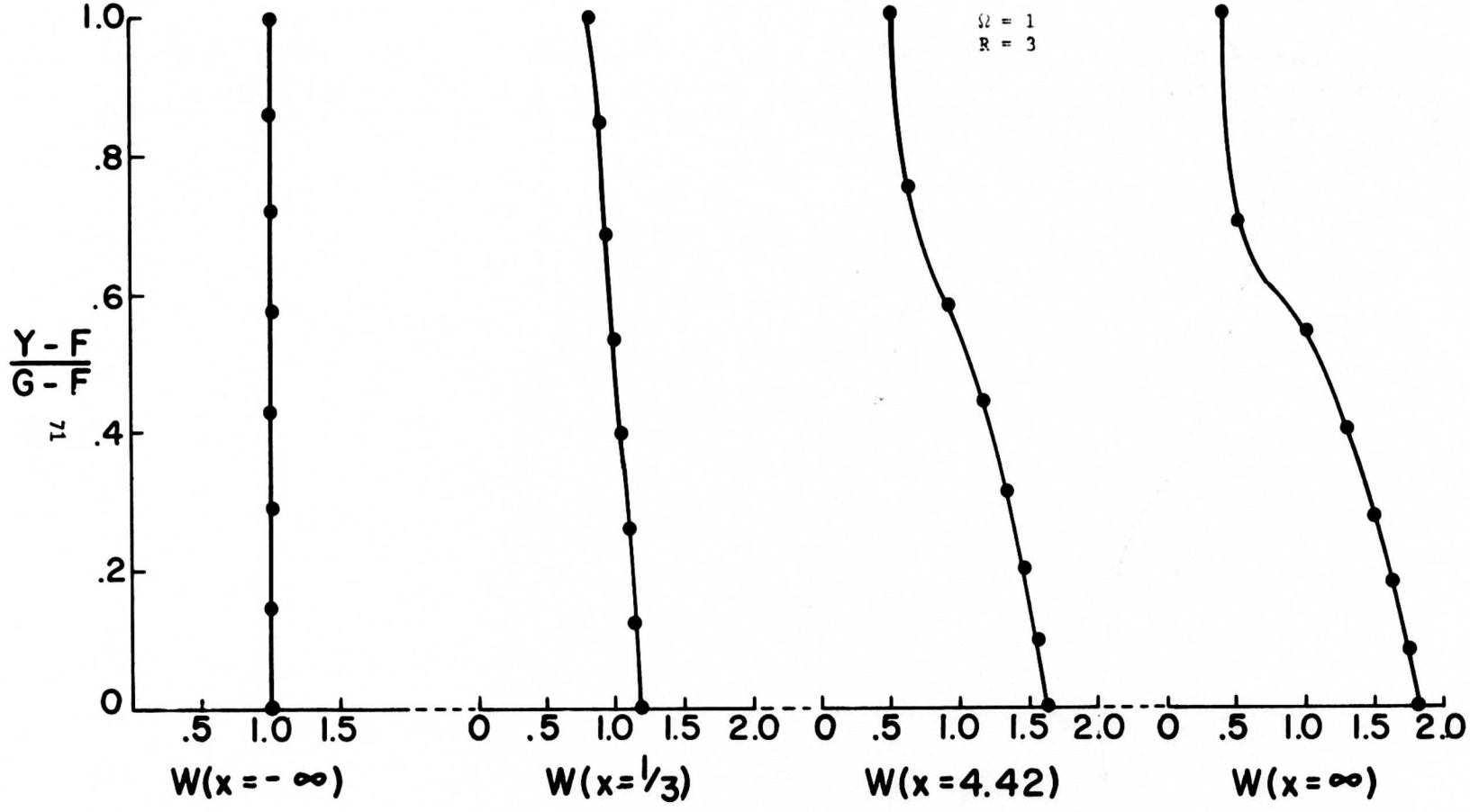

Figure 26. Axial Velocity Profiles at Four Axial Stations; $M_o = 0.2$, $\alpha = 0.5$, $\beta = 0.75$

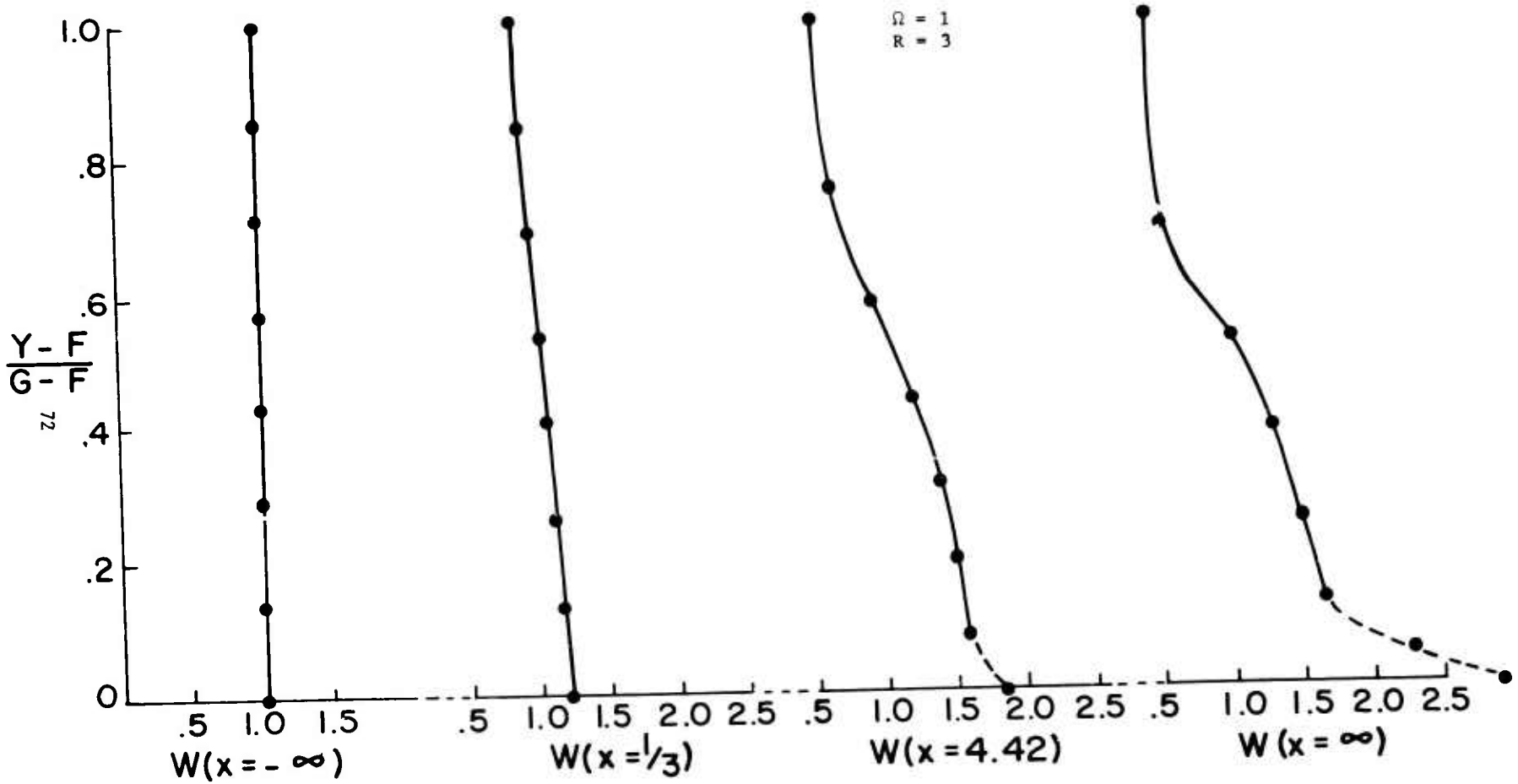

Figure 27. Axial Velocity Profiles at Four Axial Stations; $M_o = 0.3$; $\alpha = 0.5$, $\beta = 0.75$

of vorticity can be noted by observing the values of the axial velocity at the hub at downstream infinity for the two cases at $M_o = 0.2$. Thus when $\alpha = 0.4$, $W_h(\infty) = 1.67$, whereas when $\alpha = 0.5$, $W_h(\infty) = 1.85$. The latter case hence leads more rapidly to the approach to supersonic Mach numbers. This is true even though the free vortex component of swirl is reduced in the $\alpha = 0.5$ case sufficiently to cause the average outlet enthalpies to be equal.

The dotted portions of the curves appearing on Figs. 24 and 27 indicate regions where the computer program indicated the failure of the density iteration program. In such areas the density is estimated by the calculational procedure outlined in SECTION IV-4. Generally speaking the number of mesh points indicating that this procedure has been invoked decreases with successive iterations. In these cases the number of iterations was limited to ten, so it is quite possible that the few mesh points exhibiting this behavior could be removed with further iterations. As it is, the Meridional Mach number exis ing at the hub at downstream infinity, calculated utilizing the density ratio obtained by the alternate calculation procedure is .694 in Fig 24 and .975 in Fig. 27. It should be noted that the values chosen for α (0.4 and 0.5) represent very high levels of vorticity (with consequent large variations in stagnation enthalpy) compared to traditional turbomachine practice, and as such provide a demanding test for the computer program.

4. THE EFFECT OF MESH SIZE

In order to investigate the effect of Mesh size, some very highly swirling free vortex flows ($\beta = 6.66$) in an annulus of modest tip to hub ratio ($R = 10/7$) were considered. These values of β and R were taken in order, also, to compare the results to those of Hawthorne and Ringrose[10] (See also SECTION VII). The trends observed are very similar to those reported in Ref. 10, the only real differences arising because of slight differences in the value of β assumed (6.66 versus approximately 6.1 for Ref. 10), and from the much different value of wheel speed taken here ($\Omega = 1$ versus $\Omega = 2.61$ for Ref. 10).

The geometry considered has parallel walls, with the stator to rotor spacing being 0.14. (Thus approximately one third of the blade height, R-1). The mesh was constructed to have even x spacing between the stator and rotor. Upstream from the stator and downstream from the rotor the x spacing of the mesh points increases in the ratio 1.25 for each succeeding mesh point. In both coarse and fine meshes there are eight streamline mesh points. In the fine mesh, there are twelve x mesh points between stator and rotor, with fifteen further mesh points both upstream of the stator and downstream of the rotor for a total of forty two x mesh points. The coarse mesh has eight mesh points between stator and rotor with eight further mesh points both upstream of the stator and downstream of the rotor for a total of twenty four x mesh points.

When the stator alone is considered the mesh point spacing is the same as that described above. Figs. 28-31 show the behavior of the axial velocity on hub and tip throughout the flow field length. The location of the mesh points is indicated in the figures.

It is interesting to note, again, the large effect of compressibility for cases with such high swirl loading. Thus, though the entrance Mach number is

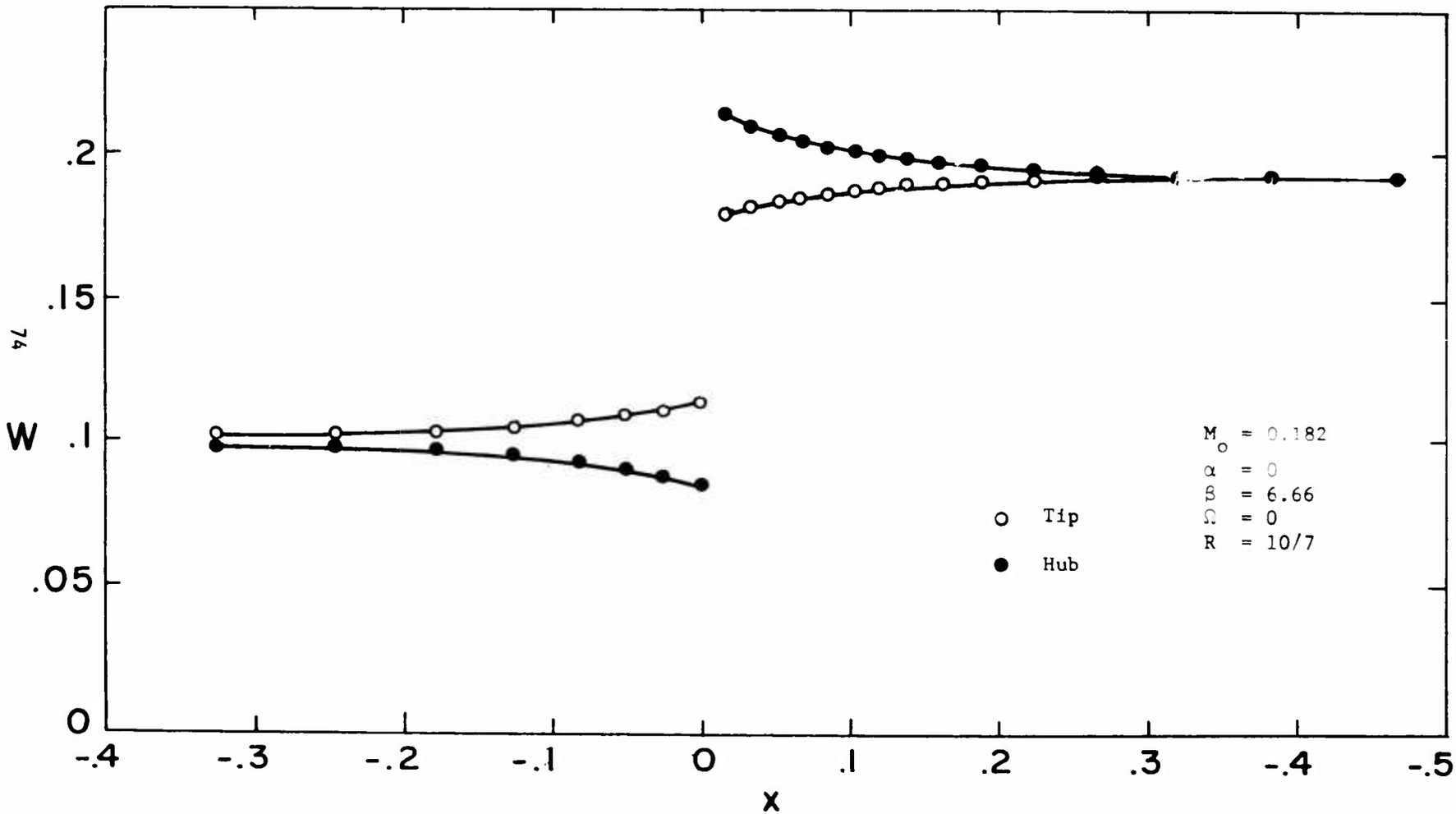

Figure 28. Coarse Mesh Results for Stator Only

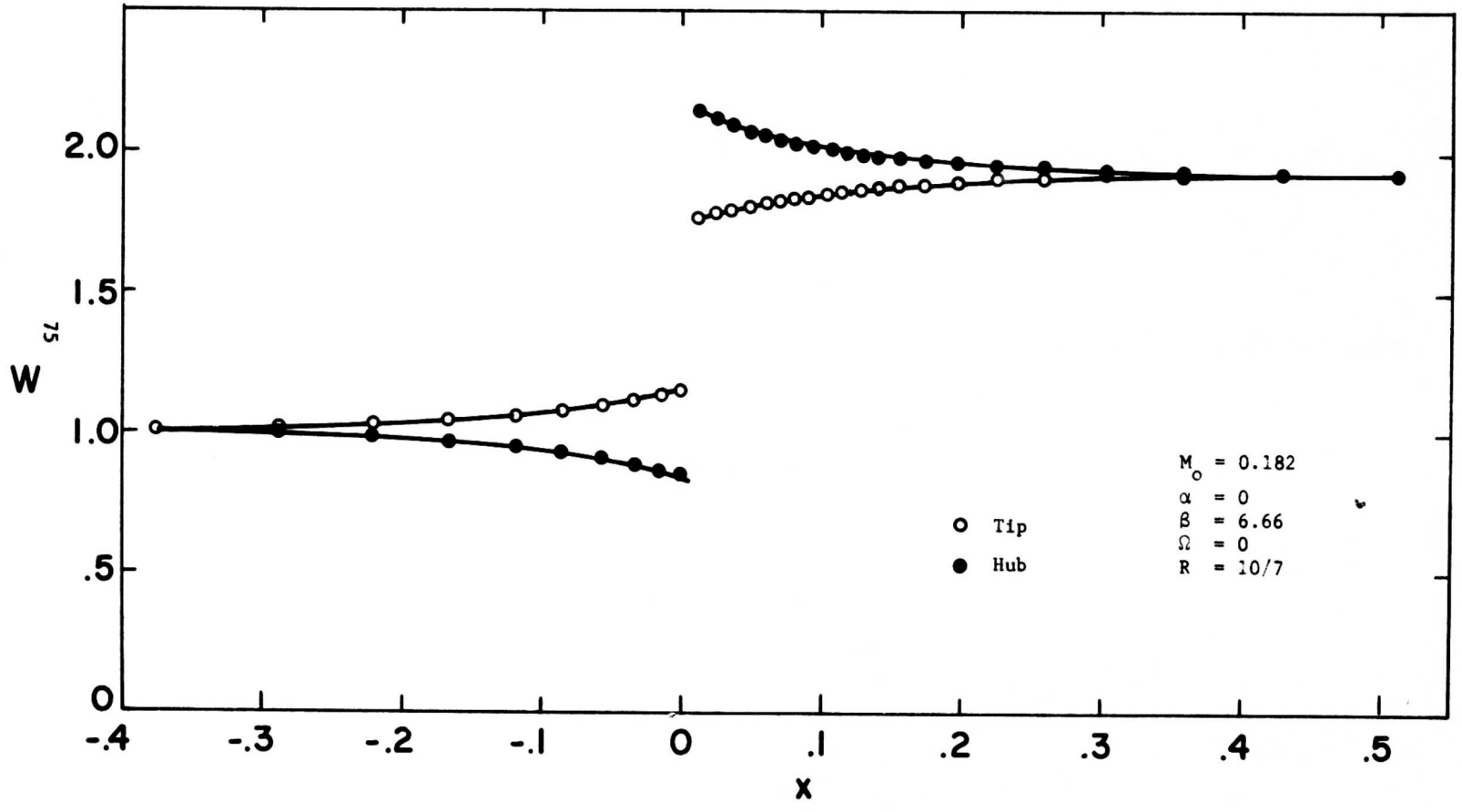

Figure 29. Fine Mesh Results for Stator Only

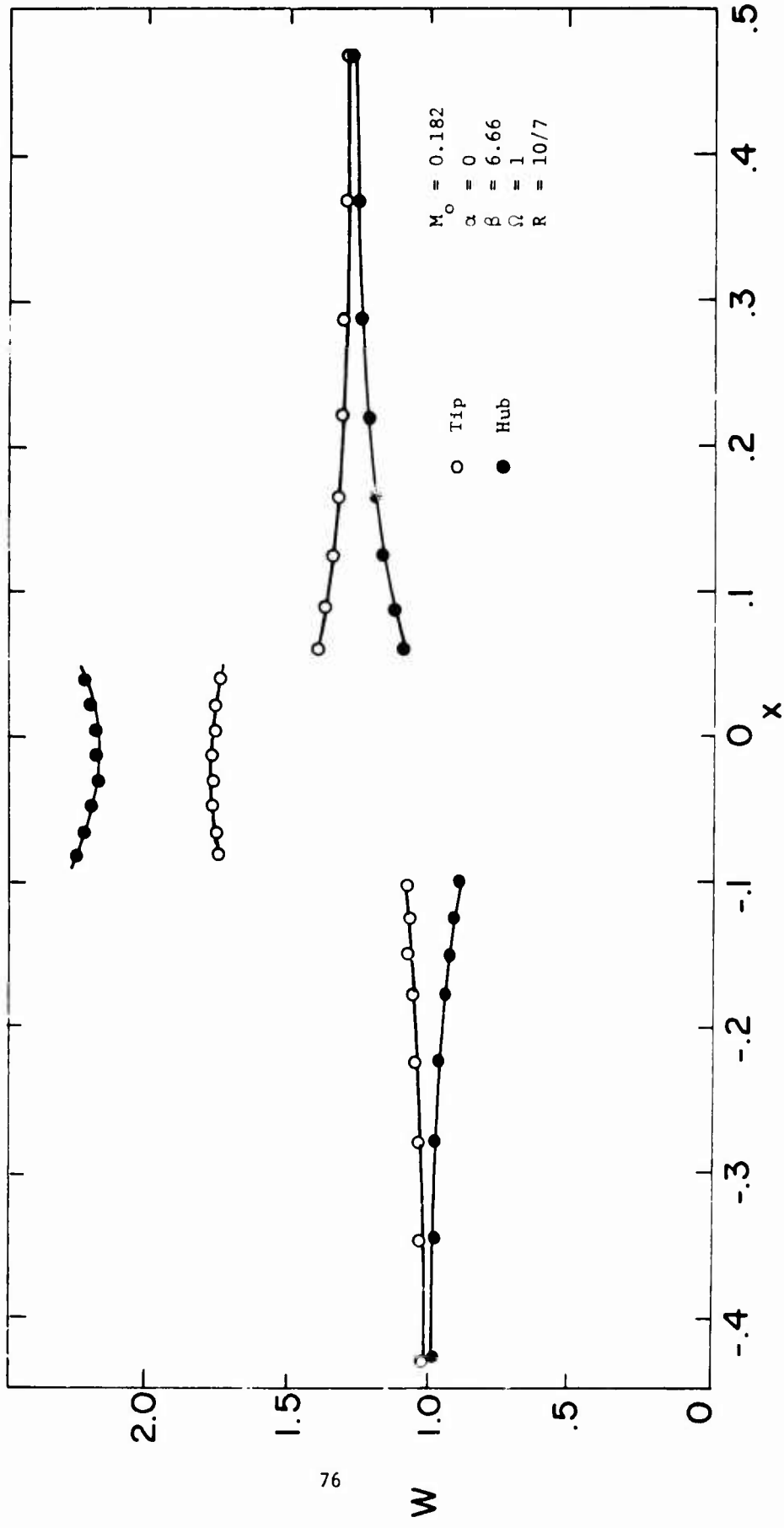

Figure 30. Coarse Mesh Results, Stator and Rotor

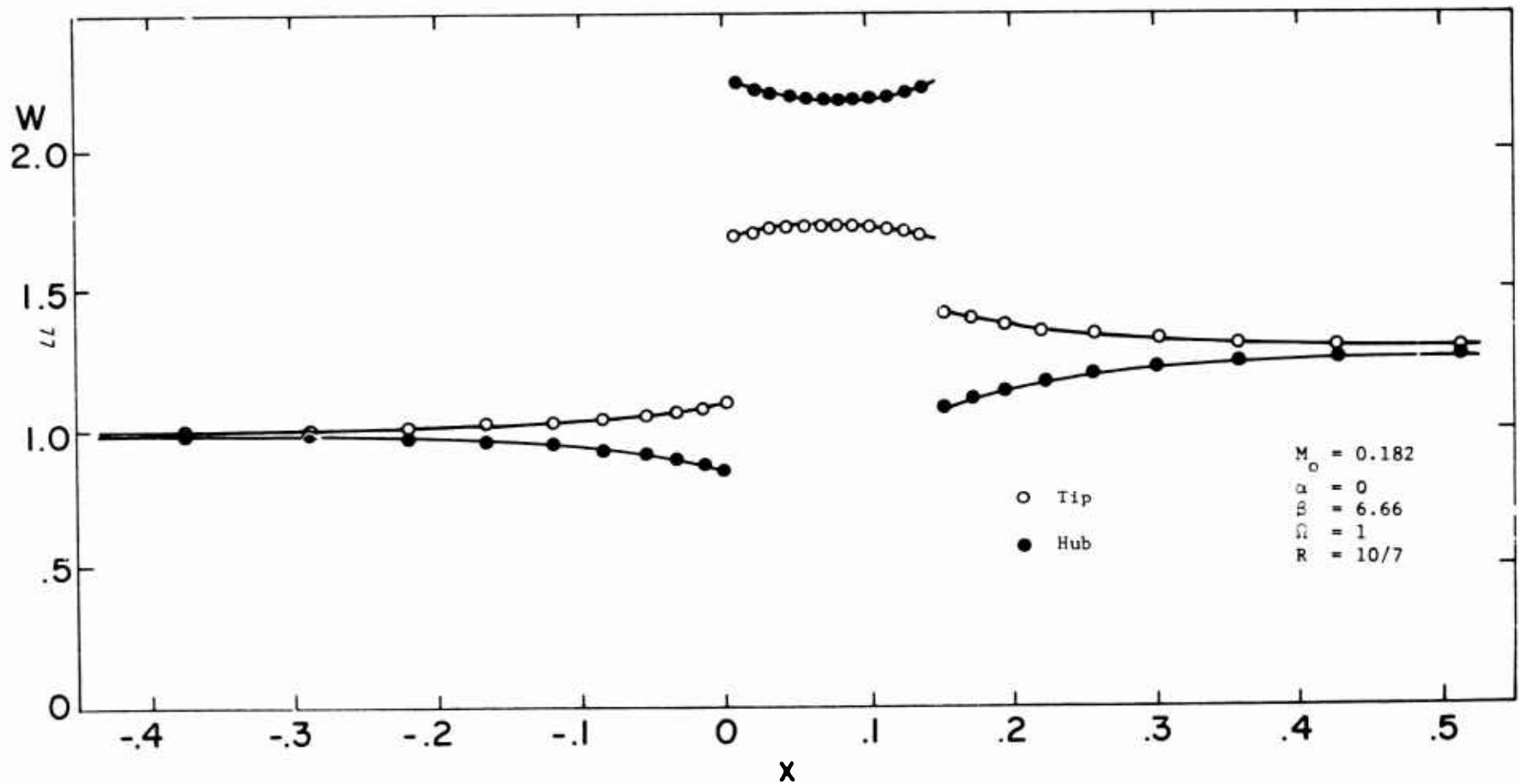

Figure 31. Fine Mesh Results, Stator and Rotor

only M_o = 0.182, the meridional Mach number at the hub just following the stator is 0.497. The total flow Mach number at this location is 1.54.

It can be seen by comparison of the figures, that the effect of decreased mesh size is very small here. (Careful perusal of the tabular output indicates changes in the predicted velocities at comparable locations of only approximately one percent). This suggests that for most calculational purposes eight streamwise mesh points and twenty four x-wise mesh points would produce sufficient computational accuracy.

5. THE EFFECT OF FINITE ASPECT RATIO

As a first approximation to the effect of finite aspect ratio the flow of fluid through a stator only was considered. The first calculation (Fig. 32) considered a single disc, whereas the second calculation (Fig. 33) considered the blade to be replaced by two actuator discs such that 62.5% of the loading was on the first disc and 37.5% of the loading on the second. Figs. 30 and 31 show the resultant axial velocity profiles existing at the position just preceding the upstream disc and just following the downstream disc. For the case of the single disc, the x = 0 origin was located so that the single disc was at the appropriate center of moment.

Comparison of the profiles, particularly at the downstream location, indicate as expected, that the flow following the single disc has proceeded more towards its asymptotic form than has that which has just departed the second of the two discs. It is obvious that this process may be continued to a larger number of actuator discs if a more accurate description of the effects of distributed blade forces is desired.

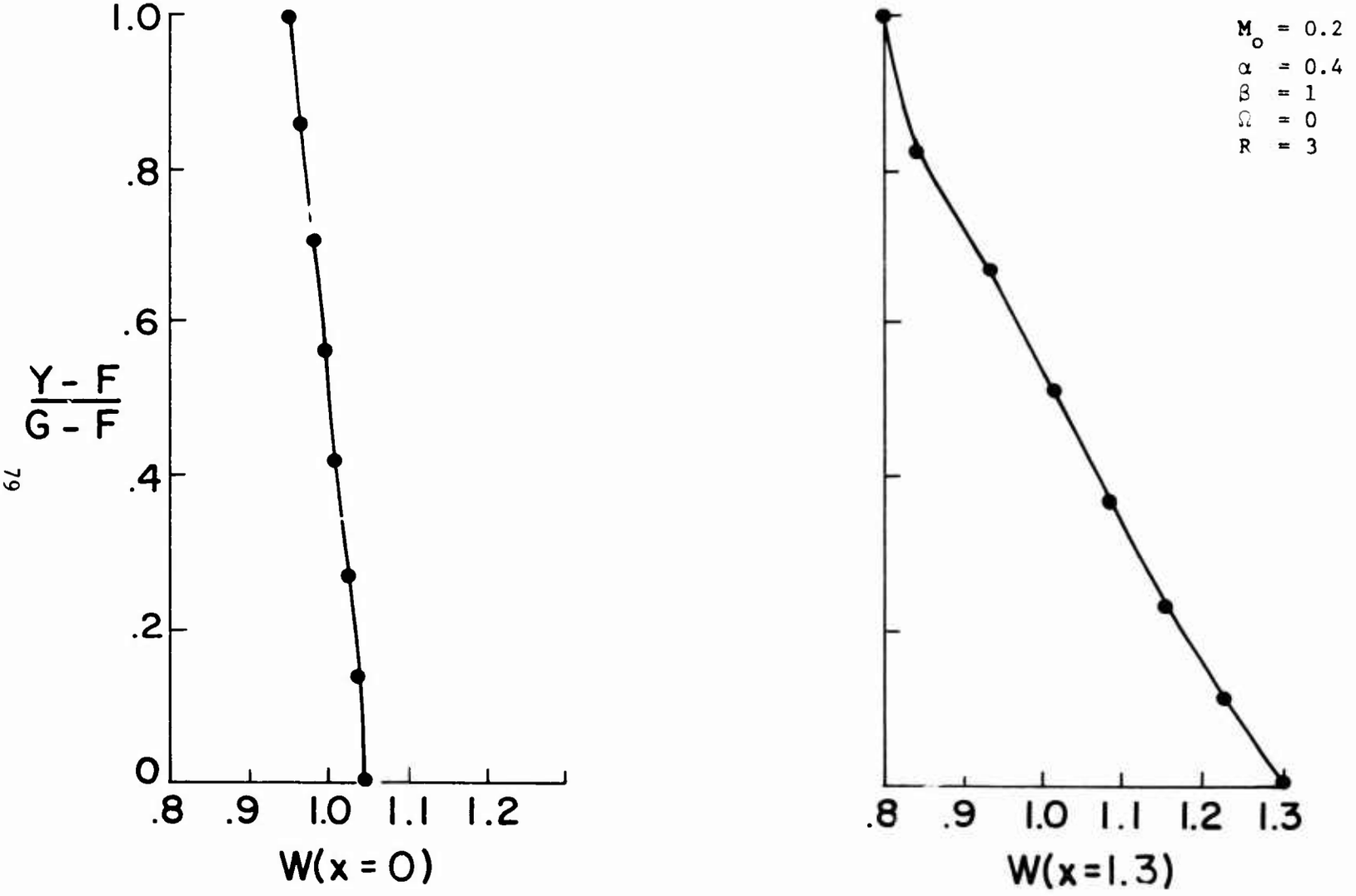

Figure 32. Single Disc Approximation to Stator

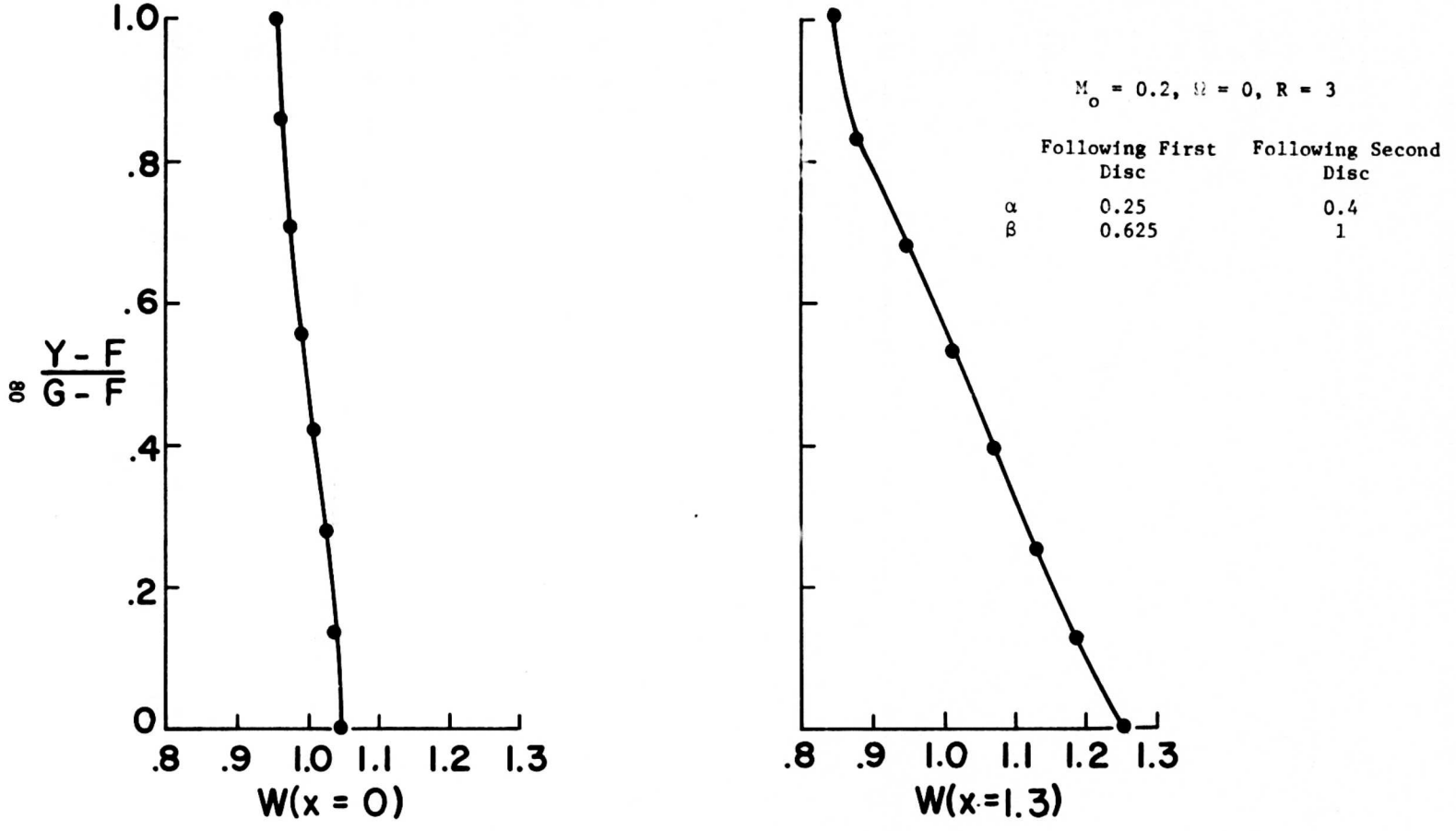

Figure 33. Two Disc Approximation to Stator

SECTION VII

COMPARISON WITH ALTERNATIVE CALCULATIONAL TECHNIQUES

Many calculational techniques for throughflow theory are available in the literature today, but we will here limit our attention to those examples that consider compressible flows.[7-10]

Creveling and Carmody[7] provide a program written to obtain the desired output variables of a turbomachine row or rows in terms of input design parameters. The study is not really directly relatable to the present study, because the detailed flow information involved in describing the flow approach to, and departure from, a blade row is not obtained. Rather, a "quasi radial equilibrium" solution is obtained for the conditions between blade rows. In this quasi radial equilibrium solution the effect of streamline curvature at the station investigated is incorporated directly by taking the supplied flow path geometry (Mod I) or by establishing the flow path geometry by computation (Mod II). It is pointed out by the authors that irregular geometry can be produced by Mod II computation, resulting in severe streamline curvature effects. In common with all the example techniques studied (and in common with this report) the computation is limited to flows in which the meridional Mach number is less than unity. By simplifynng the fluid mechanical description, the authors have made it possible to analyze the machine behavior in terms of design input variables (total pressure profile at each rotor exit, and limiting values of Rotor tip diffusion factor, Stator hub diffusion factor, Stator hub Mach number, Rotor hub relative exit angle and Rotor tip exit whirl velocity). The output of the program is the desired flow field information. (Velocities, temperatures flow angles, etc.)

The study by Marsh[8] is directed to the solution of the "direct problem" of throughflow theory wherein the blade geometry is prescribed and the resulting flow field is to be determined. As a result actuator disc theory is not used, but rather the "average forces" of the blades are related to the rate of change of angular momentum of the fluid and the blade surface geometry. The effect of blade thickness is included by adding a factor, B, in the continuity equation that is simply the ratio of the circumferential width of the blade passage to the blade pitch. The effects of imperfect flow can be included through the generation of entropy term, though the related drag effect upon the equation of motion is not included.

It is interesting to note that in common with Wu,[11] Marsh elected to solve and store the equation for density (our Eq (13)) rather than iterate for the solution at each point. In the examples considered in the present report, after the first pass for streamline location the number of iterations required for six figure density accuracy were usually only one or two. The authors of this report feel that when such accuracy is desired it is more efficient to use the iterative technique than to store the information.

The actual computational process used by Marsh involves solving a quasi-linear equation for Ψ in terms of an assumed known density field. After solution of the quasi-linear equation the density estimate is updated and the process repeated till convergence. Finite difference methods are used throughout.

The examples given by Marsh correspond to very low Mach number flows (speeds of less than 100 fps), so it is difficult to determine with certainty the reliability of the convergence of the process when applied to the analysis of flows in which large meridional Mach numbers exist. Marsh mentions that an accuracy of 10^{-3} to 10^{-4} in the streamline position estimate, $\frac{\Psi - \Psi_k}{\Psi_k}$ is normally obtained within 10 to 20 iterations.

Schröder and Schuster[9] employ a finite difference technique to solve the compressible throughflow problem in a parallel walled annulus containing one or two actuator discs. Their formulation is "quasi-direct" in the sense that they prescribe the jump in tangential velocity (and hence in enthalpy when the disc is a rotor) in terms of the spacial (r) position rather than in terms of the value of the streamfunction. By so doing, they are forced to resort to iterative corrections to the equations describing the flow downstream of a rotor because the local value of stagnation enthalpy at a given point (r,z) must be updated as the value of the streamfunction at the disc and at the point (r,z), change. As with Ref. 8 and the present report, the density is calculated by iteratively updating the streamline position estimate.

In common with the present report, Schröder and Schuster consider only radial blades. The main thrust of the paper of Ref. 9 seems to be in the direction of investigating the jump conditions at the actuator disc. It appears that their program is the most developed with regard to capability of handling high meridional Mach numbers of the papers reviewed here, but the parallel walled geometry is unfortunately restrictive. With regards to convergence, Schröder and Schuster state that "as a rule, 35 to 70 complete iteration cycles will be necessary to arrive at convergence, each cycle passing over all nodes."

The final paper considered here, that by Hawthorne and Ringrose[10] is the most restrictive physically in that it considers only free vortex flow through actuator discs contained in a parallel walled annulus. The solutions, however, are obtained in analytical form by first linearizing the equations. It is apparent that the linearizing approximation requires the presence of "small" meridional Mach numbers in order to give valid results. The paper, however, is very useful for several reasons. Most importantly the very rapid calculation of desired examples allows the easy physical interpretation of the density effects. In addition, by considering a free vortex flow field, no velocity perturbations arise from rotational effects so the effects of density variations are effectively isolated. Finally, the restriction to low meridional Mach numbers is not as restrictive as at first might seem apparent, because flows with very large swirl Mach numbers (> 1) can be considered. Such flows exhibit large compressibility effects but do not necessarily contain large meridional Mach numbers. Several computational examples have been given already in SECTION VI in which results of the present report calculations were compared to the results of Ref. 10.

SECTION VIII

SUMMARY AND CONCLUSIONS

This report has given the statement of a new variational formulation of the compressible throughflow problem. A detailed development of a finite element analysis and presentation of an associated computer program is included, together with many example calculations.

It is important to note that the variational principle is valid for a very general flow field. Thus, compressibility, entropy variations and real gas effects may all be included in the analysis. It is assumed that viscosity is zero throughout the flow field, an assumption that implies that any entropy variations arise within the blade rows. This latter assumption is, of course, consistent with conventional throughflow theory.

The analytical and numerical forms presented herein have been restricted to isentropic flows and to flows of a calorically perfect gas. This latter assumption appears primarily in the subsidiary expression for the density. It is emphasized again, however, that further development of the concept could lead to inclusion of both entropy variations and real gas effects.

The authors feel that the utilization of finite element techniques in this context promises to lead to the efficient calculation of very complex flow fields and hope that this report has made a significant step in this direction.

REFERENCES

1. Marble, F.E., "Three-Dimensional Flow in Turbomachines," Aerodynamics of Turbines and Compressors, High Speed Aerodynamics and Jet Propulsion, Vol X, Section C, Princeton, 1964.

2. Hawthorne, W.R. and Horlock, J.H., "Actuator Disc Theory of the Incompressible Flow in Axial Compressors," Proceedings of the Institute of Mechanical Engineers, Vol. 176, No. 30, 1962, pp. 789-814.

3. Oates, G.C. and Knight, C.J., "Throughflow Theory for Turbomachines," Technical Report AFAPL-TR-73-61.

4. Liepmann, H.W. and Roshko, A., "Elements of Gasdynamics," John Wiley and Sons, Inc., 1957.

5. Shen, S.F., "An Aerodynamicist Looks at the Finite Element Method," Section IV of Finite Element Methods in Flow Problems, Proceedings of the International Symposium on Finite Element Methods in Flow Problems, January 1974, Swansea, United Kingdom. UAH Press.

6. Carnahan, B., Luther, H.A. and Wilkes, J.O., "Applied Numerical Methods," John Wiley and Sons, Inc., 1969.

7. Creveling, H.F. and Carmody, R.H., "Axial Flow Compressor Design Computer Programs Incorporating Full Radial Equilibrium -- Part II: Radial Distribution of Total Pressure and Flow Path or Axial Velocity Ratio Specified (Program III), NASA Contractor Report, No. CR-54531, 1968.

8. Marsh, H., "A Digital Computer Program for the Through-Flow Fluid Mechanics in an Arbitrary Turbomachine Using a Matrix Method," National Gas Turbine Establishment (England) Report No. R282, 1966.

9. Schröder, H.J. and Schuster, P., "Actuator Disc Flow Calculated by Relaxation -- An Approach to the Analysis Problem of Turbomachinery," ASME Paper No. 72-GT-26.

10. Hawthorne, W.R. and Ringrose, J., "Actuator Disc Theory of the Compressible Flow in Free-Vortex Turbomachines," Paper 5, Proceedings of the Institution of Mechanical Engineers, 1963-1964, Vol. 178, Pt. 3I(ii), pp. 1-13.

11. Wu, H.C., "A General Theory of Three-Dimensional Flow in Subsonic and Supersonic Turbomachines of Axial, Radial and Mixed Flow Types," NACA TN 2604, 1952.

☆U.S.Government Printing Office: 1975 — 657-020/519